

Annual Report of Naka Fusion Research Establishment  
From April 1, 2000 to March 31, 2001

Naka Fusion Research Establishment

Japan Atomic Energy Research Institute  
Naka-machi, Naka-gun, Ibaraki-ken

(Received October 29, 2001)

This report provides an overview of research and development activities at Naka Fusion Research Establishment, JAERI, during the period from April 1, 2000 to March 31, 2001. The activities in the Naka Fusion Research Establishment are outstanding at high performance plasma researches in JT-60 and JFT-2M, and development in ITER EDA including technological R&Ds.

The JT-60 project aims at contributing to the physics R&D for ITER and establishing the physics basis for a steady state tokamak fusion reactor like SSTR. For the achievement of those objectives, both physical and engineering researches have been done. The JT-60 have continued to be productive in many areas covering performance improvements of high  $p$  ELMy H-mode regime and reversed shear plasma, non-inductive current drive, physics study relevant to improved modes, stabilization of MHD modes, feedback control, disruption study, understandings on energetic particles, and scrape off layer and divertor studies with increased pumping capability. Highlights of FY 2000 experiments are summarized as follows:

- 1) In the high  $p$  ELMy H-mode regime, discharges with a high total-performance have been sustained near the steady-state current profile solutions under full non-inductive current drive. In this experiment, the world record value of NB current drive efficiency  $\eta_{CD}$  of  $1.55 \times 10^{19}$  A/m<sup>2</sup>/W was achieved with increasing central electron temperature of 13keV.
- 2) The demonstration of the active control of ITB was performed by changing the direction of the toroidal momentum input. In this experiment, it is found that the change in  $E_r$  shear of outer half region of the ITB layer (near the ITB foot) was important to control the whole ITB region.
- 3) Resistive instabilities are investigated in reversed shear discharges and it is found that the radially localized resistive interchange mode near the negative shear region leads to a major collapse through nonlinear mode coupling with a tearing mode in the positive shear region.
- 4) By increasing the input power of the fundamental O-mode EC wave, the complete stabilization of Neoclassical Tearing Mode was achieved. In a typical discharge where the

complete stabilization was achieved, EC driven current density is calculated to be about  $0.15\text{kA/m}^2$ , which is about twice as large as bootstrap current density.

- 5) The deeper penetration for HFS(upper) pellet is consistent with the radial displacement based on the theoretically predicted ExB drift model. Using the HFS(upper) pellets, the accessible density region of the high  $p$  plasmas is extended to 70% of the Greenwald density with  $H_{89p}$  of 1.94.
- 6) By injecting Ar, the confinement of ELMy H-mode has been improved with high radiation loss power at high density. When the Ar density was higher than 0.5%, the  $H_H$ -factor remained near unity in the range of  $n_e < 0.65 n_{GW}$ . The confinement improvement seemed to be closely related to the high ion temperature at the pedestal.

The highlights of technological progress in JT-60 are as follows;

- 1) A new guide tube for pellet injection from the midplane at the high magnetic field side was installed inside the vacuum vessel, and the pellets have been successfully injected with a minimal speed of 0.2 km/s.
- 2) A new boronization system for the plasma surface components using  $B_{10}D_{14}$  with He as a carrier gas was developed, and in comparison with the former boronization using  $B_{10}H_{14}$ , the boronization time decreased to about one-fourth by stable glow discharge and the number of plasma discharges for wall conditioning after the boronization also decreased to one-tenth due to little hydrogen content in the boron film.
- 3) A new real-time plasma shape reconstruction system based on the Cauchy-condition surface method was successfully applied to real time plasma equilibrium control for the first time in the world.
- 4) To test the pulsed operation of the ITER super-conducting center solenoid model coil, a control gain of the poloidal field coil power supply for JT-60U has been adjusted, and as the result the pulsed operation test completed successfully.
- 5) The development for increasing the beam power on the negative-ion based neutral beam injection system has been progressed, and as the result the power level of around 5MW at 400keV has been injected stably.
- 6) The fourth gyatron and transmission system for EC heating and ECCD were installed aiming at an injection power of more than 2 MW. The antenna of the new system can scan the EC beam in both toroidal and poloidal directions.
- 7) The detailed design of the JT-60 modification utilizing superconducting coils(JT-60SC), which aims at establishing scientific and technological bases for an advanced operation in an economically attractive DEMO reactor and ITER, has been completed.

On JFT-2M, advanced and basic research of tokamak plasma is being promoted, including application of the low activation ferritic steel, with the flexibility of a medium-sized device. The pre-testing on compatibility of ferritic steel plates (FPs), covering ~20% of the inside wall of the vacuum vessel, with plasma was performed, demonstrating no adverse effects on plasmas. Boronization was introduced for the first time in JFT-2M after installation of inside FPs. High- $n_N$  discharges ( $n_N$  up to 2.8) were obtained with inside FPs and boronization. Formation of negative electric field at the H-mode transition during ECH was clarified by the heavy ion beam probe (HIBP). The MSE polarimeter system, which is capable of simultaneous measurement of a radial electric field, has been newly developed. In RF experiments, fast wave

electric field profile was directly measured for the first time using the beat wave and HIBP.

The principal objective of theoretical and analytical studies is to understand physics of tokamak plasmas. The NEXT (Numerical EXperiment of Tokamak) project has been progressed in order to research complex physical processes both in core and in divertor plasmas by using massively parallel computers.

The optimum condition of electron cyclotron (EC) beam injection has been efficiently obtained to stabilize neo-classical tearing modes (NTM). Remarkable progress has been made in the study of turbulence driven by electron temperature gradient instabilities. The study on the formation of a detached-plasma has been much progressed.

Major items of Research and Development (R&D) of nuclear fusion reactor technologies, mainly focused on ITER-related areas in FY2000 are as follows:

- 1) Blanket: Be/DSCu specimens made by HIP method with an Al interlayer have successfully withstood against a heat flux of 5 MW/m<sup>2</sup> for more than 1000 cycles.
- 2) Superconducting Magnet: The world's largest superconducting pulsed coil was successfully tested at the target field of 13 T and operating current of 46kA, with a stored energy of 640 MJ at a ramping rate of 1.2 T/s.
- 3) Negative Ion Beam: 1MV voltage folding of the beam accelerator column was successfully demonstrated. The negative ion production mechanism was clarified in detail.
- 4) RF Heating: A 170GHz gyrotron was successfully tested at 1MW level power for about 10 second (0.9MWx9.2sec).
- 5) Tritium handling: Performance of ITER-scale 2,500 m<sup>3</sup>/hr large atmosphere detritiation system was successfully confirmed. A new separation method could separate the mixture gas of H<sub>2</sub>/He to each composition gas with the enrichment more than 99%.
- 6) Plasma Facing Components of Divertor: A prototype mockup of the ITER divertor could successfully sustain a heat flux up to 20MW/m<sup>2</sup> (15sec) for more than 1000 thermal cycles.
- 7) Reactor Structure: The blanket module has been replaced under the required clearance of ± 0.25 mm between key and groove by remote handling.
- 8) Fusion Neutronics: Radiation detectors using single crystal CVD diamonds have been developed aiming the 14 MeV neutron spectrometer. A key element technology phase of IFMIF has begun to reduce the key risk factor for its construction.

An option of minimum cost still satisfying the overall programmatic objective of the ITER has been developed by the three Parties of Japan, EU and RF during the extension of the Engineering Design Activities (EDA) after the successful completion of the six year EDA in July 1998. The Outline Design Report of the newly developed ITER-FEAT was submitted in January 2000 for the review of the Parties. The technology which had been established through the plasma physics and technology R&D during the past EDA or the technology being established by the current R&D were employed in the design of ITER-FEAT. The ITER Council subsequently approved the design in June 2000 as a single mature design for ITER consistent with its revised objectives. The Draft Final Design Report of ITER-FEAT was prepared for technical review by the Technical Advisory Committee (TAC) held in February 2001. The TAC concluded that the ITER-FEAT was ready for a decision on construction with

recognition of the achievement in reducing the cost by 50%.

In April 2000, the successful DC operation of the CS Model Coil which had been developed since the beginning of the EDA was achieved in JAERI Naka. In August 2000, ten thousand cycles of pulsed operations were achieved to simulate ITER full-scale CS. The full-scale sector of the Vacuum Vessel sector with port extension for testing of the remote welding and cutting had been dismantled in March 2001 after successful completion of the test.

In fusion reactor design, the physics design of a fusion power reactor A-SSTR2 was developed on plasma current startup. At the same time, hydrogen production from biomass and other various uses of high-temperature helium gas coolant from the A-SSTR2 plant were proposed. As to safety research on A-SSTR2, a reactor design concept to reduce radioactive wastes after the decommissioning is proposed.

Keywords; JAERI, Fusion Research, JT-60, JFT-2M, NEXT, Fusion Engineering,  
ITER, EDA, Fusion Reactor

## Contents

### I. JT-60 PROGRAM

1. Experimental Results and Analyses
  - 1.1 Sustainment of High Performance and Non-inductive Current Drive
  - 1.2 Physics of Plasma Confinement
  - 1.3 MHD instabilities and High Energy Particles
  - 1.4 Plasma Control and Disruption
  - 1.5 Particle Control and Divertor/Scrape-off-Layer (SOL) Physics
  - 1.6 High Density and High Radiation Plasmas
2. Operation and Machine Improvements
  - 2.1 Tokamak Machine
  - 2.2 Control System
  - 2.3 Power Supply System
  - 2.4 Neutral Beam Injection System
  - 2.5 Radio-frequency Heating System
  - 2.6 Design Study of the JT-60 Modification Utilizing Superconducting Coils

### II. JFT-2M PROGRAM

1. Advanced Material Tokamak Experiment (AMTEX) Program
  - 1.1 Pre-testing on Compatibility with Plasma
  - 1.2 Study of Ripple Loss of Fast Ions
  - 1.3 Preparation for Testing on Compatibility with Plasma
2. High Performance Experiments
  - 2.1 Study of High Confinement Modes
  - 2.2 Radio Frequency Experiments
  - 2.3 Compact Toroid Injection
3. Operation and Maintenance
  - 3.1 Tokamak Machine
  - 3.2 Heating Systems
  - 3.3 Power Supply System

### III. THEORY AND ANALYSIS

1. Confinement and Transport
2. Stability
3. Heating and Current Drive

4. Numerical Experiment of Tokamak (NEXT)
  - 4.1 Development of Computational Algorithm
  - 4.2 Transport and MHD Simulation
  - 4.3 Divertor Simulation

#### IV. FUSION REACTOR DESIGN AND SAFETY RELATED RESEARCH

1. Fusion Reactor Design
  - 1.1 Design of A-SSTR2
  - 1.2 Design of a New DEMO Reactor
  - 1.3 Startup of DT Fusion Plant without Initial Loading of Tritium
  - 1.4 Multipurpose Use of Fusion Energy
2. Fusion Safety
  - 2.1 Structural Integrity of First Wall Made of SiC/SiC
  - 2.2 Reduction of Radioactive Waste from Tokamak Reactor

#### Appendices

- A.1 Publication List (April 2000- March 2001)
- A.2 Personnel

## I. JT-60 PROGRAM

Objectives of the JT-60 project are to contribute to the physics R&D for International Thermonuclear Experimental Reactor (ITER) and to establish the physics basis for a steady state tokamak fusion reactor like SSTR. In the fiscal year 2000, JT-60 experiments were devoted to the demonstration of steady state operation scenario in ITER, achievement of the high current drive efficiency equivalent to that required in ITER, confinement improvement at high density, divertor physics, energetic particle physics and disruption study.

Highlight in realization of high performance plasma is the successful demonstration of the high performance of  $H_H$ -factor to IPB98(y, 2) scaling  $HH_{y2} \sim 1.4$  at about 80% of the Greenwald density under a full non-inductive current drive condition in a reversed shear plasma. Total plasma current of 0.9 MA was sustained with the bootstrap current, negative-ion based neutral beam (N-NB) driven current and lower-hybrid (LH) wave driven current for  $\sim 1$  s. Increase in the triangularity of the plasma cross section at the separatrix ( $\delta$ ) from 0.3 to 0.4 was effective to improve confinement at high-density regime. A newly developed technique for the fast and precise control of the distance between RF antenna and plasma edge could keep a good LH-wave-coupling with the plasma. This new result supports the non-inductive steady-state operation scenario in ITER.

A world record on the current drive efficiency of  $1.55 \times 10^{19}$  A/m<sup>2</sup>/W by neutral beam injection was attained by N-NB injection at 360 keV in the high- $\beta_p$  ELMy H-mode with the central electron temperature of 13 keV. The efficiency is about 3 times as high as that by the conventional NB at around 100 keV. In this discharge, fully non-inductive current drive at 1.5 MA of the plasma current was realized simultaneously with high plasma performance of normalized beta  $\beta_N \sim 2.5$ ,  $HH_{y2} \sim 1.4$  under a bootstrap current fraction of  $\sim 50\%$ . Power up of the total gyrotron power from 1 MW to 3 MW was effective for obtaining high electron temperature, which lead to the high current drive efficiency.

Neo-classical tearing mode (NTM) considered as one of the dangerous instabilities in ITER was stabilized by the electron cyclotron (EC) wave injection. It has been confirmed that precise control of the injection of EC waves aiming at the magnetic island of the NTM is required to stabilize it. Furthermore, understandings of energetic particle behavior and disruptions have been steadily progressed.

The total gyrotron power was increased from 3 MW to 4 MW. Increased EC heating power is expected to be applied for suppressing NTMs at a high plasma-pressure regime and for achieving the N-NB current drive efficiency required in ITER at high electron temperature.

## 1. Experimental Results and Analyses

### 1.1 Sustainment of High Performance and Non-inductive Current Drive

With the main aim of providing physics basis for ITER and a steady-state tokamak reactor, JT-60U has been optimized the operational concepts and extending discharge regimes toward simultaneous sustainment of high confinement, high  $n_N$ , high bootstrap current fraction, full non-inductive current drive (CD) and efficient heat and particle exhaust utilizing variety of heating, current drive, torque input and particle control capabilities. In the two advanced operation regimes, i.e. the reversed magnetic shear (RS) and the weak magnetic shear (high- $p$ ) ELMy H-modes characterized by both internal and edge transport barriers (ITB and ETB) and high bootstrap current fractions  $f_{BS}$ , discharges have been sustained near the steady-state current profile solutions under the full non-inductive current drive with proper driven current profiles. It has been demonstrated that local current profile optimization is essentially important to sustain high confinement (for example, to keep a wide ITB radius) and to increase sustainable  $n_N$ . In addition, current drive capability of the high energy N-NB system in JT-60U has been extended to the reactor relevant regime.

#### 1.1.1 Enhanced Performance of the High- $p$ ELMy H-mode with High N-NB Current Drive Efficiency.

In the high- $p$  ELMy H-mode regime, characterized by the weak magnetic shear, discharges with a high total-performance have been sustained near the steady-state current profile solutions under the full non-inductive current drive with N-NB (360 keV, 4 MW) and bootstrap current [1.1-1]. Main parameters are as follows:  $I_p = 1.5$  MA,  $B_t = 3.7$  T,  $q_{95} = 4.8$ ,  $HH_{y2} = 1.4$  and  $n_N = 2.5$ . The non-inductive current was produced mainly by on-axis current drive by the N-NB (608 kA, 40% of  $I_p$ ), broad current drive by the positive ion based NBs (255 kA, 17%) and off-axis bootstrap current (760 kA, 51%). Since the NB current drive efficiency increases with  $T_e(0)$ , on-axis ECH was applied and  $T_e(0)$  reached 13 keV, and hence the world record value of NB current drive efficiency  $\eta_{CD}$  of  $1.55 \times 10^{19}$  A/m<sup>2</sup>/W has achieved. At the same time, the record values of the fusion product under the full non-inductive current drive ( $n_D(0) \cdot T_i(0) = 2.0 \times 10^{20}$  m<sup>-3</sup>skeV) has obtained. The full non-inductive high- $p$  ELMy H-mode regime has been extended to the reactor relevant regime with small values of collisionality,  $\nu_{e^*}$ , and normalized gyroradius,  $\rho_{pi}^*$ . These values are close to those for the steady-state reference design of ITER:  $\nu_{e^*} \sim \nu_{e^*}^{ITER}$  and  $\rho_{pi}^* \sim 3-4 \rho_{pi}^{*ITER}$ . Even in this low- $(\nu_{e^*}, \rho_{pi}^*)$  regime, sustainment of high  $n_N \sim 2.5$  was demonstrated with a stable set of current and pressure profiles (small  $p$  at the  $q = 2$  surface) for the neoclassical tearing modes.

In the high- $p$  ELMy H-mode regime,  $n_N H_{89P} \sim 7$  has been sustained for  $\sim 1.3$ s ( $\sim 3 \tau_E$ ) with full non-inductive current drive and  $n_N H_{89P} \sim 5.5$  for  $\sim 2.8$ s ( $\sim 12 \tau_E$ ) at  $q_{95} = 3.3$ . Here,  $H_{89P}$  is the H-factor to L-mode scaling. For the sustainment of both high  $n_N$  and high  $H_{89P}$  values, a

high triangularity operation ( $\delta > 0.3-0.4$ ) is essentially important in addition to current and pressure profile optimization because the pedestal pressure in the ELMy phase increases with triangularity. By the high triangularity operation,  $n_N = 2.8 - 3$  was sustained for 4 sec at low  $q_{95}$  of 3.4.

### 1.1.2 Extended Operational Regimes of Quasi-Steady High- $\delta$ ELMy H-mode Discharges with High Total-Performance

With the high-field-side (HFS) pellet injection, JT-60U has successfully extended the density range in the high  $\delta$  ELMy H-mode with a favorable total-performance. We adopted high triangularity at separatrix ( $\delta_x \sim 0.47$ ), since high triangularity is beneficial to achieve high confinement at high density. In addition, we injected N-NB that can keep a centrally peaked heating profile even at high density. In this regime,  $HH_{y2} = 1.05$  together with  $n_N = 2.2$  and  $f_{BS} \sim 60\%$  was achieved at  $n_e/n_{GW} \sim 0.7$  [1.1-1]. Without pellets,  $n_e/n_{GW} \sim 0.6$  was the upper density limit to achieve  $HH_{y2} > 1$ . Comparing with the discharges treated in 1.1.1, the total performance was improved in terms of density, radiation power and purity. In this case, the pedestal temperature is almost kept constant at a high value even at a high pedestal density. We found that the edge stability limit for ELMs is improving with increasing  $\delta$  in the high  $\delta$  regime.

At  $\delta_x = 0.43$ ,  $I_p = 1\text{MA}$ ,  $B_t = 3.6\text{T}$  and  $q_{95} = 4.5$ , we have demonstrated full non-inductive current drive by N-NB injection with  $n_N = 3.0$ ,  $HH_{y2} = 1.2$  and at  $n_e/n_{GW} \sim 0.6$ . At higher values of  $\delta_x = 0.5$  and  $q_{95} = 6.9$  (1MA/3.6T), we have also demonstrated full non-inductive current drive with grassy ELMs. In this case, high confinement performance of  $HH_{y2} = 1.2$  was achieved at  $n_e/n_{GW} \sim 0.6$ .

### 1.1.3 Non-inductive Sustainment of High-Confinement Reversed Shear Plasma at High Normalized-Density Regime

In order to demonstrate a high-performance steady-state plasma which is planned in ITER steady state operation, improvement and sustainment of a high-performance RS plasma have been tried via non-inductive auxiliary current profile control by means of LHCD and N-NBCD [1.1-2]. Parameters expected in the ITER steady state operations are, for example  $HH_{y2} \sim 1.5$ ,  $n_N \sim 3.2$ ,  $f_{BS} \sim 54\%$ ,  $n_e/n_{GW} \sim 0.83$  and  $q_{95} \sim 4.1$ . The target was RS plasmas of  $I_p = 0.9$  MA with  $\delta_x \sim 0.44$  at  $B_t = 2.5$  T, thus  $q_{95} \sim 7$ . The LHCD was expected to drive current just outside  $q_{min}$  position in order to extend the  $q_{min}$  position thus the ITB location. The N-NB was also utilized in order not only to increase  $\delta$  but also to increase the non-inductive current and to modify the current profile. As a result, high confinement of  $HH_{y2} = 1.4$  ( $H_{89P} = 2.4$ ) with  $n_N = 2.2$  was kept with the surface loop voltage  $V_{loop} = 0$ , which is under full non-inductive current drive for 0.8 s ( $\sim 4 \tau_E$ ). The  $f_{BS}$  was estimated as about 64% and the rest was expected to be carried by the LHCD and the N-NBCD. The LHCD contributed to extend the ITB position outward by

off-axis CD to improve confinement and N-NBCD contributed to flatten the shear reversal, as expected respectively. In addition to the high confinement, the density regime at which the experiment was carried out was also high,  $n_e/n_{GW} > 0.8$ , and almost satisfied the ITER requirement.

#### 1.1.4 Extension to High- $I_p$ /Low- $q$ Regime of High-Confinement ELMy H-mode RS Plasmas

High confinement of  $HH_{y2} \sim 2.2$  was sustained for 2.7 s ( $6 \tau_E$ ) in an ELMy H-mode RS plasma with high  $f_{BS}$  of about 80% maintaining large radius of  $q_{min}$  ( $q_{min}$ ) and that of ITB [1.1-3, 4]. However, a low- $I_p$  (0.8 MA) and high- $q$  ( $q_{95} \sim 9$ ) operation was required to sustain large  $q_{min}$  with available power (2 MW) of off-axis tangential co-beam and with attainable beta ( $\beta_N \sim 2$ ). Though stationary sustainment of  $q$  profile is not expected in a lower- $q$  regime at present,  $q$  values ( $q_{min}$  and/or  $q_{95}$ ) are supposed to affect the MHD stability significantly in RS plasmas and hence a lower- $q$  operation was attempted to address this issue. As a result, high beta ( $\beta_N \sim 2$ ) was successfully sustained for longer than  $5 \tau_E$  in a low- $q$  regime ( $q_{min} \sim 2.5$ ,  $q_{95} \sim 5.5$ ) while high confinement ( $HH_{y2} > \sim 1.5$ ) was sustained only for  $\sim \tau_E$ . Long sustainment of  $HH_{y2} > \sim 1.5$  in a low- $q$  regime has been prevented by the confinement degradation phenomena that were encountered during a high confinement phase.

#### 1.1.5 1 MA Current Drive by N-NB in High Electron Temperature Regime

The profile of the current driven by high-energy neutral beam has been experimentally identified and confirmed to agree with the theoretical prediction in the high electron temperature regime [1.1-5]. The N-NB driven current increased with the electron temperature. The measured N-NB driven current  $I_{N-NB}(exp.)$  is compared with the calculated one  $I_{N-NB}(calc.)$  in Fig.I.1.1-1. An agreement over a wide range from 0.1MA to 1MA has been obtained. Experimentally measured N-NB driven current reached up to 1MA at  $T_e = 10keV$ , which is the record of NB current drive in JT-60U. Corresponding current drive efficiency  $\eta_{CD}$  was  $1 \times 10^{19} A/m^2/W$ . Confirmation of above mentioned N-NB current drive capability with high accuracy over a wide range of electron temperature indicates validity of theoretical prediction and gives more confidence to N-NB as a current drive method in ITER and a future reactor.

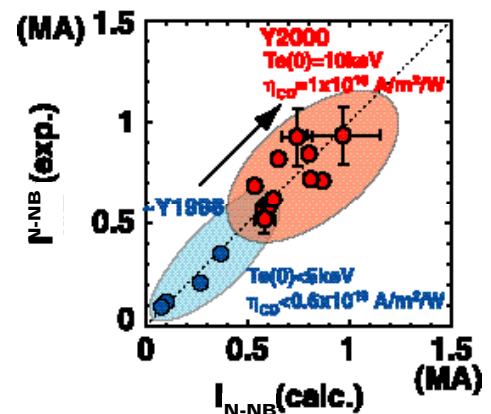


Fig.I.1.1-1 Comparison of the measured N-NB driven current  $I_{N-NB}(exp.)$  with the calculated  $I_{N-NB}(calc.)$ .

#### 1.1.6 Measurement of EC Driven Current by Motional Stark Effect Polarimeter [1.1-6]

Localized driven current profile by electron cyclotron (EC) waves was measured via

transient inductive current. The inductive current component due to temporal evolution of the internal magnetic field was evaluated by careful reconstruction of MHD equilibria with a spline function of total current and with motional Stark effect polarimetry. The EC driven current profile was evaluated by subtracting the inductive, bootstrap, and diagnostic neutral beam driven current profiles from the total current profile determined by the MHD equilibrium reconstruction. The analysis clearly shows that the EC current is driven in a thin layer of about 10% of the plasma minor radius. The determined EC driven current agrees with that calculated by ray tracing and Fokker-Planck codes. We have also confirmed that the experimentally evaluated EC driven current profile changes with the resonant location of EC waves. The current drive efficiency was about  $5 \times 10^{18}$  A/m<sup>2</sup>/W at electron temperature of 7 keV.

### References

- [1.1-1] Kamada, Y., et al., Fusion Energy 2000 (CD-ROM, IAEA, Vienna), OV1/1 (2001), to be published in Nucl. Fusion.
- [1.1-2] Ide, S. and the JT-60 team, to be published in J. Plasma and Fusion Res.
- [1.1-3] Fujita, T., et al., Fusion Energy 2000 (CD-ROM, IAEA, Vienna), EX4/1 (2001), to be published in Nucl. Fusion.
- [1.1-4] Fujita, T., et al., Phys. Rev. Lett., **87**, 085001 (2001).
- [1.1-5] Oikawa, T., et al., Fusion Energy 2000 (CD-ROM, IAEA, Vienna), EX8/3 (2001), to be published in Nucl. Fusion.
- [1.1-6] Suzuki, T., et al., "Measurement of Current Driven by Electron Cyclotron Waves in JT-60U" submitted to Plasma Physics and Controlled Fusion.

## 1.2 Physics of Plasma Confinement

Appearance of a transport barrier, which prevents energy from flowing out over a plasma column, is a key to access high-confinement regime. A barrier can be formed at the plasma boundary, which is so called "H-mode pedestal" or "edge transport barrier (ETB)". Another one which is formed inside the plasma is referred to as "internal transport barrier (ITB)". The ITB can be observed both in the reversed magnetic shear and the high  $\beta_p$  plasmas. In this year, a large amount of effort has been made for the study of the basic physics and characteristics of these barriers as well. On the ITB, physics issues such as conditions for its formation, confinement scaling and characteristics with electron heating have been studied mainly in RS plasmas. Also a scheme to control the ITB has been investigated. Concerning the ETB, edge parameters at the ETB formation, its structure especially at high density and effect of triangularity on pedestal temperature and the core confinement have been investigated. Furthermore compatibility of the ITB and the ETB was studied in RS plasmas. Moreover, the characteristics of the ETB have been investigated based on multi-machine database.

### 1.2.1 Effect of Electron Heating on Improved Confinement Plasmas

In these days' high-confinement plasma experiments, main heating scheme is NB heating with beam acceleration energy of around 100 keV which mainly heats ions. On the other hand, in a fusion plasma electron heating by alpha particles will be dominant. Also fueling is quite

different between current experiments (central beam fueling) and fusion plasma (almost no particle source) [1.2-1]. Furthermore, suppression of the Ion Temperature Gradient (ITG) mode, which is expected to play a large role in confinement improvement, can be different when  $T_e$  becomes higher than  $T_i$  and density gradient becomes smaller. In order to investigate the impact of electron heating on an improved-confinement-plasma, electron cyclotron heating (ECH) and N-NB heating with the acceleration energy of around 350 keV were applied to RS ( $I_p = 1.3$  MA) and high- $\beta_p$  ( $I_p = 1$  MA) plasmas. In both plasmas, more than 50% of the input power was fed into electrons. In the case of RS, the ITBs were found to remain in both the temperature and density. High confinement of  $H_{89p} = 2.4$  was maintained. In the case of high  $\beta_p$ , although ITBs in  $T_i$  and  $n_e$  became weaker, high confinement of  $H_{89p} = 2.4$  was still maintained. In both plasmas,  $T_e/T_i$  exceeded unity and reached about 1.2 in the core region.

### 1.2.2 On ITB Formation Condition in an RS Plasma

In order to clarify key parameters for ITB formation, parameter scan was carried out on RS plasmas. The first one is on toroidal rotation velocity. Since radial variation of the toroidal rotation velocity can be connected to the gradient of the radial electric field which is expected to be important for suppression of micro-instabilities. In the experiment, necessary perpendicular beam power to form ITB in an RS plasma at  $B_t = 3.7$  T was compared between tangential co- and counter-beams. It was found that when the plasma was rotating to counter direction with tangential counter injection ITB was found to be formed at around  $I_p = 0.6$  MA, while no ITB was found when the plasma was rotating to co-direction with tangential co-injection although the injection power was almost the same. The second one is to investigate if power necessary to form ITB depends on  $I_p$ . Since  $I_p$  is an important factor from the viewpoint of designing a new machine. Dependence on  $B_t$ , which is one of other important parameters, had been found to be weak already [1.2-1]. In the experiments, ITB was intended to be formed during  $I_p$  ramp-up phase as usual RS experiments. Therefore different sets of  $I_p$  and  $dI_p/dt$ , (0.3 MA, 0.4 MA/s) and (0.6 MA, 0.6 MA/s), were used in order to extend the range of  $I_p$  where ITB is formed. In the lower  $I_p$  cases, it was found that ITB tended to be formed with smaller NB power. The results suggest  $I_p$  dependence. However, since the discharges had not yet been optimized, similar or further study will be continued with finer optimization of parameters such as the current or shear profiles, which are expected to be important local parameters.

### 1.2.3 Active Control of Internal Transport Barrier in JT-60U RS Plasmas

The active control of ITB was demonstrated by changing the direction of the toroidal momentum input. The RS plasma with the strong ITB, which is characterized by steep pressure gradient, was generated in the standard scenario of balanced injection. In a quasi-steady state phase after the current flat-top, the directions of toroidal momentum input was changed with the

fixed total NB power from initially balanced injection to co-injection, then to ctr-injection and finally to the balanced injection again. The ion temperature gradient was degraded during the co-injection phase, then recovered at the balanced injection phase as shown in Fig.I.1.2-1. The change in  $E_r$  shear of outer half region of the ITB layer (near the ITB foot) was important to control the whole ITB region. This indicates that there is a non-

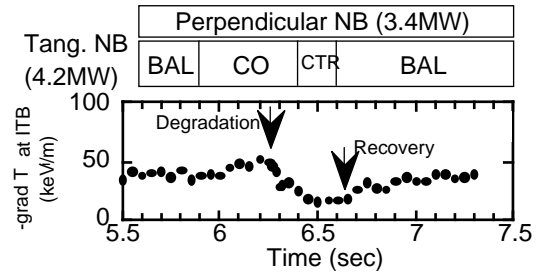


Fig.I.1.2-1 Time evolution of the ion temperature ( $T_i$ ) gradient at the ITB for a combination of NB types of balance injection (BAL), co-injection (CO) or counter injection (CTR).

local nature in relations between the  $E_r$  shear and the reduction of transport. The behaviors of electron temperature and electron density profiles were similar to ion temperature profile. [1.2-2]

#### 1.2.4 Scaling of Stored Energy in JT-60U RS Plasmas

Confinement properties of RS plasmas with L-mode edge were investigated under the discharge conditions of  $B_t = 4$  T,  $0.03 < \beta_p < 0.1$ ,  $1.7 < R_p < 2.0$ ,  $3.08 < R_p < 3.18$ ,  $0.5 < r_{foot}$  (the position of the ITB foot)  $< 0.75$ , nearly balanced NB injection. The stored energy evaluated diamagnetically,  $W_{dia}$ , was correlated with  $I_p$ . The  $W_{dia}$  increased with increasing  $r_{foot}$  due to the larger improved confinement region when  $I_p$  was fixed. Therefore the confinement property might be characterized by local parameter such as poloidal magnetic field at  $r_{foot}$ . The dependence of  $W_{dia}$  on  $B_p^{foot}$  was studied. It is found that the stored energy was strongly correlated with the poloidal magnetic field at the position of ITB foot,  $B_p^{foot}$ , rather than  $I_p$ , and was proportional to  $(B_p^{foot})^{1.5}$ . The ITB width,  $\Delta_{ITB}$ , becomes narrower during the evolution phase of the ITB and the lower boundary of the ITB width is proportional to the ion poloidal gyroradius at the ITB center,  $\rho_{pi}^{ITB}$ . This indicates that the transport property at the ITB layer can be characterized by the ratio of  $\Delta_{ITB}$  to  $\rho_{pi}^{ITB}$ . We consider the dependence of this ratio, and then  $W_{dia}$  scaling for RS plasmas was rewritten by

$$W_{dia} = 27.1 \times B_p^{foot 1.5} \times \Delta_{ITB} / \rho_{pi}^{ITB -0.25}$$

(in MJ, T and m). The RMSE for this fit is 6.86%. This scaling indicates that confinement property of RS plasma with the ITB is characterized by the local parameter at the ITB, and  $W_{dia}$  is almost independent of the heating power in this scaling expression. The investigation on the physical mechanism of this confinement property is the future work. [1.2-3]

#### 1.2.5 Compatibility Conditions of the Edge and Internal Transport Barriers

Having in mind that it is prerequisite to seek for the compatibility conditions of internal and edge transport barriers to establish the steady state high performance plasmas with superior

stability characteristics in a fusion experimental reactor, the L-H transition power has been investigated in plasmas with an internal barrier. It was found that the transition power is substantially higher than the conventional scaling established for plasmas without the internal barrier [1.2-4-6]. However, the criteria for the edge density and temperature to induce the L-H transition is similar between the cases with and without the internal barrier, and the edge density is extremely low in plasmas with strong internal barrier, which substantially increases the heating power to attain the H-mode. Thus, it was found that the scaling of L-H transition power, which does not separate the core transport and transition physics, is not generally applicable for plasmas with the internal barrier.

It was shown that the degradation of the quality of the transport barrier, in terms of the changes of toroidal rotation profile or equivalently the radial electric field distribution [1.2-7], resulted in the increase of edge density and thus inducing the L-H transition. Therefore, it is concluded that the degree to what extent the threshold power is modified depends on the quality of the internal barrier, indicating that the additional "hidden" parameter is present in plasmas with internal barrier.

#### 1.2.6 Edge Structure in JT-60U High-Density H-mode Plasmas

In order to explore the physics of confinement degradation at high density, which has been an issue of controversy for the ITER design, the edge structure and its interaction with the core structure have been intensively investigated. In this respect, it has addressed that the width of the  $E_r$  shear layer is reduced with an increase of edge density [1.2-8], and the pedestal width is concomitantly reduced. However, the correlation length of the density fluctuations is much less than the pedestal width [1.2-9,10]. It was also found that the direct influence of the neutral particles on the global confinement is not obvious [1.2-11]. In addition, the interaction of ITB and H-mode was first addressed in the reference of [1.2-11], in terms of the modification of edge conditions through the changes of  $\omega_{EXB}/\gamma_{LIN}$  profile in the plasma interior. Where the  $\omega_{EXB}$  is the angular frequency by ExB rotation and the  $\gamma_{LIN}$  is the linear growth rate of micro-instabilities.

The causalities of increased L-H threshold power at high density, exceeding the ITER scaling [1.2-12], have been intensively investigated emphasizing the edge parameters, including the neutral-particle density. It was hereby found that an increase of edge collisionality caused by the substantial reduction of the edge temperature could be a direct candidate. It was also suggested that the substantial increase of the threshold power at high density might be related to an increase of the edge density itself, exceeding the counter effect of inhomogeneity of neutral particles on the flux surface [1.2-13].

### 1.2.7 Triangularity Effects on Thermal-Energy-Confinement in ELMy H-mode Plasmas

The density scans of the energy confinement and pedestal properties were carried out in high- and low-triangularity ELMy H-mode plasmas. High triangularity discharges at low densities ( $n_e/n_{GW} \sim 0.4$ ) produced the higher pedestal pressure, at which higher pedestal temperature was obtained at a given density. The core electron and ion temperatures increase in roughly proportion to the pedestal temperature, and are independent of the triangularity. The profiles of temperature are stiff in the sense that there is a minimum scale length of temperature gradient, which can be achieved and the energy transport adjusts to maintain this scale length. The core temperature profiles are self-similar, as can be observed by a roughly constant shift on the logarithmic plot as the boundary temperature is varied. High- $\beta_p$  H-mode plasmas due to high power heating produced further high pedestal confinement. The improvement of the edge stability by increased triangularity leads to higher pedestal temperature, which in turn raises the core temperature, and thus the high thermal-energy-confinement is obtained.

### 1.2.8 Edge Plasma Parameters at L-H Transition after the Modification of Divertor Geometry [1.2-14]

Substantial reduction of the L-H threshold power was observed under the W-shaped divertor, in comparison with the open divertor. From a viewpoint of edge plasma parameter, it was found that edge plasma pressure just before the L-H transition in the case of W-shaped divertor became smaller than that in the case of open divertor. After the modification of divertor geometry, lower edge ion collisionality just before L-H transition ( $\nu_{i\text{eff}}^*(\text{L-H})$ ) was established with lower NB power. It was suggested that reduction of  $\nu_{i\text{eff}}^*(\text{L-H})$  arose from the decrease of neutral particles near the X-point by the analysis of poloidal profile of neutral-particle density. Therefore, neutral particles near the X-point prevented the threshold power for the L-H transition from reducing furthermore. According to this result, it is predicted that we can reduce the threshold power for the L-H transition further by using fueling which does not increase the neutral-particle density near the X-point.

### 1.2.9 Understanding of the H-mode Pedestal Characteristics using the Multi-Machine Pedestal Database [1.2-15]

With the use of a multi-machine pedestal database, essential issues for each regime of ELM types are investigated. They include (i) understanding and prediction of pedestal pressure during type I ELMs which is a reference operation mode of ITER, (ii) identification of the operation regime of type II ELMs which have small ELM amplitude with good confinement characteristics, (iii) identification of upper stability boundary of type III ELMs for the access to the higher confinement regimes with type I or II ELMs, (iv) relation between core confinement and pedestal temperature in conjunction with the confinement degradation in high density

discharges. Scaling and model based approaches for expressing pedestal pressure are shown to roughly scale the experimental data similarly well and initial predictions for the future reactor case could be performed by them. It is identified that  $q$  and  $\beta_p$  are important parameters to obtain the type II ELM regime. A theoretical model on type III ELMs is shown to reproduce the upper stability boundary reasonably well. It is shown that there exists some critical pedestal temperature, below which the core confinement starts to degrade. It is also shown that improved pedestal conditions for good confinement in high-density discharges are possible by increasing the plasma triangularity.

## References

- [1.2-1] Ide, S. and the JT-60 team, *Phys. Plasmas*, **7**, 1927 (2000).
- [1.2-2] Sakamoto, Y., et al., *Nucl. Fusion*, **41**, 865 (2001).
- [1.2-3] Sakamoto, Y., et al., "Characteristics of Internal Transport Barrier in JT-60U Reversed Shear Plasmas", submitted to *Journal of Plasma and Fusion Research SERIES*.
- [1.2-4] Fukuda, T., et al., *Nucl. Fusion*, **37**, 1199 (1997).
- [1.2-5] Fukuda, T., et al., *Plasma Phys. Control. Fusion*, **40**, 827 (1998).
- [1.2-6] Fukuda, T., et al., *Plasma Phys. Control. Fusion*, **42**, A289 (2000).
- [1.2-7] Fujita, T., et al., *Nucl. Fusion*, **39**, 1627 (1999).
- [1.2-8] Asakura, N., et al., *Plasma Phys. Control. Fusion*, **39**, 1295 (1997).
- [1.2-9] Fukuda, T., et al., *Nucl. Fusion*, **37**, 1199 (1997).
- [1.2-10] Hatae T., et al., *Plasma Phys. Control. Fusion*, **42**, A283 (2000).
- [1.2-11] Fukuda, T., et al., *Plasma Phys. Control. Fusion*, **40**, 543 (1998).
- [1.2-12] Snipes, J. A., et al., *Plasma Phys. Control. Fusion*, **42**, A299 (2000).
- [1.2-13] Fukuda, T., et al., *Plasma Phys. Control. Fusion*, **42**, A289 (2000).
- [1.2-14] Tsuchiya, K., et al., *Fusion Energy 2000 (CD-ROM, IAEA, Vienna)*, EXP5/26 (2001).
- [1.2-15] Hatae, T. et al., *Nucl. Fusion*, **41**, 285 (2001).

## 1.3 MHD instabilities and High Energy Particles

### 1.3.1 Resistive Interchange Modes in Reversed Shear Discharges

Resistive instabilities were investigated in reversed shear discharges and the following results were obtained. First, burst-like MHD activities which often emerged in reversed shear discharges with large pressure gradient were identified as the resistive interchange mode through direct observation of localized electron temperature perturbations by using the measurement of the electron cyclotron emission, ECE. The burst-like MHD activities with  $n=1$  were observed in the negative shear region with large pressure gradient near the internal transport barrier at  $n_N$  of about unity or even lower, and higher  $n$  ( $= 2, 3$ ) modes were also observed in higher  $n_N$  regime. The burst-like MHD activities are benign to the internal transport barrier and no clear degradation of the plasma-stored energy is observed by the activities. Second, resistive MHD instabilities that give rise to major collapse were studied through detailed analyses of a process of a major collapse. We found that the radially localized resistive interchange mode near the negative shear region leads to a major collapse through nonlinear mode coupling with a tearing mode in the positive shear region [1.3-1].

### 1.3.2 Wall Stabilization and Resistive Wall Mode (RWM)

Stabilizing effects by the resistive wall were investigated. We confirmed that both of

the resistive (tearing) and the ideal modes can be stabilized by the conducting wall that is close enough to the plasma surface (typically  $d/a < 1.3$ ;  $d$ : wall radius,  $a$ : plasma minor radius) and high- $\beta_p$  discharges with  $N > N^{\text{no-wall}}$  were obtained. Magnetohydrodynamic perturbations which have the growth rate of  $\sim \omega^{-1}$  and the toroidal rotation frequency  $f_{\text{tor}} \sim 1/(2\tau_w)$  were observed in the wall-stabilized high- $\beta_p$  discharges and were attributed to the resistive wall mode. Plasma rotation frequency in the toroidal direction  $f_{\text{tor}}$  near the mode rational surfaces at the outer  $q = 3$  or  $q = 4$  surfaces was  $\sim 4$  kHz and no clear reduction of  $f_{\text{tor}}$  was observed within the time resolution of 16.7 ms before occurrence of the resistive wall mode. Although  $f_{\text{tor}}$  does not decrease under the condition that  $N > N^{\text{no-wall}}$ , the RWMs grow and the discharge end up with the major collapse or disruption. The result suggests that the toroidal rotation frequency  $f_{\text{tor}} = 4$  kHz ( $\sim 10^{-2} v_A / (2R)$ ) is insufficient for stabilization of RWMs by the resistive wall [1.3-1], where the  $v_A$  is the Alfvén velocity. The wall stabilization effect can be weak when safety factor near the plasma edge,  $q^*$ , is close to integer values, then RWMs appear with significantly large  $\gamma_{\text{RWM}}$ . Characteristics of RWMs with respect to current-driven  $n = 1$  kink modes were also studied by employing current ramp-up discharges. It seems that dependence of  $\gamma_{\text{RWM}}$  on  $d/a$  is consistent with a theoretical one using a cylindrical model with certain plasma flow [1.3-2].

### 1.3.3 Complete Stabilization of a Neoclassical Tearing Mode by ECCD/ECH

Tearing mode stabilization experiment was started in 1999 using one-unit of EC system. The stabilization experiments have been performed using the fundamental O-mode electron cyclotron wave, which is the same as in ITER. In 2000, two gyrotrons were newly installed. Design value of the total generation power was increased up to 3 MW, which corresponds to the injection power of about 2.3 MW. In addition, control system for the steerable mirror was modified so that the mirror angle can be changed during a discharge. Stabilization experiment was performed in the similar way as in 1999, where the mode location was estimated from the profiles of electron temperature perturbations and the safety factor. Mode location was also identified by scanning the steerable mirror during a discharge. By fixing the mirror angle at the optimum one, a neoclassical tearing mode with  $m/n = 3/2$  was completely stabilized. In a typical discharge where the complete stabilization was achieved, EC driven current density is calculated to be about 0.15 kA/m<sup>2</sup>, which is about twice as large as bootstrap current density. Total EC driven current is calculated to be about 25 kA, which is 2% of plasma current [1.3-3].

### 1.3.4 Characteristics of Neoclassical Tearing Modes (NTMs) in High- $\beta_p$ H-mode Discharges

Onset condition of NTMs in high- $\beta_p$  H-mode discharges, such as density dependence of  $N$  at the NTM onset, has been investigated. Collisionality dependence of  $N$  at the NTM onset normalized by Larmor radius has been also investigated and founded that dependence of ion Larmor radius  $\rho_{i*}$  is stronger than that of electron collisionality  $\nu_e^*$  ( $N/\rho_{i*} \propto \nu_e^{*0.36}$ ). In some discharges, the NTM is not observed even when the value of  $N/\rho_{i*}$  exceeds the threshold for the

mode onset. This fact suggests that there is another factor that determines the onset of NTMs. Effects of current and pressure profiles on the mode onset have been investigated by comparing between the high- $\beta_p$  H-mode discharges with and without N-NB. It was found that by replacing a part of positive-ion based NB power with N-NB, an  $m/n = 2/1$  mode was suppressed in spite of higher beta. One of the reasons is considered to be a difference in pressure profiles: by injecting N-NB, pressure gradient at  $0.3 < r/a < 0.7$  was decreased and thus bootstrap current was decreased. This fact suggests that the  $\beta_N$  at the NTM onset can be improved by pressure profile optimization using N-NB [1.3-4,5].

### 1.3.5 Influence of MHD Instability on N-NB Current Drive

Current drive capability of N-NB was evaluated experimentally, and validity of theoretical prediction was confirmed for MHD-quiescent plasmas in section 1.1.5. Influence of beam driven instability and NTM on current drive has been also studied [1.3-6]. A beam-driven instability appeared in the central region of the plasma with large fraction of beam pressure. This instability occurred in burst-like behavior and fast frequency sweeping was observed. It was observed that a burst of long frequency sweeping caused loss of N-NB ions carrying non-inductive current from central region ( $r/a < 0.3$ ). The lost driven current in the central region was experimentally estimated to be  $\sim 40$  kA (7% of total driven current). Influence of NTM on beam ions was evaluated from comparison of the measured neutron yield with the calculated one by the transport code. The NTM caused loss or redistribution of fast ions. Influence of NTM was larger for higher energy NB (N-NB) and was enhanced with increasing activity of the instability.

### 1.3.6 Edge Stability of Giant and Grassy ELMs

The dependence of the edge stability on plasma shape and local pressure gradients,  $P$ , in the DIII-D and JT-60U tokamaks was studied. The stronger plasma shaping in DIII-D allows the edge region of the DIII-D discharges with type I (“giant”) ELMs to have access to the second region of the stability for the ideal ballooning modes and larger edge  $P$  than JT-60U type I ELM discharges. These JT-60U discharges are near the ballooning mode first regime stability limit. The DIII-D results support an ideal stability based working model of type I ELMs as low to intermediate toroidal mode number,  $n$ , MHD modes. Results from stability analysis of JT-60U type I ELM discharges indicate that predictions from this model are also consistent with JT-60U edge stability observations [1.3-7].

### 1.3.7 Collapse of Density Pedestal by Giant ELM

In JT-60U ELMy H-mode discharges, the detailed behavior of type I ELM was studied using a heterodyne O-mode

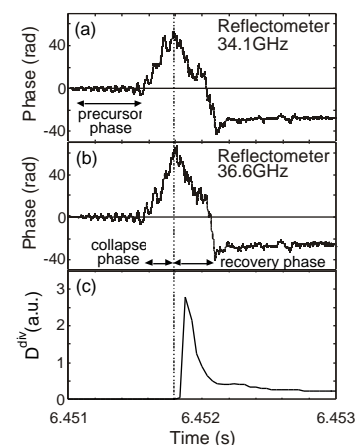


Fig.I.1.3-1 (a), (b) Phase changes of reflectometer and (c)  $D$  intensity during an ELM.

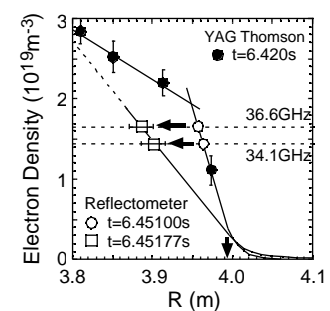


Fig.I.1.3-2 Electron density profile measured with YAG Thomson scattering and reflectometer.

reflectometer system in order to understand the collapse mechanism of the pedestal structure and consequences on the core/edge plasma. The phase signal of the reflectometer exhibits the movement of the cutoff layer (density layer) due to the collapse of the pedestal in a density profile by an ELM. The sequence of the ELM event can be classified into a precursor phase, a collapse phase, a recovery phase and a relaxation phase as shown in Fig.I.1.3-1. The typical time scale of each phase is 200-500 $\mu$ s, 100-350 $\mu$ s, 200-500 $\mu$ s and 6-10ms, respectively. Figure I.1.3-2 shows the reconstructed density profiles at the end of collapse phase shown in thin line in Fig.I.1.3-2. The maximum displacement was 6.1cm and 7.1cm for 34.1GHz and 36.6GHz reflectometer, respectively. In this case the reflected position reached 10cm inside the separatrix, which corresponds to twice the pedestal width of about 5cm [1.3-8].

### 1.3.8 Alfvén Eigenmodes Driven by Energetic Particles

In N-NB experiments [1.3-9,10], we have explored the parameter regime near the alpha particle birth domain in ITER, which could not be achieved by using NB, IC wave and alpha particles in the previous works, in term of two fast ion parameters: the volume averaged hot ion beta,  $\langle \beta_h \rangle$ , and the ratio of the beam ion velocity parallel to the magnetic field to the Alfvén velocity,  $v_{b\parallel}/v_A$ . We observed three different types of frequency sweeping modes in this regime: a slow frequency-sweeping (Slow FS) mode, a fast frequency-sweeping (Fast FS) mode, and an abrupt large-amplitude event (ALE). The slow FS mode appears with the frequency inside the Alfvén continuum spectrum and its frequency increases to a gap frequency of the toroidal Alfvén eigenmodes (TAE) on the time scale of the equilibrium change. One possibility of the Slow FS mode is considered to be a resonant TAE which belongs to a kinetic ballooning mode branch in a low frequency by using non-perturbative HINST code [1.3-11]. The ALEs and Fast FS modes appear inside a TAE gap and have a pulsating nature. The mode amplitude of the fluctuating poloidal magnetic field to its field,  $B_{\perp}/B_z$ , in ALEs reaches about  $10^{-3}$  at the first wall. The drop of neutron emission rate and the enhancement of the neutral-particle fluxes were observed on the occurrence of the ALEs, which indicates significant transport of energetic ions. The Fast FS modes, which often follow up-down frequency chirping, also induce fast ion loss when its amplitude is large. The transport mechanism is considered as “mode-particle pumping” from the energy dependence of the neutral-particle fluxes [1.3-12].

### References

- [1.3-1] Takeji, S., et al., Fusion Energy 2000 (CD-ROM, IAEA, Vienna), EX7/2 (2001).
- [1.3-2] Takeji, S., et al., to be submitted.
- [1.3-3] Isayama, A, et al., Plasma Phys. Control. Fusion, **42**, L37 (2000).
- [1.3-4] Isayama, A, et al., J. Plasma Fusion Res. SERIES **3**, 94 (2000).
- [1.3-5] Isayama, A, et al., Nucl. Fusion., **41**, 761 (2001).
- [1.3-6] Oikawa, T., et al., Fusion Energy 2000 (CD-ROM, IAEA, Vienna), EX8 (2001).
- [1.3-7] Lao, L.L., et al., Fusion Energy 2000 (CD-ROM, IAEA, Vienna), EXP3/06 (2001).
- [1.3-8] Oyama, N., et al., Plasma Phys. Control. Fusion, **43**, 717 (2001).
- [1.3-9] Kusama, Y., et al., Nucl. Fusion, **39**, 1837 (1999).
- [1.3-10] Shinohara, K., et al., Nucl. Fusion, **41**, 603 (2001).
- [1.3-11] Gorelenkov, N. N., et al., Nucl. Fusion, **40**, 1311 (2000).
- [1.3-12] White, R. B., et al., Phys. Fluids, **26**, 2958 (1983).

## 1.4 Plasma Control and Disruption

In addition to the further development of real time feedback control schemes, namely the

NTM suppression and  $T_e$  control aimed at the enhancement of steady-state plasma performance, low voltage start-up studies with ECH and runaway current experiment were performed in the 2000 campaign.

#### 1.4.1 Low Voltage Start-Up Assisted with Electron Cyclotron Heating

The development of low voltage startup scheme is prerequisite particularly in large tokamaks with super-conducting coils. The EC assisted startup experiment has been undertaken, and one turn voltage of as low as 4 V ( $E \sim 0.26$  V/m) was attained, satisfying the ITER requirement. We have found that the rate of development in  $I_p$  decreases with the filling pressure and also influenced by the toroidal magnetic field and EC wave injection angle. In the recent campaign, where the second harmonic EC wave was applied, the stable plasma production with the initial break down voltage of 4 V was possible with EC wave power of 690kW, but not with that of 400kW. The current was ramped up to 1 MA only when the resonance layer was in the center of a plasma, namely  $B_t = 1.83$  T and EC wave injection angle of  $52^\circ$ .

#### 1.4.2 Runaway Current Termination at the Plasma Disruption

Termination of the runaway electron current was successfully performed during the simulated vertical plasma displacement event, where the safety factor at the plasma surface,  $q_s$ , decreased. For all of the discharges with runaway electron generation, runaway current started to decrease with the appearance of spikes in magnetic fluctuations, and disappeared before  $q_s$  decreased to 2. Many spikes in magnetic fluctuation appeared during the runaway termination. The dominant mode of the spikes in the magnetic fluctuations was  $m=3/n=1$ . The first magnetic fluctuation with a fast growth rate of about  $3 \times 10^4$  s<sup>-1</sup> was followed by repeated magnetic fluctuations of which growth rate was slowed down to approximately  $5 \times 10^3$  s<sup>-1</sup>. Those fluctuations with slow growth rate decayed and terminated the runaway current. Corresponding to the loss of runaway electrons by magnetic fluctuations, the heat flux at the inner divertor plates was measured, which is an indicator of the wall interaction with the runaway electrons. Deposited power during the current decay was in a form of intensive pulses with each duration of the order of hundred micro seconds, and it did not deposit at the constant heat load during the current decay. On the other hand, the halo current, measured by the Rogowski coils, during the runaway termination was small, and increased after the runaway termination (at  $q_s < 2$ ) with a dominant toroidal mode of  $n=1$  [1.4-1].

#### Reference

[1.4-1] Tamai, H., et al., Fusion Energy 2000 (CD-ROM, IAEA, Vienna), EX9/2 (2001), to be published in Nucl. Fusion.

## 1.5 Particle Control and Divertor/Scrape-off-Layer (SOL) Physics

### 1.5.1 Pellet Injection Characteristics [1.5-1]

In order to extend the operational region to high density without confinement degradation, multiple pellet injector was installed for injections from low-field-side midplane, LFS(mid), and high-field-side at the top, HFS(upper). For the HFS(upper) pellet injection, the guide tube with a minimum curvature of 600 mm is used. The size of a pellet is 2.1mm cube and 30-40 pellets can be injected in each discharge. So far, the injection frequency of  $f=10$  Hz (designed maximum value is 20 Hz) and the injection speed of  $v=100-1000$  m/s, as designed, have been achieved.

For the LFS(mid) pellet injection, a large density spike is observed with a fast decay time of about 1 ms in the NB heated plasma. The fast decay could be due to a displacement in the direction of the major radius, because the fast decay is observed only for the LFS(mid) pellet injection. The initial density rise for the LFS(mid) pellet is almost the same in the OH and NB heated plasmas. The typical initial rise of the density in the OH plasma with the HFS(upper) pellet is about 30% smaller than that with the LFS(mid) pellet, which can be considered as the transmission loss in the guide tube. The initial rise of density for the HFS(upper) pellet in the NB heated plasma is 40% smaller than that in the OH plasma. One of the reasons for this reduction could be the ablation loss in the SOL. The neutral-gas-shielding (NGS) model suggests a 20% loss in the SOL of NB heated plasma for the HFS(upper) pellets. For the HFS(upper) pellet, deeper penetration than the prediction calculated by NGS model is observed in the NB heated plasma. The deeper penetration for the HFS(upper) pellet and the fast decay of density for the LFS(mid) pellet in the NB heated plasma are consistent with the radial displacement theoretically predicted based on the  $E \times B$  drift model. Using the HFS(upper) pellets, the accessible density region of the high  $p$  plasmas is extended to 70% of the Greenwald density limit with  $H_{89p}$  of 1.94.

### 1.5.2 Helium Exhaust and Forced Flow Effects [1.5-2]

Helium exhaust characteristics in the reversed shear plasmas have been studied by using He-NB injection under the W-shaped divertor. In the case of low-recycling divertor, it is difficult to achieve good helium exhaust capability. However, the helium exhaust efficiency is improved with high recycling divertor, although confinement degrades with increasing recycling. The simple model using the helium transport coefficients estimated based on gas-puff modulation technique suggests that helium removal from the core plasma inside ITB is possible with sufficient pumping rate (with high recycling divertor) even in the high confinement plasma. Simultaneous sustainment of high confinement and high recycling is the remaining issue.

The pumping rate is improved up to 5% with both-leg pumping in a W-shaped configuration from 3% with inner-leg pumping at the high-density region. Carbon impurity reduction is observed with gas-puffing and effective divertor pumping. Carbon impurity level

is effectively reduced with both-leg pumping due to the effect of flow produced by puff and pump.

### 1.5.3 Impurity Transport [1.5-1]

In order to understand impurity transport in the main plasma, transport coefficients are estimated using a gas-puff modulation technique, and these are compared with the theoretical predictions based on the neoclassical theory and turbulence model. The Multi-Mode Model (MMM) is used as a turbulence model, in which the Ion Temperature Gradient (ITG) modes, Trapped Electron Modes (TEM) and drift-resistive ballooning modes, as well as smaller contributions from kinetic ballooning modes, are included. In the ELMy H-mode plasma ( $I_p=1.0$  MA,  $B_t=2.1$  T,  $P_{NB}=11.1$  MW and  $H_{89p}=1.3-1.5$ ), which has no ITB and positive magnetic shear, helium particle diffusivity ( $D$ ) is in the range of  $1-2$  m<sup>2</sup>/s. In the high  $\beta_p$  plasma ( $I_p=1.5$  MA,  $B_t=3.6$  T,  $P_{NB}=17.5$  MW and  $H_{89p}=1.9$ ), which has ITB with a small gradient and weak positive magnetic shear,  $D$  is in the range of  $1-3$  m<sup>2</sup>/s, and seems to be reduced in the ITB region. However, the reduction is less than a factor of 2. In the reversed shear (RS) plasma ( $I_p=1.0$  MA,  $B_t=2.1$  T,  $P_{NB}=7.3$  MW and  $H_{89p}=1.9$ ), which has ITB with a large gradient and reversed magnetic shear, the  $D$  is in the range of  $0.3-2$  m<sup>2</sup>/s, and is reduced by a factor of 5-6 in the ITB region compared with that in the inside and outside regions. The value of  $D$  in the ITB region of the RS plasma is only higher by a factor of 2-4 than the neoclassical value. The convection velocity,  $v$ , in the ITB region of the RS plasma is the same level as the neoclassical prediction. In the ELMy H-mode and high  $\beta_p$  plasmas, the  $D$  is two orders of magnitude higher than neoclassical predictions, and is smaller by a factor of 3-5 than the turbulence model. The values of  $v$  for neoclassical and turbulence model predictions are in the range of error bar of the measurements in the ELMy H-mode plasma.

### 1.5.4 Impurity Control by Boronization and Optimization of the Wall Temperature

Boronization using deuterated decaborane has been applied to suppress oxygen production and the vessel temperature has been optimized to reduce carbon generation originating from chemical sputtering. The boronization decreases the oxygen content in the core plasma from  $\sim 3\%$  to  $\sim 0.5\%$ . The oxygen content of  $\sim 0.5\%$  is kept by additional boronization about every 100 shots. By lowering the vessel temperature from 540 K to 420 K, chemical sputtering yield decreases by  $\sim 40\%$  at carbon divertor plates. For hydrogen plasmas, the carbon content reduces from 3.1% to 1.8% in L-mode discharges with NB heating power of 13 MW and from 2.4% to 1.7% in reversed shear discharges.

### 1.5.5 SOL Plasma Physics

Control of the plasma flow in the SOL and divertor, using a pumping system, is

considered to be important because of its implications for the exhaust of helium ash and impurity retention in the divertor. In 2000, effect of the divertor pumping on the SOL plasma flow (SOL flow) was investigated in the partially detached divertor. Prompt heat load after ELM events has been a crucial issue to determine the life time of the divertor target for ITER. An infrared TV (IRTV) system was prepared for the fast measurement of the divertor heat load. The results on ELM energy loss and heat load on the W-shaped divertor target were summarized. Measurements of particle flux and SOL flow caused by ELM events were carried out using reciprocating Mach probes at the outer midplane and the X-point. Understanding of the SOL flow pattern in ELMy H-mode plasma and evaluations of convection and conduction of ELM power flow started.

#### 1.5.5.1 Divertor Detachment and SOL Plasma

With application of inner and outer divertor pumping (both-side pumping started in 1999), neutral-particle flux from the inner divertor to the outer divertor through under-dome was relatively small that the in-out asymmetry of the neutral-particle recycling did not change. The SOL plasma flow pattern, i.e. flow reversal at the midplane and flow towards the divertor near the X-point [1.5-3], did not change comparing with that for the inner divertor pumping (1997-1998). However, it was found that, in the partially detached divertor, an increase in the plasma flow velocity below X-point was larger for the both-side pumping, and that the subsonic plasma flow was maintained in the wider range of the main plasma density ( $\bar{n}_e$ ) without appearance of X-point MARFE [1.5-4]. These results show that the detachment front is located below the X-point by a reduction in the down-stream plasma pressure, using the divertor pumping from the private flux region. Pumping at both-sides of the divertor was favorable for maintaining the partially detached plasma.

#### 1.5.5.2 ELM Heat Load and Energy Loss

The ELM energy deposition, its time scale and deposition area are critical issues for evaluating ELM heat load on ITER divertor plate. International database of the high H-factor and high density plasmas are required to predict those parameters under the ITER operation. The ELM energy loss ( $W_{ELM}^{IRTV}$  evaluated from fast IRTV and  $W_{ELM}^{dia}$  from fast diamagnetic signal) were summarized for the high triangularity ELMy H-mode plasmas, i.e. (1) at low density ( $n_e/n^{GW}=0.4-0.5$ ), (2) at high density ( $n_e/n^{GW}=0.6-0.75$ ) with argon gas puff, and (3) at high safety-factor (grassy ELM). Comparison of  $W_{ELM}^{IRTV}$  and  $W_{ELM}^{dia}$  shows that the heat flux measurement (particularly inner divertor) may be overestimated by a factor of 2-3, presumably due to toroidal asymmetry of the heat flux and/or due to over estimation of the thermal conductivity of carbon.

The ELM energy fraction to the pedestal energy, its time and width for type-I ELM were

$W_{\text{ELM}}^{\text{dia}}/W_{\text{ped}} = 0.08-0.11$  (average),  $\tau_{\text{dep}}$  about or less than 0.25ms (one line scan of IRTV), and  $R_{\text{dep}}=1.5-1.7\text{cm}$  (mapped to outer midplane), which was 1.5 times wider than the value between ELMs, respectively. For the Ar gas puffing case,  $W_{\text{ELM}}^{\text{dia}}/W_{\text{ped}}$  was slightly smaller, and ELM frequency was decreased. It was comparable to previous DIII-D&JET database (at relatively low density), which implies unfavorable prediction for the ITER operation. For the grassy ELM,  $W_{\text{ELM}}^{\text{dia}}/W_{\text{ped}} = 0.03-0.05$  was small (1/2-1/4 of type I ELM). It is required to extend the operation at the low safety-factor. These data contributed in the ITER physics R&D works to deduce a simple scaling from the SOL collisional transport model [1.5-5].

### 1.5.5.3 SOL Plasma Flow Caused by ELMs

The SOL flow pattern just after ELM event is an important issue because it determines particle transport in ELMy H-mode plasma and affects exhaust of impurity ions. It is also important to clarify a transport of ELM heat flow, i.e. conduction and convection, since there were a few fast measurements. Simultaneous measurements of ELM heat flux (by IRTV), particle flux and Mach number (by reciprocating Mach probes) were performed in ELMy H-mode plasmas with low heating power. Heat flux deposition time and width were  $\sim 250\mu\text{s}$  and 1-1.5cm (mapped to outer midplane), respectively. Those values were comparable to the period ( $\sim 350\mu\text{s}$ ) and the region (1-1.5cm) of the SOL-flow-velocity enhancement, which reached the ion sound velocity, measured with the X-point Mach probe. This suggests that the convective transport of heat flux in SOL is important contribution to the divertor heat load.

### References

- [1.5-1] Takenaga, H., and the JT-60 team, Phys. Plasmas, **8**, 2217 (2001).
- [1.5-2] Sakasai, A., et al., Fusion Energy 2000 (CD-ROM, IAEA, Vienna), EX5/5 (2001).
- [1.5-3] Asakura, N., Sakurai, S., Shimada, M., et al., Phys. Rev. Lett., **84**, 3093 (2000).
- [1.5-4] Asakura, N., Sakurai, S., Tamai, H., et al., J. Nucl. Mater., **290-293**, 825 (2001).
- [1.5-5] Loarte, A., et al., Fusion Energy 2000 (CD-ROM, IAEA, Vienna), ITER/2-ITER/11 (2001).

## 1.6 High Density and High Radiation Plasmas

Confinement of the ELMy H-mode plasmas is degraded in the high-density regime in many tokamaks, and this degradation is a critical issue for the ITER design. High radiation is needed for mitigating the severe problem of concentrated power loading on the divertor plates. Controlled injection of impurity gases is a promising technique for enhancement of radiation loss power. Moreover, by injecting impurities, the confinement has been improved with high radiation loss power in the high-density regime in some tokamaks. In JT-60U, Ar has been injected into ELMy H-mode plasmas for confinement improvement and the radiation loss enhancement due to a radiating mantle at high density [1.6-1, 2, 3]. The properties of confinement improvement at the pedestal and core plasmas and radiation loss enhancement have been investigated. On the other hands, the RS plasma is a promising candidate for advanced

steady-state tokamak operation. In order to extend such an operation toward high density and high radiation, Ar and Ne have been injected into the RS plasmas with high confinement [1.6-1,4]. Radiation enhancement and divertor plasma detachment have been investigated.

### 1.6.1 Ar Seeded ELMy H-mode Plasmas [1.6-1,2,3]

The  $H_H$ -factor ( $HH_{y2}$ ) is plotted for different Ar densities against the electron density in Fig.I.1.6-1 (a). In the plasmas without Ar injection, the  $HH_{y2}$  decreased from 0.9 to 0.6 as the  $n_e/n_{GW}$  ratio increased from 0.45 to 0.60. On the other hand, the  $HH_{y2}$  was kept high in the plasmas with Ar injection. When the Ar density was higher than 0.5%, the  $H_H$ -factor remained near unity in the range of  $n_e < 0.65n_{GW}$ . The  $HH_{y2}$  was about 50% higher than that in plasmas without Ar injection at  $n_e = 0.65n_{GW}$ . The improvement in confinement more than compensated for the deuterium density reduction by impurity contamination, resulting in higher neutron production rates. The confinement was improved in both the pedestal and core regions. Figure I.1.6-1 (b) illustrates relation between the ion temperature at the pedestal and the line averaged electron density. The ion temperature at the pedestal decreased as the electron density increased in the case without Ar injection. However, with Ar injection, the ion temperature remained rather high even in the high-density regime. The confinement improvement seemed to be closely related to the high ion temperature at the pedestal.

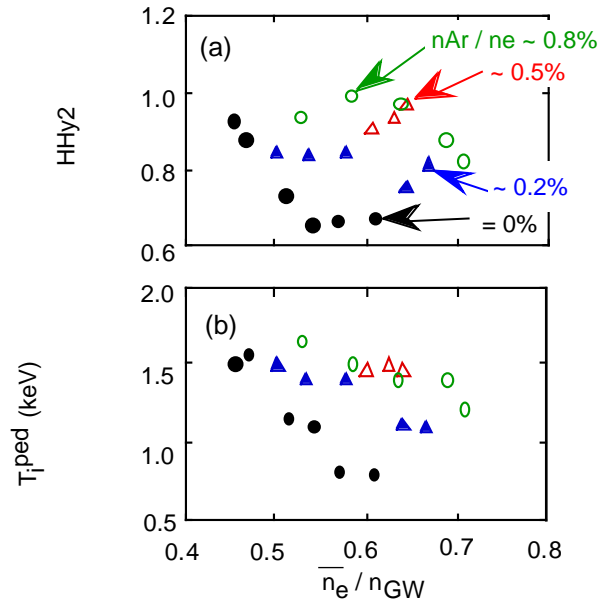


Fig.I.1.6-1. (a)  $H_H$ -factor ( $HH_{y2}$ ) and (b) ion temperature at the pedestal for different Ar densities against the line averaged electron density normalized by the Greenwald density limit.

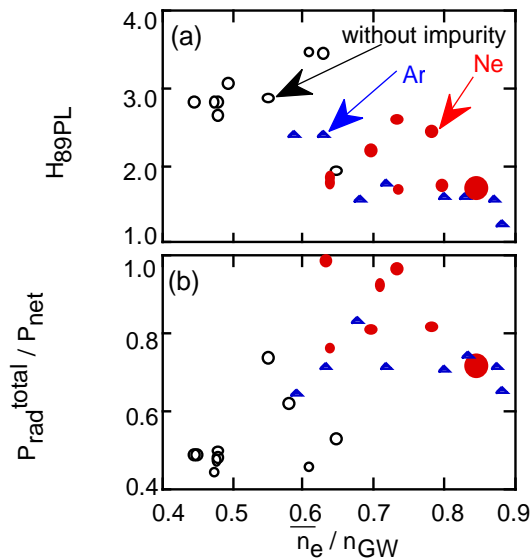


Fig.I.1.6-2. (a) H-factor ( $H_{89}$ ) and (b) ratio of the total radiation loss power to the net heating power against line averaged electron density normalized by the Greenwald density limit. The large closed circles indicate a discharge with divertor plasma detachment.

### 1.6.2 Impurity Seeded RS Plasmas [1.6-1,4]

The H-factor ( $H_{89P}$ ) and the ratio of the total radiation loss power ( $P_{\text{rad}}^{\text{total}}$ ) to the net heating power ( $P_{\text{net}}$ ) are plotted against the electron density in Fig.I.1.6-2. With Ar injection, as the electron density increased from  $0.6 n_{\text{GW}}$  to  $0.9 n_{\text{GW}}$ , the  $H_{89P}$  decreased from 2.4 to 1.2 while  $P_{\text{rad}}^{\text{total}}/P_{\text{net}}$  stayed around 0.7. Then, the electron temperature at the plasma center decreased from  $\sim 6$  keV to  $\sim 2$  keV, and the ratio of the radiation loss power from the main plasma to the total radiation loss power increased from 0.35 to 0.8. Since some of Ar ions were not fully ionized in this temperature range, the radiation loss power inside the ITB increased with Ar injection. With Ne injection, high confinement ( $H_{89P} > 2.4$ ,  $HH_{y2} > 1.6$ ) and high radiation loss ( $P_{\text{rad}}^{\text{total}}/P_{\text{net}} > 0.8$ ) were simultaneously obtained at high density ( $n_e > 0.7n_{\text{GW}}$ ). Then, the radiation loss power increased both in the edge of the main plasma and in the divertor plasma, and the internal transport barrier was strongly maintained. At an electron density of  $0.84n_{\text{GW}}$ , the divertor plasma became detached with  $H_{89P} = 1.8$  ( $HH_{y2} = 1.2$ ) and  $P_{\text{rad}}^{\text{total}}/P_{\text{net}} = 0.73$ . Under the conditions of divertor plasma detachment and an X-point MARFE, the ITB became more pronounced and the  $H_{89P}$  increased from 1.3 to 1.8.

#### References

- [1.6-1] Sakurai, S., Kubo, H., Takenaga, N., et al., J. Nucl. Mater., **290-293**, 1002 (2001).
- [1.6-2] Kubo, H., Sakurai, S., Asakura, N., et al., Nucl. Fusion, **41**, 227 (2001).
- [1.6-3] Ongena, J., Budny, R., Dumortier, P., et al., Phys. Plasmas, **8**, 2188 (2001).
- [1.6-4] Kubo, H., Sakurai, S., Asakura, N., et al., "RADIATION ENHANCEMENT AND IMPURITY BEHAVIOR IN JT-60U REVERSED SHEAR DISCHARGES", Proc. of 28th EPS Conf. on Cont. Fusion and Plasma Physics (Madeira), to be published.

## 2. Operation and Machine Improvements

### 2.1 Tokamak Machine

The operation and maintenance of JT-60 was carried out on schedule in this fiscal year. As for the gas feeder system, an air leakage was found on a piezoelectric valve (PEV) in the April experimental operation. The valve fortunately could be repaired quickly without replacement which needs a vent of the JT-60 vacuum vessel to the atmosphere. In the shutdown time from July to August, the vessel was vented for maintenance works inside the vessel and an anode electrode for glow discharge cleaning (GDC) was repaired since its voltage-holding degraded in the April operation. During the shutdown regular inspections of the high pressures gas facility of liquid N<sub>2</sub> tank were performed. In the next shutdown from January to February, the condition of the cooling pipes inside the toroidal magnetic field coils was inspected, in which small water leakages were found twice in 1992-1995, and no abnormality was recognized as in the previous year. The inspections were conducted in two ways. One is observation of the inside pipe with a fiber scope, and the other is checking of leakage tightness using highly pressurized air. The extension of the existing cracks and newly produced cracks on the inside wall of the cooling pipes have not been found.

As for the centrifugal pellet injector which delivers cube deuterium pellets of  $(2.1)^3$  mm<sup>3</sup> with velocities of 0.2~1.0 km/s at frequencies of 1~10 Hz [2.1-1], a new guide tube for injecting from the midplane in the high-field side (HFS) has been installed. As shown in Fig. I.2.1-1, the HFS midplane guide tube of 5 mm in inner diameter and ~5 m in length has been installed inside the vacuum vessel in addition to the former guide tube for injecting from the HFS top side equipped outside of the vessel. Since the conventional guide tube in the low-field side (LFS) midplane was removed, a line selector is used only to choose an injection direction between HFS midplane and HFS top side. The guide tube has two major bends on the way to the nozzle at P-10 port section. The curvature of the first bend is

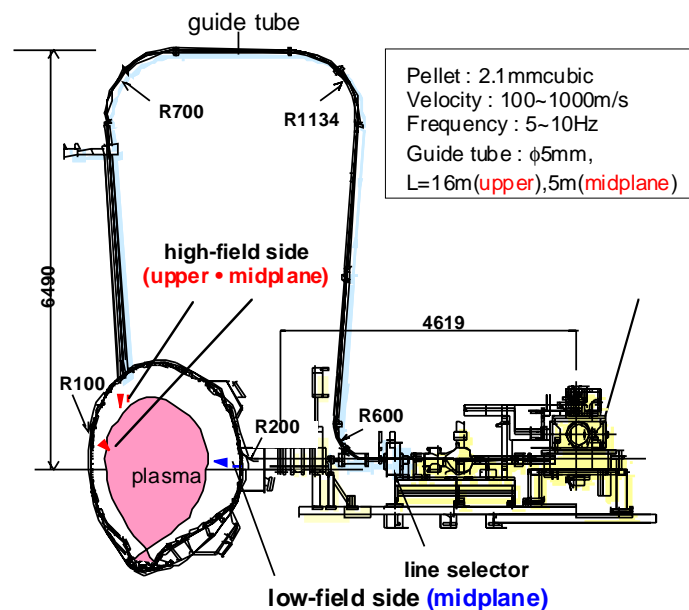


Fig. I.2.1-1 Schematic drawing of the pellet injection system for JT-60.

R=200mm at the outboard port and the second is R=100mm at the inboard nozzle point. An outer rotor motor for accelerating the pellets has also been modified so as to meet a lower velocity region less than 0.2 km/s that improves a fueling efficiency with HFS guide tubes. Consequently the minimal pellet velocity of 0.1km/s has been obtained. Pellet injection experiments from HFS midplane in the velocity range of 0.1-0.2km/s began in the end of March 2001 and the pellets have been successfully injected.

As regard the in-situ boronization system [2.1-2], boron coating discharges with deuterated decaboran ( $B_{10}D_{14}$ ) and He as a carrier gas, which was newly applied for the decaborane-based boronization in the previous fiscal year, have been operated successfully five times. Comparing to the former method using hydride decaboran ( $B_{10}H_{14}$ ), boron coating time was reduced to  $\sim 1/4$  due to the GDC stabilization without precise control of methane gas. The number of discharge conditioning shots after boronization were also reduced to  $\sim 1/10$  due to a reduction of hydrogen content inside a boron film as shown in Fig. I.2.1-2. It was made clear that the boronization time was actually shortened and efficiency of the first wall conditioning after the vessel vent was drastically improved by adoption of the deuterated decaboran.

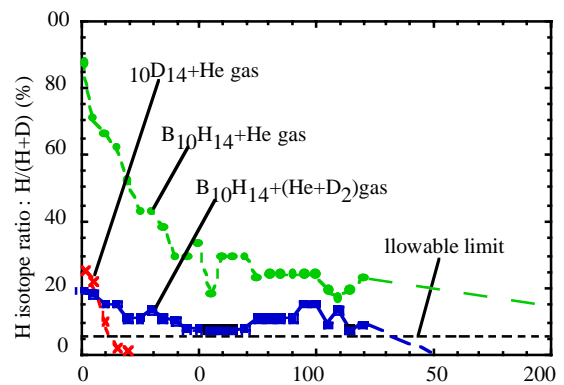


Fig. I.2.1-2 Reduction of the number of total conditioning shot after boronization.

In a plasma-surface interaction study, some preparations have been done to begin a tritium analysis for the carbon first wall tiles used in JT-60 DD experiments. An application for a licensing of the tritium use at Naka site in JAERI was filed in June 2000 to Science Technology Agency (STA) based on the law of radiation protection regulations and it was accepted in December. After the permission, the analysis room in the radioactive waste storage building was arranged for radiation exposure managements to undertake a tritium analysis, by installing a hood and setting up the tritium monitoring systems. Some systems for surface analysis such as a secondary ion mass spectrometry system (SIMS), a liquid scintillation system and a hood etc., were installed in the room. The arrangement has also been made for the cooperative research program between JAERI and universities using the JT-60 first wall, which will start at the beginning of next fiscal year.

**References**

- [2.1-1] K. Kizu, H. Hiratsuka, et al, JAERI-Tech 2001-022.
- [2.1-2] J. Yagyu, T.Arai, et al, Boronization using deuterated-decaborane in JT-60U , submitted to IEEE 19th Symp. on Fusion Engineering.

**2.2 Control system**

**2.2.1 Replacement of the discharge control computer system**

The discharge control system (DCS) with 20 years old mini-computers was fully reconstructed with UNIX workstations and VME-bus systems, and the replacement was completed in March 2001. The schematic configuration of the new DCS is shown in Fig. I.2.2-1. Functionally, the workstation communicates with the VME controllers of plant subsystems on the network by TCP/IP protocol, checks consistency of the plant status before executing the discharge sequence control and collects experimental data after plasma discharges. The VME-bus system performs the discharge sequence control by transferring commands to the workstations and receiving the status data from them. Since the CAMAC system has been used for some of the plant subsystem controllers and timing system, the old mini-computer system remains just as a CAMAC interface. Most of programs for these functions had been checked using a proto-type DCS system before the replacement. Owing to such careful procedures, the new DCS could start successfully without serious troubles. The data acquisition speed of the new system is about twice as faster as the old one.

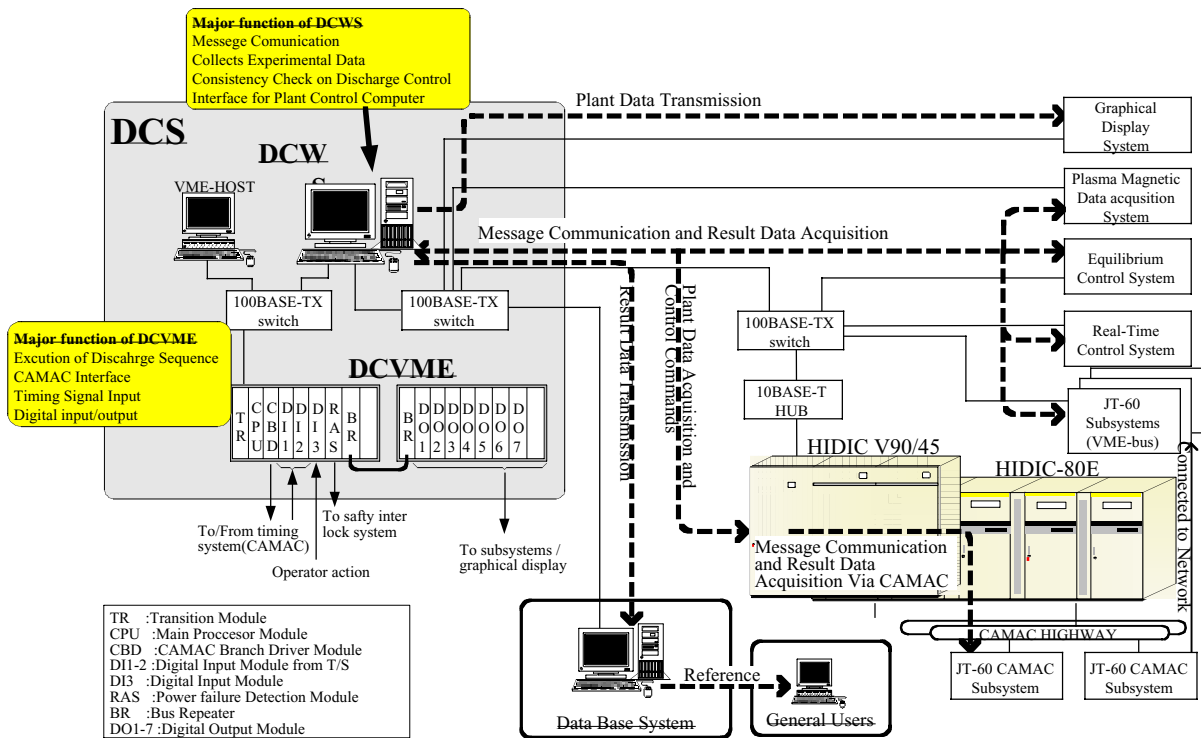


Fig. I. 2.2-1 Schematic structure of the new discharge control system.

### 2.2.2 A real-time plasma shape reconstruction system for JT-60 plasma feedback control

A new real-time plasma shape reconstruction system, which had been developed on the basis of Cauchy-condition surface method[2.2-1], was successfully applied to the real-time plasma equilibrium control for the first time in the world. The total calculation time of major equilibrium parameters, vertical position, horizontal position, x-point height, triangularity, etc., was designed to be within 500 $\mu$ sec. The actual calculation time for plasma vertical position was approximately 240  $\mu$ sec using one processor dedicated only to this calculation. However, the calculation times for the rest parameters, which were calculated using another processor, was about 800  $\mu$ sec in total. Therefore, the control cycle for the plasma vertical position that requires fast control was set at 250  $\mu$ sec and those for the rest parameters were set at 1 ms. Fig.I.1.2.2 shows the experimental results of the real-time plasma control with this system.

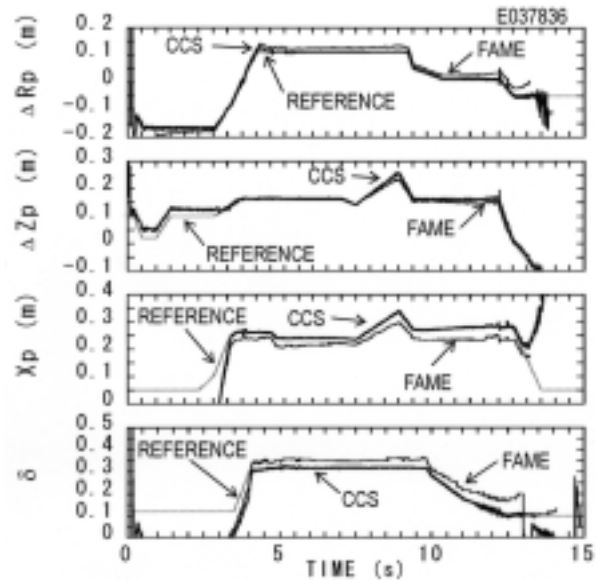


Fig. I.2.2-2 Experimental results of the real-time control of major equilibrium parameters. CCS stands for the control results with the real-time plasma reproduction system, FAME stands for the calculation results using SELENE code.

### 2.2.3 Development of A Large Input Voltage Range and Low Drift Digital Integrator

Digital integrators with a voltage-frequency converter (VFC) and an up-down counter (UDC) have been used for magnetic measurements in JT-60. Functionally, the VFC generates the number of pulses in proportion to the time integration of the input voltage between sampling cycles, and the UDC counts it. By summing up the counts, the time-integrated signal is obtained. Very low drift performance (30mVs/3000sec in average) has been realized for this integrator[2.2-2]. However, after disruptions, it often outputs an integration result with a large shift from the correct one. This is because the input voltages at disruptions are far beyond the upper and lower limits of voltage-frequency conversion.

To solve this problem, a digital integrator constructed with three internal integrators in parallel and a digital signal processor (DSP) has been developed. Each internal integrator has a pre-amplifier with a fixed gain of 0.01, 1 or 10 ( 1 kV, 10 V or 1 V in voltage range). The DSP selects a count of the internal integrator with the highest gain at every cycle (10 kHz) when the

input voltage is within the limits, but switches it to that with a lower gain when the voltage beyond the limits is input. Then, the DSP sums up these counts at every cycle to yield a time-integrated signal. Performance tests of the switching action and integration showed satisfactory results. On-site test under JT-60 experimental conditions is now being carried out to verify the performance.

#### References

- [2.2-1] Kurihara, K., et al., Fusion Engineering and Design 51-52 (2000) 1049-1057.  
[2.2-2] Kurihara, K. and Kawamata, Y., Proc. of 17<sup>th</sup> Symp. on Fusion Engineering, 799-802 (1998).

### 2.3 Power Supply System

#### 2.3.1 Modification of Direct Digital Control (DDC) Algorithm for Poloidal Field Coil Power Supply

Each coil current of poloidal field coils, F-, V-, H-, Q- and M-coils, frequently turned to increase during the coil current ramp-down phase, causing failures of thyristor bank currents and interruption of the gate block(GB) sequence. This is because the coil current was suddenly induced in each coil by mutual inductions from other coils when each power supply shifted to the by-pass pair (Bpp) mode where the thyristor banks are turned on. In particular, the F-, V- and Q-coil power supplies are strongly affected since the mutual inductance between the coils is large.

The DDC algorithm for the GB-sequence of those power supplies was modified to solve the problem. In the previous GB-sequence, the DDC system output a constant thyristor firing angle of 120 degrees to give negative voltage till the current decreases to a preset level, and shifted to the Bpp-mode. In the new GB-sequence, the DDC system outputs negative voltage in order to decrease the coil current linearly to zero in 2 seconds, then outputs a constant thyristor firing angle of 120 degrees for 0.5 seconds, finally shifts to the Bpp-mode and stops the power supply by GB at 2.5 second. After the modification, the coil currents and circuit currents have been controlled to decrease to zero as expected and no failure has occurred due to the mutual inductions.

#### 2.3.2 Operation of Poloidal Field Coil Power Supply for the Tests of the ITER Super-conducting Central Solenoid Model Coil

As one of the Engineering Design Activities (EDA) of ITER, the pulsed operation test of the super-conducting central solenoid (CS) model coil was carried out using the poloidal field coil power supply for JT-60. The CS model coil with no resistance and large inductance of 0.6 H may resonate with the voltage ripple of 1800 —2000 Hz in the power supply, which may cause damage in the coil layers. Therefore high frequency characteristics of the CS model coil and the loop voltage in each of 18 coil layers were measured before the test. The measured impedance of

the coil showed a sharp peak at about 500 Hz, indicating the existence of resonance frequency. However, at the ripple frequency of the power supply, the voltage in each coil layer was only about three or four times as large as the voltage equally distributed to each coil layer. The estimated voltage was about 150 —280 V for the ripple voltage of 50 - 70 V, which was sufficiently smaller than the limit of the allowable voltage for the CS model coil [2.3-1].

To simulate the pulse operation of the CS model coil, a transfer function and an equivalent circuit of the coil were estimated using its frequency characteristics. In the simulation, feedback gains for the F-coil and V-coil power supplies were adjusted so as to stably control the coil current.

The first pulsed operation test in May 2000 was carefully started with a moderate feedback gain not to apply an unexpected high voltage to the coil. In the first operation, the current settling time for the flat-top was found to be too slow, about 2 s, for lack of the feedback gain. On the other hand, the coil current was not zeroed after the GB-sequence. A residual coil current of about 0.5 kA decreased very slowly to zero with the time constant of the super-conducting coil circuit. This was because the coil current decreased with a delay against the reference for lack of the feedback gain, and did not decrease to zero before the end of the GB-sequence. Therefore the feedback gain was increased to twice, and

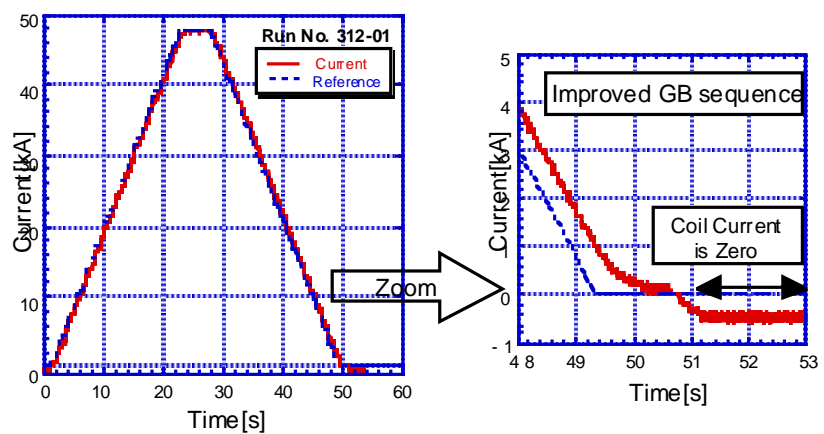


Fig.I.2.3-1. Pulse Operation test of CS Model Coil.

the following provisional measures were taken. The reference of the coil current in the final stage of current ramp-down phase was set at a negative value to surely decrease the coil current to zero before the GB-sequence ended. Furthermore, before the second pulse operation test planned in July 2001, as permanent measures, the GB-sequence algorithm was changed to give negative voltage to the coil for 1 - 2 sec to ensure the decrease in coil current to below zero. Thus the second pulse operation test was successfully carried out. The test up to a coil current of 46 kA, which corresponded to the magnetic field strength of 13 T and a magnetic stored energy of 640MJ, was performed as planned. The result is shown in Fig.I.2.3-1.

#### References

[2.3-1] Shimada K., Miura Y. M., Terakado T., et al., Characteristics of the high frequency impedance of a large super-conducting coil and its effect on the coil excitation, in Proc. of 8<sup>th</sup> IEEJ Ibaraki, Hitachi, p.141-142 (2000) (in Japanese).

## 2.4 Neutral Beam Injection System

### 2.4.1 Development of Negative-Ion Based Neutral Beam (N-NB) Injection System

In this fiscal year, the 500keV negative-ion based neutral beam (N-NB) injection system for JT-60U has injected a neutral beam power of 5.2 MW at 380keV for 2~2.5 sec and 5.1 MW at 410keV, which are all somewhat less than what was planned [2.4-1]. The neutral beam power is limited by the excessive heating of the accelerator grids of ion sources and a beam limiter in the beam line, which would result from a divergent energetic beam [2.4-2]. The divergent beam comes from mis-matching of local beam perveance due to the strong spatial non-uniformity of the ion source plasma that yields to local variations in the current density extracted from different areas on the plasma grid. So we have implemented several techniques to correct the non-uniformity in these sources.

The most successful technique has involved installing resistors whose value can be changed independently in the circuit for each of the eight filament groups, and, in addition, masking about 19 % of the grid area to avoid extracting divergent beamlets from remaining areas of lower plasma density [2.4-3]. Figure I.2.4-1 shows the ion saturation current profiles with the arc series resistor of 150 mΩ and 100 mΩ. The ion saturation current was measured with Langmuir probes located at the left and right side of

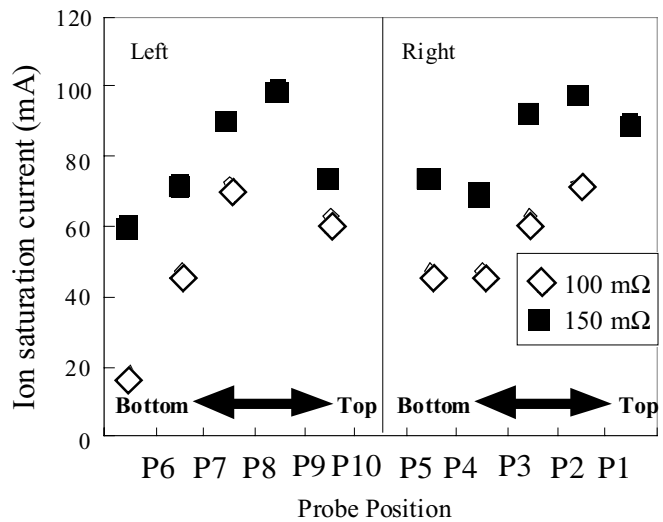


Fig.I.2.4-1 Effect of arc series resistors of 100 mΩ and 150 mΩ.

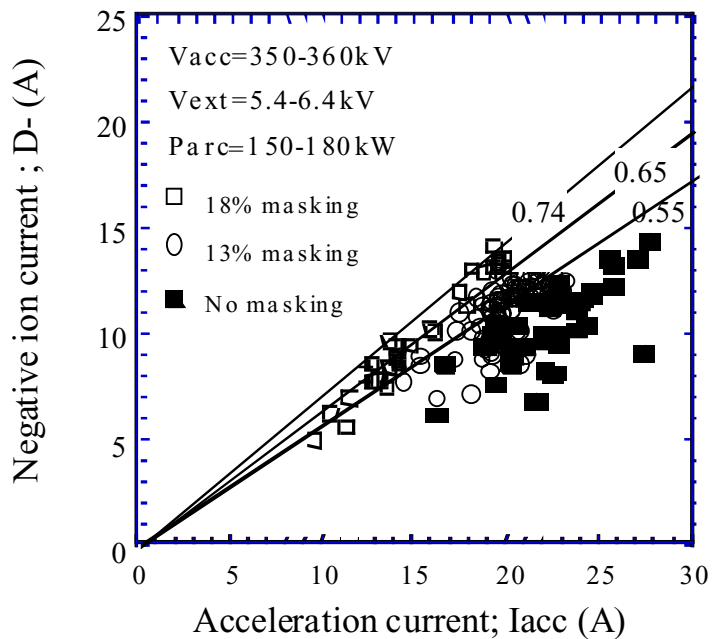


Fig.I.2.4-2 Masking effect on acceleration efficiency.

plasma grids. The non-uniformity has improved largely with higher arc series resistors. The masking was done on top and bottom of the plasma grid with thin molybdenum plates. Owing to these countermeasures, the acceleration efficiency of the deuterium negative ion beams in the accelerator has improved by more than 30%, as shown in Fig.I.2.4-2. These results show that the masking is very effective in improving the beam performance, though the accelerated drain current decreased a little bit with increasing the masking area.

#### 2.4.2 Stable Operation of Positive-Ion Based Neutral Beam Injection System

Concerning the positive-ion based neutral beam (NB) injection system in this fiscal year, the computer control system for the beam operation has been altered from a mini-computer to a workstation system in order to match a great variety of beam injection parameters [2.4-4]. In the modification, the CAMAC system for the data acquisition has been exchanged with a VME bus-system, and the load of the workstation has been mitigated by taking a part of function of the workstation.

The NB injection system has also injected stably a deuterium beam power of 20-25 MW at around 90 keV for 8-9 sec with 11 beam lines. The cryopumps of the three beam lines also have been used as the pumping system for JT-60 divertor. The cryopump can effectively evacuate helium gas by the argon gas trapping method.

#### References

- [2.4-1] Kuriyama, M., Akino, N., Ebisawa, N., et al., "Study of Increasing the Beam Power on the Negative Ion Based Neutral Beam Injector for JT-60", to be published in Proc. of 21th Symposium on Fusion Technology, Spain, (2000).
- [2.4-2] Grisham, L.R., Kuriyama, M., Kawai, M., et al., in Proc. of 18th IAEA Fusion Energy Conference, Sorrent, Italy, (2000).
- [2.4-3] Umeda, N., Akino, N., Ebisawa, N., et al., Fusion Technology 39(2-Part2) 1135 (2001).
- [2.4-4] Oohara, H., Akino, N., Ebisawa, N., et al., Fusion Technology 39(2-Part2) 1140 (2001).

## 2.5 Radio-Frequency Heating System

### 2.5.1 Improvement of the RF Control System

A 15-year-old Radio-Frequency (RF) control system for Ion Cyclotron (IC) and Lower Hybrid (LH) heating systems using a mini-computer and CAMAC system was replaced by a new system, featuring industrial computers which are a sort of personal computer improved in tolerance for electromagnetic noise, dust and mechanical shock, workstations and VME modulus shown in Fig. I.2.5-1. We expect that frequent troubles due to the decrepit control system will be reduced dramatically. On the new control system, RF power and phase, controlled with the RF mini-computer on aging mode so far, have been managed with the JT-60 Control System on experiment mode. In the aging mode, RF operators make the waveforms of the power and

phase including its timing. Contrary in the experiment mode, operators of an experiment team will make the waveforms as well as other parameters for plasma control. The latter mode has an advantage in unification of the parameter control in JT-60U, especially in the case that many experiments are planned in one shot. In the new control system, though the waveform is not sent to the RF system before shot, the power level and phase orders are sent every 10 ms. To realize this scheme having a simple interface between the RF control system and JT-60 control system, with entirely safety for the RF hard wares, a real time limitation controller has been developed. The controller checks the power level order from the JT-60 control system every 10 ms, and modifies its level automatically using the parameters of the maximum power, pulse width and rate of power increment, set by the RF operator according to the conditioned situation of the RF hardware such as antenna breakdown voltage at that time.

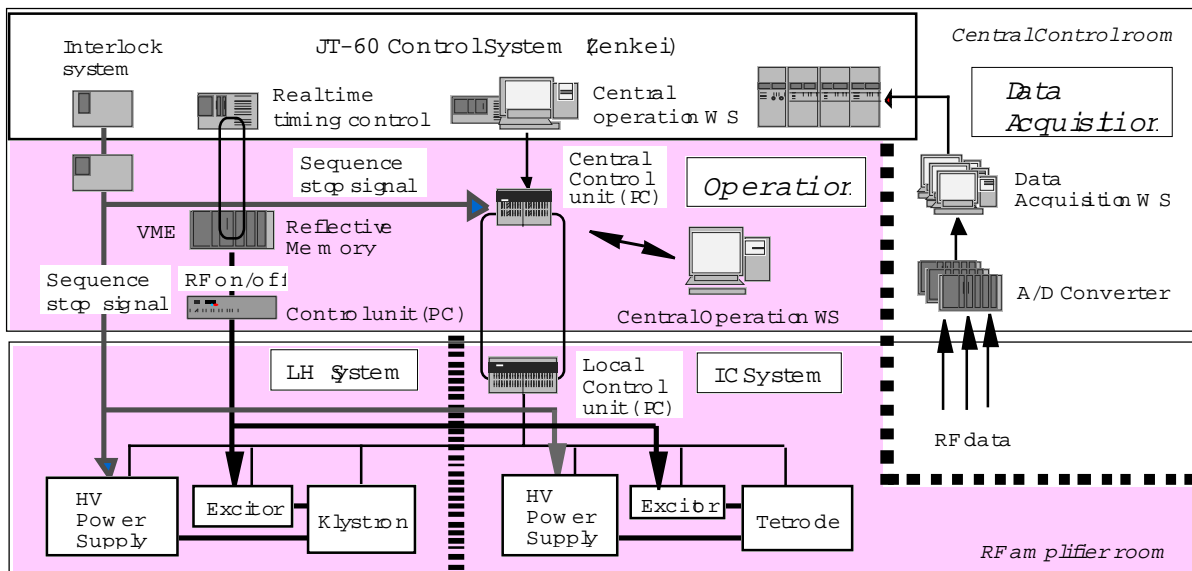


Fig. I.2.5-1 New control system for the IC and LH systems has been completed featuring industrial computers (improved personal computers; PC), workstations (WS) and VME system to replace the 15-year-old RF control system using a mini-computer and CAMAC system suffering from frequent troubles.

### 2.5.2 Operation of the IC and LH Systems

The IC system was operated at a power level of around 3 MW for the experiments such as analysis of high energetic ions with an innovative diamond detector, Alfvén-eigen mode

investigation and wall conditioning with RF discharge plasmas. Preliminary trials for antenna coupling improvement were done using CH<sub>4</sub> gas-puff expecting increase in scrape-off-layer density without reduction in breakdown voltage of the antenna.

The LH system was successfully operated for the following experiments. 1) Phase control, which is essential for LH system operation, was checked by comparison between measured hard X-ray profiles and predicted ones for typical phase differences. 2) LH power was injected to sustain the negative shear plasma configuration with high  $\beta_N$ . Here, CH<sub>4</sub> gas was puffed to improve LH coupling and to suppress RF-breakdown. The distance between plasma and wall was controlled precisely by Cauchy-condition surface method [2.5-1] to keep good coupling. 3) Plasma current profile control was performed by combination of LH and EC injection.

### 2.5.3 Upgrade of EC system featuring a new antenna

The Electron Cyclotron (EC) program was started to study the local heating and current drive in JT-60U in 1999 [2.5-2]. The frequency of 110 GHz was adopted to couple the fundamental O-mode from the low field side with an oblique toroidal injection angle for the current drive, which is the same scheme for EC current drive (ECCD) in ITER. A schematic view of the EC system for JT-60 is shown in Fig. I.2.5-2. In 1999, the first one unit was completed and successfully generated RF power up to 1 MW. In 2000, the EC system was upgraded adding two units to generate the total RF power of 3 MW [2.5-3].

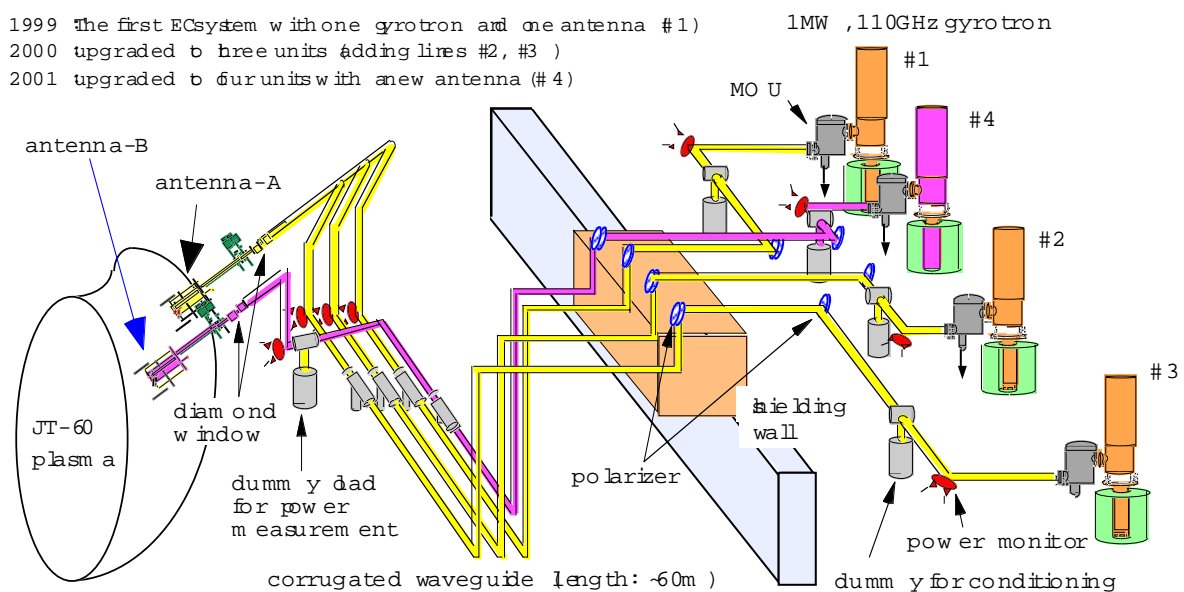


Fig. I.2.5-2 Schematic view of the 110 GHz - 4 MW EC system in JT-60U.

The RF power is connected to the antenna-A, which focuses the deposition of three EC beams within ~15 cm in plasmas. The antenna also controls the EC beam in the poloidal direction with the steerable mirror during a plasma discharge. A strongly peaked  $T_e$  profile with  $T_{e0} \sim 15$  keV was obtained by on-axis EC heating alone. Also, the local EC heating clearly resulted in the different properties of the thermal transport with and without the internal transport barrier. The local change in the current profile was directly confirmed by the motional Stark effect diagnostics [2.5-4]. Therefore, the system showed its high availability for the local profile control at an injected power level of 1.5 - 1.6 MW for 3 sec. The available power was limited by a parasitic oscillation of the gyrotrons, which heated the cathode and then shifted the gyrotron operational condition during a pulse.

In 2000, the fourth RF unit was newly designed and constructed to study EC heating/ECCD at injection power more than 2 MW. This unit has a new antenna (antenna-B), which can control the EC beam in the toroidal and poloidal directions with two steerable mirrors [2.5-5]. A new gyrotron was also redesigned so as to suppress the parasitic oscillation by installing an RF absorber in its beam tunnel. The design of the antenna-B featuring a new function of two-dimensional EC beam scan is challenging because it must be placed at a small, shallow port-box of the vacuum vessel with the depth of ~20cm. We adopt an antenna consisting of two main parts in order to make it compact. One is a steerable flat mirror system to control the EC beam in the poloidal direction, fixed in the port-box, and the other is a rotatable focusing mirror system incorporated with the wave-guide to realize toroidal beam scan, supported from the outside of the vacuum vessel. It rotates on the waveguide axis with  $\sim 20^\circ$ . This new system will start in April 2001.

#### References

- [2.5-1] Kurihara, K., et al., Fusion Eng. and Design, **51-52** 1049 (2000).
- [2.5-2] Ikeda, Y., et al., Fusion Eng. and Design, **53** 351 (2001).
- [2.5-3] Kajiwara, K., et al., J. Plasma Fusion Res. SERIES, Vol.3 372 (2000).
- [2.5-4] Ikeda, Y., et al., Fusion Energy 2000(CD-ROM,IAEA, Vienna),Exp 4/03 (2001).
- [2.5-5] Moriyama, S., et al., Upgrade of ECH system in JT-60U featuring an antenna for toroidal/poloidal beam scan, Proc, 14<sup>th</sup> Top. Conf. on Radio Frequency Power in Plasmas, Oxnard, USA, 7 to 9 May, 2001.

## 2.6 Design Study of the JT-60 Modification Utilizing Superconducting Coils

The modification of JT-60 utilizing superconducting coils (SC) is planned as a full superconductor tokamak (JT-60SC) as shown in Fig.I.2.6-1. Typical machine parameters proposed are as follows: the plasma current  $I_p = 4$  MA, the toroidal magnetic field  $B_t = 3.8$  T, the major radius  $R_p = 2.8$  m and the minor radius  $a_p = 0.85$  m with elongation at 95% flux  $\kappa_{95} \sim 1.7$  and triangularity  $\delta_{95} \sim 0.35$ . The mission of the JT-60SC program is to establish scientific and technological bases for an advanced operation in an economically attractive DEMO reactor and

ITER. To accomplish this mission, the major objectives for researches have been established (1) to control high beta plasmas, (2) to achieve steady-state operation using non-inductive current drive with high bootstrap current fraction, and (3) to control and remove heat flux and particles in the divertor region.

Conceptual design for the JT-60SC has been studied as follows (Fig.I.2.6-2):

(i) As a superconducting cable for toroidal field (TF) coils (18 unit coils), feasibility of Nb<sub>3</sub>Al or Nb<sub>3</sub>Sn conductor with a high copper ratio of 4 has been investigated. The cable-in-conduit conductor is optimized with the operation current  $I_{op} = 19.4$  kA at the maximum magnetic field in the windings  $B_{max} = 7.4$  T and enables a compact magnet design with realizing high current density. The central solenoid (CS) coil, which consists of 4 modules and is made of Nb<sub>3</sub>Sn cable-in-conduit conductor with  $I_{op} = 20$  kA at  $B_{max} = 7.4$  T, is designed with capability of providing a flux swing of 40 V-sec for  $I_p = 4$  MA and a pulse length of 100 s.

(ii) The vacuum vessel made of stainless steel with low Co contamination is designed to be a double-walled structure located within the bore of the TF coils. The double walls are filled with water for cooling and neutron shielding. And high Mn steel plates are installed for  $\gamma$ -ray shielding.

(iii) The TF ripple reduction with low-activation ferritic steel such as F82H is required in JT-60SC. In order to reduce the TF ripple as low as 0.4%, ferritic steel plates are mounted inside the vacuum vessel of JT-60SC. The optimization of ferritic steel plates mounting is a key issue for wide range of  $B_t = 2.0 - 3.8$  T to obtain a high beta plasma of  $\beta_N \gtrsim 3$ .

(iv) The in-vessel components consist of divertor, inboard first wall, stabilizing plates (passive stabilizer for vertical displacement events (VDE) and the stabilization of ideal MHD modes), cryopumps, the resistive wall modes (RWM) control coils and vertical/horizontal position control coils. The engineering task for divertor design is to demonstrate steady-state

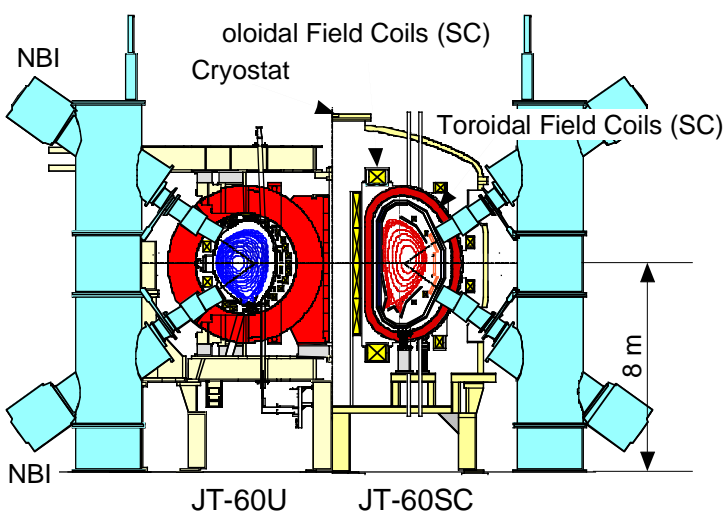


Fig.I.2.6-1 Comparison of JT-60U and JT-60SC.

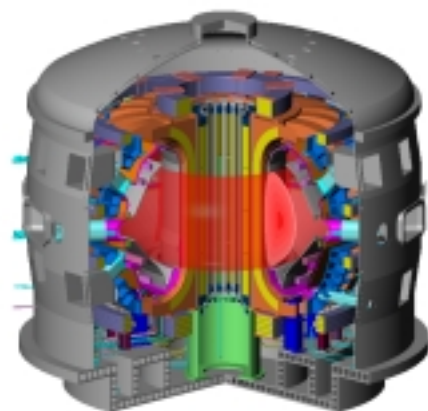


Fig.I.2.6-2 Schematic drawing of JT-60SC.

heat removal at high heat flux of 10 —15 MW/m<sup>2</sup> by metal armors under the high performance of a break-even class operation (planned total heating power of 44 MW/10 s and 15 MW/100 s including N-NB and EC wave).

(v) The effects of magnetic error field on locked mode disruptions and the neoclassical tearing mode (NTM) with installation of stabilizing plates, pedestal plates of inboard first wall and ripple reduction plates made of F82H steel were evaluated.

## II. JFT-2M PROGRAM

On JFT-2M, advanced and basic research for the development of high performance tokamak plasma is being promoted, making use of the flexibility of a medium-sized device and the research cooperation with universities and other institutions. In this fiscal year, we performed the preliminary test on compatibility of ferritic steel plates (FPs) inside the vacuum vessel (covering ~20% of the vacuum vessel wall) with plasma, as the second stage of AMTEX (Advanced Material Tokamak Experiment). No adverse effects on plasmas, including H-mode production, were observed. Boronization was introduced for the first time in JFT-2M after installation of inside FPs in order to investigate compatibility of FPs with higher performance plasmas. High- $n$  discharges ( $n$  up to 2.8) were obtained with inside FPs and boronization. As for the high performance experiments, the H-mode research with the heavy ion beam probe (HIBP) was continued, clarifying formation of negative electric field at the H-mode transition triggered by ECH. The MSE polarimeter system, which is capable of simultaneous measurement of a radial electric field, has been newly developed for high performance experiments. In RF experiments, fast wave electric field profile was directly measured for the first time using the beat wave and HIBP. Compact toroid (CT) injection experiments were continued to clarify the dynamics of fuelling by CT injection.

### 1. Advanced Material Tokamak Experiment (AMTEX) Program

#### 1.1 Pre-testing on Compatibility with Plasma

In the second and third stages of the AMTEX, the low activation ferritic steel (F82H) plates (FPs) are installed inside the vacuum vessel to simulate a blanket wall of a demo-reactor. In order to investigate the problems preliminarily, 20% of the vacuum vessel surface area was covered with the FPs in the 2nd stage. The position of FPs and its effect on plasma are schematically shown in Fig.II.1.1-1. The distance between the plasma and the FPs became much smaller, compared to the first stage, and thus, enhancement of the MHD instability might be caused. The plasma control can be affected because a part of the magnetic probes and flux loops are affected due to the magnetization of FPs and also FPs have an effect to draw a plasma column. In addition, impurity release from the FP might be a problem during the plasma discharge with higher heating power, though it was predicted from the experiment in the test chamber [1.1-1] and the HT-2 tokamak [1.1-2, 3] that it would not be so severe at least for the vacuum properties and the ohmic plasmas. The behavior was

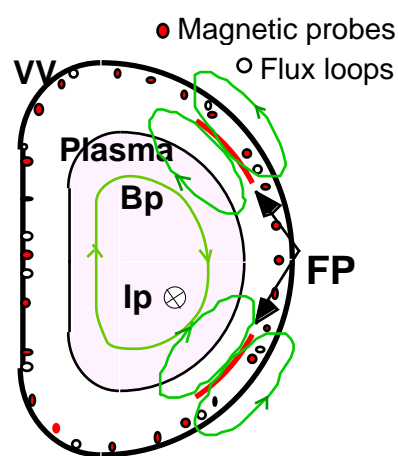


Fig II.1.1-1 Schematic cross-sectional view of the vacuum vessel (VV), FP, magnetic sensors and magnetic fields.

checked prior to the 3rd stage, where high performance plasma would be required [1.1-4]. A boronization system was installed to reduce impurity desorption, and to obtain high performance plasma with reduced impurities [1.1-5]. Checking the effect of the boron coating was also important in the 2nd stage.

Before the boronization, experiments were carried out to check the effects of bare FPs on the plasma performance. The impurity desorption from the ferritic steel was not remarkable even when the neutral beam (800kW) was injected. The plasma was produced by the same procedure as before, although a relative shift of ~1cm was observed in the plasma position compared to the calculated position without FPs, mainly due to the effect of FPs to the magnetic sensors [1.1-5]. For the locked mode disruption, operational region became rather wider [1.1-6]. Thus it is concluded that effects of the ferritic steel is not so large in this experimental condition.

After the series of the experiments, the boronization was carried out with DC glow discharge in the mixture gas of 1% B(CH<sub>3</sub>)<sub>3</sub> (tri-methyl-boron) + 99% He. After the boronization, the total radiation loss power reduced to 1/3, and oxygen ion line intensities measured by a visible spectroscopy also reduced to 1/20. The carbon line intensity also decreased slightly though the main components of the deposited film is C (the composition ratio; B/C = 0.18). The normalized beta value up to 2.8, which is the highest value obtained in JFT-2M, is achieved with FPs after the boronization, indicating that magnetic effects of FPs do not disturb high  $n_N$  discharge at least up to  $n_N$  2.8. Thus encouraging results were obtained in the second stage of AMTEX.

#### References

- [1.1-1] Odaka, K., Sato, O., Ohtsuka, M., et al., J. Plasma Fusion Res., **73**, 1001 (1997) (in Japanese).
- [1.1-2] Nakayama, T., Abe, M., Tadokoro, T., et al., J. Nucl. Matter., **271&272**, 491 (1999).
- [1.1-3] Abe, M., Nakayama, T., et al., J. Plasma Fusion Res., **73**, 1290 (1997).
- [1.1-4] Kimura, H., Sato, M., Kawashima, H., et al., "Progress of Advanced Material Tokamak Experiment (AMTEX) Program on JFT-2M", to be published in Fusion Eng. Design.
- [1.1-5] Tsuzuki, K., et al., "Testing for Compatibility of Reduced Activation Ferritic Steel with Plasma on JFT-2M -Partial Coverage of the Vacuum Vessel with Ferritic Steel -", submitted to J. Plasma Fusion Res., (in Japanese).
- [1.1-6] Isei, N., et.al., Fusion Technol., **39**, 1101 (2001).

## 1.2 Study of Ripple Loss of Fast Ions

In the first stage of the AMTEX program, reduction of the toroidal field ripple was examined by insertion of ferritic steel plates (FPs) between the toroidal field coils and the vacuum vessel (outside FPs). It was demonstrated that the FP insertion reduced the toroidal field ripple and the losses of fast ions produced by tangential co-NB injection. By optimizing the FP thickness, such that the fundamental mode ripple was minimized to be 0.07% at the shoulder part, the ripple-trapped loss was reduced to be almost negligible (Fig.II.1.2-1). It was found that the reduction of the fundamental mode ripple and the ripple banana diffusion coefficient at the shoulder part was the most effective to reduce the ripple ion losses [1.2-1]. The ripple loss study was continued in the second stage of AMTEX, where both outside and inside FPs were present (the latter has no effect on the ripple). Effectiveness of the ripple reduction mentioned

above was compared with other injection angle cases, such as tangential ctr- or perpendicular- NB. Experimental results showed that the fast ion losses were effectively reduced due to the ripple reduction at the shoulder part by FPs, irrespective of NB injection angle [1.2-2].

**References**

- [1.2-1] Kawashima, H. and JFT-2M Group, Nucl. Fusion, **41**, 257 (2001).
- [1.2-2] Kawashima, H., Tsuzuki, K., Isei, N., et al., Proc. 28<sup>th</sup> Eur. Conf. On Controlled Fusion and Plasma Physics (Madeira EPS 2001) P4.004.

**1.3 Preparation for Testing on Compatibility with Plasma [1.1-4]**

A conceptual drawing of the cross-section of the vacuum vessel in the third stage, where inside wall of the vacuum vessel is fully covered with the ferritic steel wall, is shown in Fig.II.1.3-1. The ferritic steel wall is divided into a number of FPs of 32 pieces and 16 pieces in the outboard and inboard sides, respectively, in the toroidal direction (16: the number of TFCs) and 7 pieces in the poloidal direction. The thickness of FPs is in the range of 6-10.5 mm, depending on the location. Each FP is fixed to the vacuum vessel with bolts. An example of dynamical analyses of the electromagnetic forces on FPs during disruption is given in Ref. [1.3-1]. In order to reduce the toroidal field ripple ideally, the optimization of the poloidal distribution of the FP thickness and the periodicity in the toroidal direction are required [1.3-2]. The layout of FPs is determined carefully considering these requirements. We aim at further reduction of the ripple magnitude in the third stage (say, both the fundamental mode ripple  $\delta_{16}$  and the second harmonic ripple  $\delta_{32}$  are less than 0.2% at  $B_t = 1.3T$  over a wide range in the poloidal direction on the outboard side), compared to the one in the first stage, where toroidal periodicity of FPs is not so rigorously kept because of spatial limitation. Magnetic sensors, such as magnetic probes and saddle coils etc., will be mainly installed on the plasma side of FPs to minimize shielding effects of ferritic steel on the plasma control. Graphite tiles will

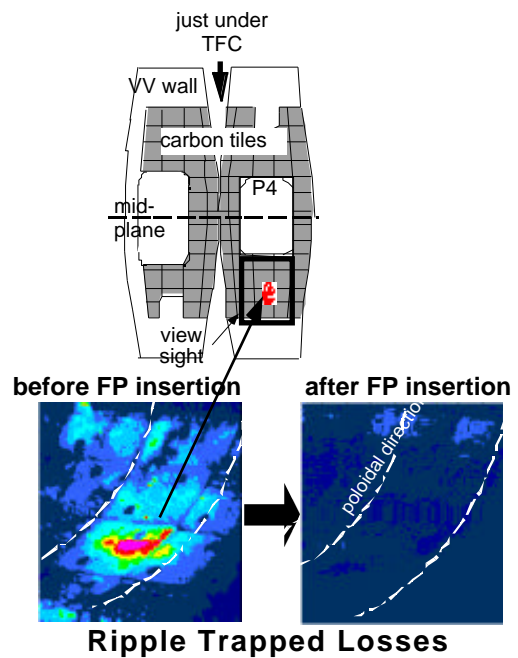


Fig.II.1.2-1 The profiles of the incremental wall temperature  $T_s$  due to the ripple-trapped losses before and after FP insertion, respectively. The highest  $T_s$  before FP insertion reaches to 70 °C.

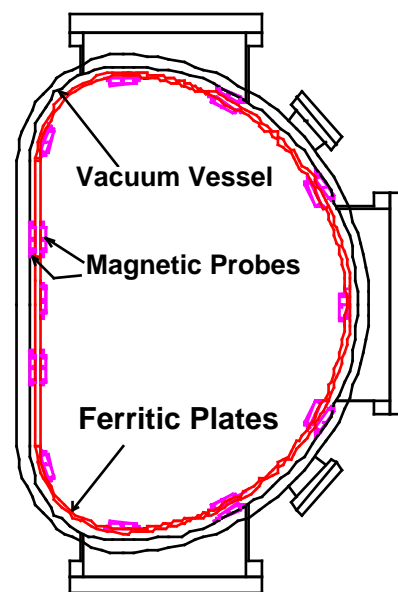


Fig.II.1.3-1 A conceptual drawing of the cross-section of the vacuum vessel in the 3rd stage of AMTEX.

be installed on FPs (continuously on the inboard side and partially on the outboard side and near the divertor legs) for the protection of FPs and magnetic sensors from high heat flux. We will perform detailed measurements of the magnetic field inside the vacuum vessel using Hall elements before and after the installation of FPs, to estimate ripple magnitudes and error fields. The relative position of the vacuum vessel to the center of the toroidal field coils is to be measured, from which we can also estimate error fields due to FPs.

#### References

- [1.3-1] Urata, K., et al., "Dynamical analyses of electromagnetic force on ferritic board for AMTEX on JFT-2M", to be published in Fusion Eng. Design.
- [1.3-2] Nakayama, T., et al., "Development of a decision method for optimum ferromagnetic board arrangements to reduce toroidal magnetic field ripple", to be published in Jpn. J. App. Phys.

## 2. High Performance Experiments

### 2.1 Study of High Confinement Modes

#### 2.1.1 ECH H-mode

Negative edge electric field ( $\sim 100$  V/cm) around the edge transport barrier, or pedestal, developed during the H-mode by the peripheral electron cyclotron heating (ECH) on JFT-2M tokamak. Edge plasma potential was measured by Thallium heavy ion beam probe (HIBP) method [2.1-1]. The edge potential decreased at the H-mode transition, whereas the potential increased during the L-mode. The H-mode was triggered by a heat pulse generated by the sawtooth activity. The edge potential/density fluctuation in the frequency range of 10~100kHz was gradually suppressed in accordance with the gradual potential decrease at the H-mode transition in spite that the low frequency fluctuation ( $< 10$  kHz) did not change during the transition. Thus the decrease of the high frequency fluctuation seems to be related with the confinement improvement by the H-mode. Further the precursor fluctuation of the edge localized mode (ELM) was clearly found in the potential fluctuation signal. The fluctuation frequency went down from  $\sim 150$  kHz to less than 100 kHz just before the ELM. The potential increases during the ELMs, as during the L-mode. We found that the behavior of the edge potential in the H-mode with ECH is not much different from the H-mode by the neutral beam heating, and that the heat pulse by the sawtooth rather seems to play a larger role for the transition to the H-mode.

#### 2.1.2 Development of MSE Diagnostics [2.1-2]

A multi-channel motional Stark effect (MSE) polarimeter system, which is capable of simultaneous measurement of a radial electric field, has been developed on JFT-2M. The diagnostic can measure the polarization angle at 18 radial locations, which cover a region between just inside the magnetic axis and the outboard edge of the plasma. By viewing two neutral beam lines (one is co-parallel to the plasma current and the other is counter-parallel) simultaneously and near tangentially to the toroidal magnetic field from only one spectroscopic instrument, it provides

the best sensitivity in radial electric field measurements with good spatial resolution. The magnetic field pitch angle is also measured with the smallest uncertainty. Preliminary data for L-mode plasma has been obtained. It is found that the statistical uncertainty of the magnetic field pitch angle and the radial electric field are about  $0.1^\circ$  and 4 kV/m, respectively, with a time resolution of 10 ms.

#### References

- [2.1-1] Ido, T. et al., Plasma Phys. Control. Fusion, **42**, A309 (2000).  
 [2.1-2] Kamiya, K., Kimura, H., et al., "The Multichannel Motional Stark Effect Diagnostis Discriminating Radial Electric Field in the JFT-2M Tokamak", to be published in Rev. Sci. Instrum., (2001).

### 2.2 Radio Frequency Experiments [2.2-1]

It is important to understand the propagation and absorption of the fast waves in plasma for the basic study of the fast wave current drive, which is one of the promising current drive methods for a tokamak fusion reactor. The spatial pattern of the fast wave electromagnetic field in plasma had not been measured directly because of its difficulty, although detailed calculation had been possible with full wave codes. In JFT-2M, the direct measurement was performed for the first time in collaboration with

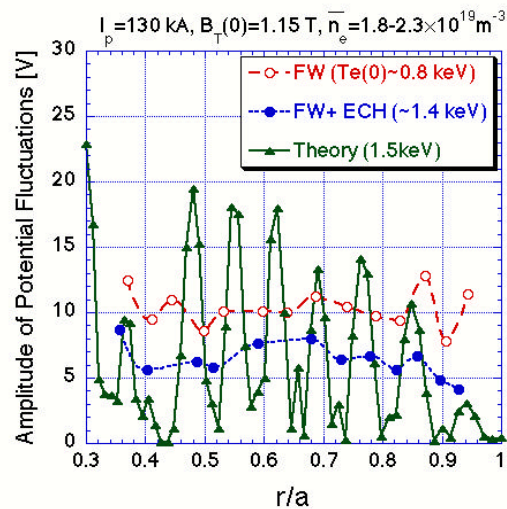


Fig.II.2.2-1 Radial profiles of potential fluctuations. Amplitude of potential fluctuations was reduced with ECH because of improvement in the fast wave absorption due to increase in the electron temperature.

Ibaraki University and the National Institute for Fusion Science. The basic principle is such that the ponderomotive pseudo-potential of a beat wave between the two fast waves ( $\omega_1$  and  $\omega_2$ ) is excited and the potential fluctuation pattern (frequency;  $|\omega_1 - \omega_2|$ ) is measured with HIBP. The experiments were done with launching fast waves at two frequencies (200 MHz and 199.91 MHz) from the comb-line antenna [2.2-2] with and without ECH. The potential fluctuation profiles at the beat wave frequency (90 kHz) were measured with HIBP. The experimental results are consistent with computational results by the full wave code (TASK/WM) as shown in Fig.II.2.2-1.

#### References

- [2.2-1] Saigusa, M., Kanazawa, S., Ogawa, T. et al., Proc. of International Conference of Plasma Physics (ICPP2000), **3** 844 (2000).  
 [2.2-2] Ogawa, T. and JFT-2M group, Fusion Energy 2000 (CD-ROM, IAEA, Vienna), EXP4/06 (2001).

### 2.3 Compact Toroid Injection

Injection of a compact toroid (CT) is a potential refueling method for fusion plasmas. In JFT-2M, CT injection experiments were performed under the collaboration between JAERI and Himeji Institute of Technology. We demonstrated successfully penetration of a CT plasma into

the core region of JFT-2M plasma with  $B_t = 0.8T$ . As a result, averaged electron density increased by  $\bar{n}_e = 0.4 \times 10^{19} \text{ m}^{-3}$  and a fueling efficiency of 40% was obtained [2.3-1]. In order to understand the dynamics of CTs which traverse across the magnetic field, new electrostatic probe array was installed on JFT-2M. From the probe measurement, it was found that CT plasma reaches to the equivalent position of the divertor separatrix even if the external field of 1.0-1.4 T was applied and that there exists a trailing plasma behind the CT. We also observed a large amplitude fluctuation on the ion-saturation current and magnetic coil signal [2.3-2]. Time-frequency analyses suggest that the time-scale of this fluctuation agrees with that of the magnetic reconnection between the CT plasmoid and the external magnetic field estimated from the three-dimensional MHD simulation [2.3-3, -4].

#### References

- [2.3-1] Ogawa, T., et al., J. Nucl. Matter., **290-293**, 454 (2001).
- [2.3-2] Niimi, H., et al., Proc. of Int. Conf. Plasma Physics, (ICPP2000), **3**, 1987 (2000).
- [2.3-3] Suzuki, Y., et al., Nucl. Fusion, **40**, 277 (2000).
- [2.3-4] Nagata, M., et al., "Behavior of Compact Toroid Injected into the External Magnetic Field", to be published in Nucl. Fusion.

### 3. Operation and Maintenance

#### 3.1 Tokamak Machine

As for the JFT-2M facility, the ferritic steel plates (FPs) had been installed to cover about 20% of the area inside the vacuum vessel at the end of former FY. The evacuation and baking of the main equipments such as vacuum vessel and NB system were carried out, and the preparation to operate for experiments had been finished. An initial conditioning of the first wall was carried out by Taylor-type discharge cleaning (TDC) together with baking. The plasma production test was done next, and the whole of the systems were confirmed to be in good condition. The experiments were started on schedule from May, and continued up to February '01. A wall conditioning to decrease the gas desorption from the first wall, especially installed FPs, was performed by glow discharge cleaning (GDC) and boron-coating by using tri-methyl boron.

The vacuum vessel was opened from the end of September to October to check the inside components. The vacuum vessel was opened again in the end of February for preparation of full covering of FPs for the third-step of Advanced Material Tokamak Plasma Experiment (AMTEX) to be carried out in the next FY. The FPs that had been installed outside and inside of the vacuum vessel and inside components were almost removed. For this fiscal year, the number of plasma discharge was 2940shots, discharge cleaning (TDC and GDC) was 230 hours, and coil-energizing operation was 316 shots. The number of the boronization was 4 times (18 hours in total).

In order to improve reproducibility of CT plasmas, a new power supply system for the fast gas puffing of the CT injector was installed. This system consists of 4 capacitors bank discharge systems, each of which can be controlled independently and drive each fast gas-puffing valve. By careful control of the power supply system, a same amount of gas flow was obtained

from each fast gas-puffing valve and reproducibility of the CT plasma production was improved.

### **3.2 Heating Systems**

As for the NB system, successive maintenances were carried out over the year, and injection experiments were carried out. The annual check of the NB system was also carried out. The electrolytic capacitors of the power supply were renewed for preventive maintenance. After finishing the aging of gyrotrons, the EC wave experiment was started from July. The annual check of the EC power supply and control equipment were carried out in October. After the power test of the gyrotrons, the injection experiments were restarted from December. But, #4 gyrotron had a trouble due to cracking of the output window during the experiment. High confinement mode (H-mode) experiments were performed using the NB and EC heating systems

### **3.3 Power Supply System**

As for the DC generator (DCG) for the toroidal-magnetic-field power supply, operation was done smoothly, because the DCG building was newly equipped with dust filters. The conditions of brush and insulation performance of the DCG were maintained in the good condition. But, the electric-current-error-alarm of DCG appeared by a trouble of the commutator at the maximum magnetic field. Therefore, the maintenance of commutator was carried out. The trouble did not recur by this maintenance and by careful operation such as increasing the magnetic field step by step.

### III. THEORY AND ANALYSIS

The principal objective of theoretical and analytical studies is to understand physics of tokamak plasmas. Much progress was made on analyzing dynamics of the internal transport barrier in JT-60U reverse shear plasmas. Progress was also made on the study of stability micro and macro instabilities. The NEXT (Numerical EXperiment of Tokamak) project has made progressed in order to research complex physical processes both in core and in divertor plasmas by using massively parallel computers. Remarkable progress was made in the study of the turbulence driven by electron temperature gradient instabilities.

#### 1. Confinement and Transport

The Reverse Shear (RS) plasmas with Internal transport barrier (ITB) realize the favorable energy confinement properties in JT-60U. The transport properties of such plasmas are studied by the "transient" transport analysis method [1-1]. A new source of the heat pulse propagation is found in RS plasmas. This heat pulse propagation is created by the ITB-event. The region of strong rise of temperature ( $\sim 20$  keV/s) is initially well localized ( $\sim 4$  cm) in space. Later on, a slow diffusive broadening of the rising T perturbation is seen. Outward heat pulse propagation is analyzed in the region with  $\sim 8$  cm width fully located in positive shear space zone. Values of the electron dynamic heat diffusivity as low as  $\sim 0.1$  m<sup>2</sup>/s are found. The important consequence of the analysis is the absence of electron and ion heat pinch in the ITB region [1-1]. Transport evolution in reverse shear (RS) and normal shear (NrS) JT-60U tokamak plasmas with ITB is described as a combination of various fast and slow time scales processes. Abrupt in time and wide in space ( $\sim 30\%$  of minor radius) variations of electron and ion heat diffusivities (seen as spontaneous-like simultaneous rise and decay of  $T_{e,i}$  in two spatial zones) are found for weak ITBs in both RS and NrS plasmas [1-2].

In order to predict the energy confinement property of ITER and fusion reactors from present-day tokamaks, the transport properties of NB heated ELM My H-mode plasmas in JT-60 have been clarified by using the nondimensional plasma parameters [1-3]. The thermal diffusivity and energy confinement time of both electron and ion are normalized by the Bohm diffusion and their dependence on the normalized Larmor radius,

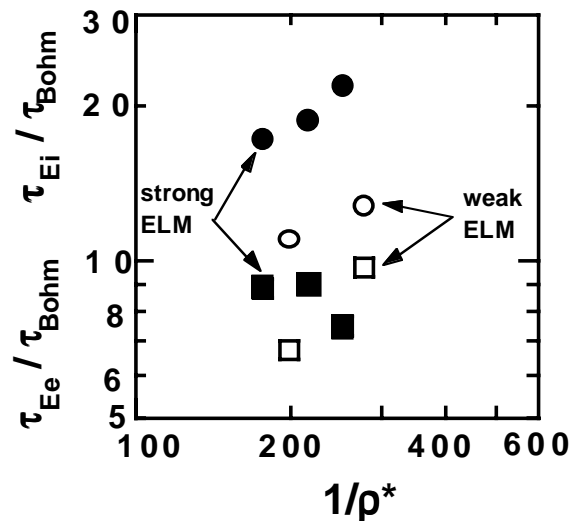


Fig.III.1-1. The  $(1/\rho^*)$  dependence of the normalized energy confinement time for electrons (circles) and ions (squares) in cases of weak ELM (open symbols) and strong ELM (closed symbols).

$\rho^*$ , and the normalized collision frequency,  $\nu^*$ , are studied in detail. The dependence of the normalized energy confinement time of electron and ion,  $\tau_{Ee}/\tau_{Bohm}$  and  $\tau_{Ei}/\tau_{Bohm}$ , on  $(1/\rho^*)$  in JT-60U ELMy H-mode plasmas is shown in Fig.III.1-1. In the case of relatively weak ELM (open symbols), both the electron and ion energy confinement increase with  $(1/\rho^*)$ . In the cases of strong ELM (closed symbols), the ion energy confinement has nearly independence of  $(1/\rho^*)$ , which is unfavorable for the fusion reactors because of their large  $(1/\rho^*)$  value.

#### References

- [1-1] Neudatchin, S.V., Takizuka, T., Shirai, H., et al., Plasma Phys. Control. Fusion, **43**, 661 (2001).
- [1-2] Neudatchin, S.V., Takizuka, T., Dnestrovskij, Yu., N., et al., Fusion Energy 2000 (CD-ROM, IAEA, Vienna), EXP5/20 (2001).
- [1-3] Shirai, H., Takizuka, T., Koide, Y., et al., Plasma Phys. Control. Fusion, **42**, 1193 (2000).

## 2. Stability

Double tearing modes (DTM) are considered as one of the possible candidates for the low beta disruption in negative shear plasmas. Linear and nonlinear features of DTM are investigated systematically in the cylindrical reduced MHD model with the helical symmetry. The new nonlinear phenomenon, which is caused by the deformation of a magnetic island structure, is found in the weakly coupled region of DTM. It is shown that DTM is nonlinearly destabilized after slow growth in the Rutherford-type regime. During the period of this regime, the nonlinear mode coupling between the main and higher harmonics enhances the higher harmonics, which cause the triangular deformation of magnetic islands and the following abrupt growth of DTM [2-1].

Validation studies of the neutral point against vertical displacement events had been carried out in the Alcator C-Mod and the ASDEX-Upgrade tokamaks under international collaborations. The disruption experiments of the Alcator C-Mod tokamak had clarified that the neutral point does exist at 2-3 cm above the horizontal midplane, as the tokamak-simulation-code (TSC) has predicted. As for the ASDEX-Upgrade, the disruption database indicates that the vertical location of the neutral point is rather unclear comparing with the JT-60U. The TSC simulations on the neutral point sensitivity to the plasma profile parameters are now in progress [2-2].

Stabilizing effects of the externally applied current profile, such as electron-cyclotron-current-drive (ECCD), on the neoclassical tearing mode (NTM) have been numerically analyzed. Peaking of the external current profile is shown to be effective for the stabilization. When the external current profile is modulated in phase with the island rotation, the stabilizing effect is more effective than that in the case of no modulation. The stabilizing effect of the peaked current is sensitive to the relative location between the rational surface of the island and the external current. The low magnetic shear through the equilibrium modified by the external current destabilizes the NTM island [2-3].

The effect of NTM on the confinement degradation is studied by using a 1.5D time-dependent simulation code TOPICS. The NTM island width is calculated according to the modified Rutherford's equation. In the case that a neutral beam is injected before sawtooth starts, a bootstrap current modifies a total current profile and makes a conventional tearing stability index  $\Delta'$  positive. 3/2 mode NTM arises a few seconds after NB which is the same order as the local resistive skin time. In the case of NB after sawtooth, the NTM arises only with high NB power. At the same NB power, the confinement degradation by 3/2 mode island in the former case is larger than that of the latter case [2-4].

#### References

- [2-1] Ishii, Y., Azumi, M., Kurita, G., et al., Phys. Plasmas, **7**, 4477 (2000).
- [2-2] Lister, J.B., Khayrutdinov, R., Limebeer, D.J.N., Lukash, V., Nakamura, Y., et al., Proceedings of 27th European Conference on Controlled Fusion and Plasma Physics (EPS, Budapest, 2000), **24B**, 181-184 (2000).
- [2-3] Ozeki, T., Tokuda, S., Hamamatsu, K., "Stabilizing Effects of a Width of Externally Applied current on Neoclassical Tearing Mode", 42nd Annual Meeting of APS, Quebec (2000).
- [2-4] Hayashi, N., Ozeki, T., Shirai, H., et al., "Effect of Neoclassical Tearing Mode on Confinement Degradation", 42nd Annual Meeting of APS, Quebec (2000).

### 3. Heating and Current Drive

An electron cyclotron (EC) wave is very attractive for stabilization of neo-classical tearing modes (NTM). To obtain the optimum condition of the EC beam injection to stabilize NTM, we have developed a ray-tracing code which can save computation time. The ray trajectories are calculated by the standard method and the driven current is calculated by using the adjoint equation for the full relativistic Fokker-Planck equation [3-1]. By scanning the launching direction in both the toroidal and poloidal directions, the optimum direction of beam injection is obtained to drive a current with a maximum value of  $I_t/\rho_w$  at the desired magnetic surface, where  $I_t$  is the total driven current and  $I_t/\rho_w$  is the radial width of the driven current. When the current is driven at the position where a ray trajectory becomes tangent to the magnetic surface ('tangential resonance'), Doppler broadening of the current profile is significantly reduced and  $I_t/\rho_w$  reaches the maximum value. In the case of tangential resonance, the driven current width is mainly determined by the effects of the beam divergence. The width of the driven current is kept in a range of 2 ~ 5 % of the minor radius when a beam divergence is  $2\beta$ . The dependence on both the location of beam injection and the wave frequency has been also obtained [3-2].

#### References

- [3-1] Hamamatsu, K., Fukuyama, A., Fusion Engineering and Design, **53**, 53 (2001).
- [3-2] Hamamatsu, K., Fukuyama, A., Plasma Phys. Control. Fusion, **42**, 1309 (2000).

## 4. Numerical Experiment of Tokamak (NEXT)

### 4.1 Development of Computational Algorithm

A new scheme for inner layer equations in resistive MHD stability theory has been developed. The new scheme solves the inner layer equations as an initial-value problem. The full implicit finite-difference-approximation to time yields equations including derivatives only with respect to the radial variables. The differential equations thus derived are to be solved with the given asymptotic condition at infinity. This asymptotic matching problem is transformed into a boundary value problem for which finite difference methods are applicable [4.2-1].

#### Reference

[4.1-1] Tokuda, S., Fusion Energy 2000 (CD-ROM, IAEA, Vienna), THp2/10 (2001).

### 4.2 Transport and MHD Simulation

Linear and nonlinear properties of slab drift waves are studied in the negative sheared slab configuration modeling the  $q_{\min}$ -surface region of negative shear tokamaks, where  $q_{\min}$  is the minimum value of a safety factor  $q$ . Linear calculations show that both the ion and the electron temperature gradient driven (ITG and ETG) modes become strongly unstable around the  $q_{\min}$ -surface. Nonlinear simulations are performed for the ETG turbulence that evolves in a much faster time scale than the ITG turbulence. It is found that quasi-steady  $E_r \times B$  zonal flows are generated by an inverse wave-energy-cascade-process. Linear stability analyses of the electrostatic Kelvin-Helmholtz (K-H) mode show that the quasi-steady  $E_r \times B$  zonal flow profile is closely related to the  $q$ -profile or the magnetic shear, which has a stabilizing effect on the K-H mode. It is shown that the microscopic quasi-steady  $E_r \times B$  zonal flows arising from the ETG turbulence have a strong stabilizing effect on the slab ITG mode [4.3-1~5].

The  $m = 2$  collisionless DTM has been studied with the gyro-kinetic particle simulation to clarify the effect of the electron inertia on the MHD phenomena in the reversed shear configuration of a tokamak plasma. The collisionless DTM are found to grow up with the Alfvén time scale due to the coupling of two perturbations originated in each resonant surface. It is also found that the internal collapse occurs on the Alfvén time scale due to the rapid growth of the  $m = 2$  electrostatic potential. The  $E \times B$  flow due to an  $m=2$  electrostatic potential surviving after the collapse induces the secondary reconnection and the re-distribution of the current profile, which produces a new reversed shear configuration [4.3-6].

The process of fueling by injection of a spheromak-like compact toroid (SCT) is investigated by using MHD numerical simulations, where the SCT is injected into a magnetized target plasma region corresponding to a fusion device. We proposed, on the basis of simulation

results, a theoretical model that determines the penetration depth of the SCT into the target region. It is revealed that the fluctuations of the target magnetic field propagate with the Alfvén velocity determined by the magnetic field and the density in the device region, which leads to the relaxation of the magnetic tension force. The model is shown to be useful for estimating the penetration depth of the SCT [4.3-7].

#### References

- [4.2-1] Idomura, Y., Tokuda, S., Wakatani, M., *Phys. Plasmas*, **7**, 2456 (2000).
- [4.2-2] Idomura, Y., Tokuda, S., Wakatani, M., *Phys. Plasmas*, **7**, 3551 (2000).
- [4.2-3] Idomura, Y., Tokuda, S., Kishimoto, Y., et al., *Fusion Energy 2000* (CD-ROM, IAEA, Vienna), TH2/6 (2001).
- [4.2-4] Idomura, Y., JAERI report, JAERI 1341 (2001).
- [4.2-5] Idomura, Y., Tokuda, S., Kishimoto, Y., et al., *Nuclear Fusion*, **41**, 437 (2001).
- [4.2-6] Matsumoto, T., Naitou, H., Tokuda, S., et al., *Fusion Energy 2000* (CD-ROM, IAEA, Vienna), TH3/3 (2001).
- [4.2-7] Suzuki, Y., Hayashi, T., Kishimoto, Y., *Physics of Plasmas*, **7**, 5033 (2001).

### 4.3 Divertor Simulation

Physical characteristics of the scrape-off-layer (SOL) and divertor plasmas have been investigated by using an advanced particle-simulation-code PARASOL. The effect of diffusive particle loss and radiative energy loss on the formation of detached plasma was studied in a one-dimensional system [4.3-1]. The generation of supersonic flow in the presence of above losses was found, which can bring about the detachment. Heat transport along magnetic field lines in open-field plasmas was studied [4.3-2]. We found a new analytic expression for the heat flux in the collisionless regime through PARASOL simulation results. Two-dimensional PARASOL code was developed. With the use of this code, effects of the radial gradients including diamagnetic drift flow on SOL and divertor plasmas were studied [4.3-3]. Detailed explanation on the PARASOL code was presented elsewhere [4.3-2, 4.3-4].

#### References

- [4.3-1] Takizuka, T., Hosokawa, M., Shimizu, K., *J. Nucl. Mater.*, **290-293**, 753 (2001).
- [4.3-2] Takizuka, T., Hosokawa, M., Shimizu, K., *Trans. Fusion Tech.*, **39**, 111 (2001).
- [4.3-3] Takizuka, T., Shimizu, K., Hayashi, N., Hosokawa, M., *Fusion Energy 2000* (CD-ROM, IAEA, Vienna), THP1/22 (2001).
- [4.3-4] Hosokawa, M., Takizuka, T., JAERI-Data/Code 2000-025 (2000).

## IV. FUSION REACTOR DESIGN AND SAFETY RELATED RESEARCH

Research on fusion reactor design and safety was mainly devoted to physics and plant designs of a fusion power reactor A-SSTR2, multi-purpose uses of fusion energy, a reduction of radioactive wastes from the plant, etc. At the same time, conceptual design study of a fusion demo plant has started in the last fiscal year to bridge a gap between ITER and A-SSTR2.

### 1. Fusion Reactor Design

#### 1.1 Design of A-SSTR2

In 1999, the design of a new tokamak reactor A-SSTR2 that orients both economical and environmental acceptance has started, adopting the advantages of SSTR, A-SSTR and DREAM. A-SSTR2 (Fig.IV.1.1-1) aims at a high power density with the combination of high toroidal field (11 T on the plasma axis and 23 T at the peak) and moderate normalized beta ( $\beta_N = 4$ ), producing 4 GW of fusion power output at a compact machine size ( $R_p = 6.2$  m) [1.1-1].

Center solenoid (CS) coils are removed to set the support for the enormous electromagnetic force. Accordingly, CS-less plasma current rise is one of the key issues of A-SSTR2. Recent assessment found the following three options feasible to provide the initial current up to 2-3 MA: 1) multipath absorption of electron-cyclotron-resonance waves (390 GHz), 2) lower hybrid current drive (10-15 GHz), and 3) induction by a compact startup assist coil with a capability of 30 Vsec. Above 2-3 MA, the overdrive by bootstrap and neutral-beam-driven current is expected to boost the plasma current up to the flatter of 12 MA.

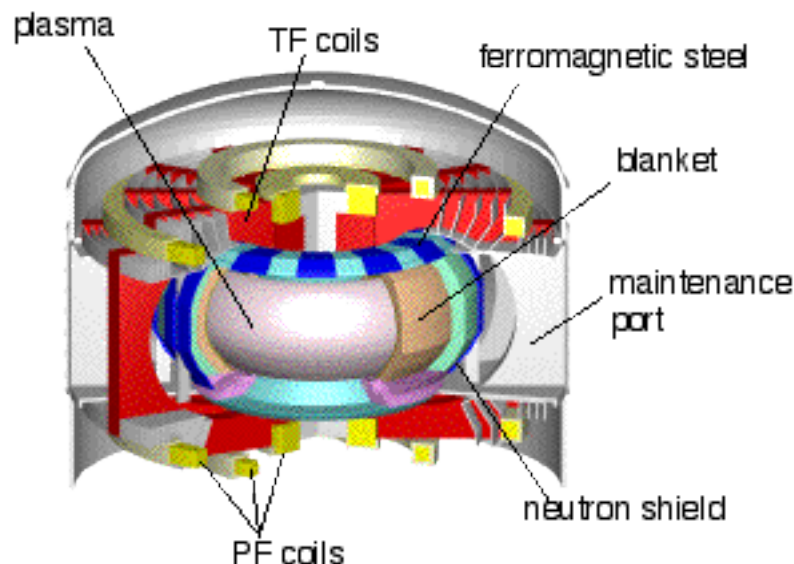


Fig.IV.1.1-1 Cutaway view of A-SSTR2 (TF/PF: toroidal/poloidal field)

#### Reference

[1.1-1] Nishio, S., et al, 18th IAEA Fusion Energy Conf. FTP2/14 (2000).

## **1.2 Design of a New DEMO Reactor**

Design activity of a fusion reactor was embarked on in FY2000. The concept of the DEMO reactor is a minimum-sized fusion power plant on the basis of the plasma technologies that will be established in ITER, bridging the gap between ITER and A-SSTR2. Using future technologies in 2030's such as a high temperature superconductor, the reactor is designed to have the fusion gain of  $\sim 40$ , the fusion output of 2.3 GW and the bootstrap current fraction of 80% at the maximum toroidal field of 20 T (9.5 T at the plasma center) and  $R = 5.8$  m. For the sake of high heat efficiency, the reactor adopts ODS steel (Oxide-Dispersed-Strengthened steel) as the structural material of blanket and supercritical pressurized water as coolant. Through the initial design study, the following high priority issues were extracted to be resolved in the coming years: countermeasures against disruptions, erosion of the wall material by neutral particles, contamination of coolant by tritium, efficient heat cycle, and safety issue related with supercritical pressurized water.

## **1.3 Startup of DT Fusion Plant without Initial Loading of Tritium**

Even in the plasma without initial tritium loading, DD reaction produces a small amount of tritium and neutrons that is converted to tritium in a breeding blanket. The recirculated tritium can burn in DT reaction and yield more tritium, resulting in exponential breeding. A model analysis, on the basis of the conventional fusion reactor plant consisting of a fuel circulation system and breeding blanket, indicated that a full power operation with 50% tritium in the plasma is achievable in operation of the order of 100 days [1.3-1]. Thus, to prepare initial tritium for fusion plant is not mandatory.

### **Reference**

[1.3-1] Konishi, S., et al., J. Plasma Fus. Res., **76**, 1309 (2000).

## **1.4 Multipurpose Use of Fusion Energy**

Use of fusion energy for various applications not limited for electric power generation was considered to improve its attractiveness and to expand potential market. At a coolant temperature above 600°C where advanced reduced activation material can be used, many of the plants such as petro-chemical, paper, gas and other chemical plants can be operated, and besides electricity generation is more efficient than light water reactor temperature.

Under constraint of global environment problem, this feature of fusion energy improves its attractiveness by production of low carbon fuels such as hydrogen or alcohol, as well as electricity. One of the important use of heat from fusion will be hydrogen production that is anticipated to become major fuels for dispersed generators such as micro gas turbine or fuel cell, or transportation because of preferred effects on reduction of carbon dioxide emission. Steam

reforming reaction,  $C_mH_n + H_2O \rightarrow CO_2 + H_2$  is endothermic reaction that requires large amount of heat, and can be regarded as transformation of fusion energy to the form of  $H_2$  chemical energy. While fossil fuel can be used as raw material, biomass, possibly wastes, will be more attractive to generate hydrogen. Chemical process to generate hydrogen to be attached to A-SSTR2 was designed and found to have attractive features. At the coolant temperature of 900°C, vapor electrolysis, another form of conversion of fusion energy to hydrogen will also be possible.

## **2. Fusion Safety**

### **2.1 Structural Integrity of First Wall Made of SiC/SiC**

In the SiC/SiC composite which is regarded as a promising material for the first wall in a future fusion reactor, a micro-crack can be generated and developed in the matrix. On the other hand, SiC fibers can suppress the crack development. In order to assess the structural integrity of SiC/SiC first wall, the wall with a crack was modeled to fit with the finite element method. The preliminary calculation confirmed that the fibers reduce the crack opening displacement [2.1-1].

#### **Reference**

[2.1-1] Kurihara, R., et al., Fusion Eng. Design, **54**, 465 (2001).

### **2.2 Reduction of Radioactive Waste from Tokamak Reactor**

The "radwaste (radioactive waste) minimum" concept of fusion reactor design is proposed to lead to a significant reduction of radioactive waste. The new concept considers that the role of a neutron shield is to keep the outer structural components from considerable activation, rather than to ensure the function of superconducting magnets during discharges. The presented concept requires some reinforcement of shielding with a minimal change of reactor size, which can be met by the use of an advanced shield material such as a metal hydride. An estimate based on the concept indicates that the radwaste from A-SSTR2 can be as low as 17% in weight fraction, whereas the radwaste expected in the conventional way amounts to 92% [2.2-1].

#### **Reference**

[2.2-1] Tobita, K., et al., "Fusion reactor design towards radwaste minimum with advanced shield material", J. Plasma Fus. Res., (in press).

## Appendix A.1 Publication List (April 2000 - March 2001)

### A.1.1 List of JAERI report

- 1) Abe, T., Hiroki, S., Tanzawa, S., et al., "Preliminary Joining Experiment of Alumina Pipes by using Ceramics Sleeve", JAERI-Research 2001-029 (2001).
- 2) Hosokawa, M. and Takizuka, T., "Development of PARASOL Code", JAERI-Data/Code 2000-025 (2000).
- 3) Ida, M., Nakamura, H., Sugimoto, M., et al. "International fusion material irradiation facility Key Element technology Phase Task description", JAERI-Tech 2000-052 (2000).
- 4) Idomura, Y., "Gyrokinetic analysis of micro-instabilities in negative shear tokamaks", JAERI report, JAERI 1341 (2001).
- 5) Inoue, T., Suzuki, Y., Miyamoto, K., et al., "Steering of H- ion beamlet by aperture displacement", JAERI-Tech 2000-051 (2000).
- 6) Iwai, Y., Yamanishi, T., and Nishi, M., "A design study of hydrogen isotope separation system for ITER-FEAT", JAERI-Tech 2001-027 (2001).
- 7) Kamiya, K. and Miura, Y., "The Multichannel Motional Stark Effect Diagnostics in the JFT-2M Tokamak", JAERI Tech 2000-090 (2000) (in Japanese).
- 8) Kasugai, Y., Ikeda, Y., Uno, Y., et al., "Activation Cross Section Measurement at Neutron Energy from 13.3 to 14.9 MeV using FNS Facility", JAERI-Research 2001-025 (2000).
- 9) Kizu, K., et al., "Development of the centrifugal pellet injector for JT-60U", JAERI-Tech 2001-12 (2001).
- 10) Maebara, S., "Study of Lower Hybrid Current Drive System in Tokamak Fusion Devices", JAERI-Research 2000-061 (2000).
- 11) Murata, I., Nishio, T., Terada, Y., et al., "(n,2n) Reaction Cross Section Measurement with A Beam DT Neutron Source -Measurement Method-", Proceedings of the 2000 Symposium on Nuclear Data, Tokai, Japan, November 2000, JAERI-Conf 2001-006 (2001).
- 12) NBI heating laboratory, Proceedings of the joint meeting on plasma surface interaction (PSI) and plasma facing components (PFC)", JAERI-Conf 2001-001 (2001).
- 13) Nakamura, H., Hayashi, T., Suzuki, T., et al., "Analysis on Tritium Permeation in Tritium Storage Bed with Gas Flowing Calorimetry", JAERI-Research 2000-044 (2000) (in Japanese).
- 14) Nakamura, H., Ida, M., Nakamura, H., et al., "Experimental Study on the Effect of Nozzle Surface Finishing in High-Speed Water Jet", JAERI-Research 2000-068 (2000) (in Japanese).
- 15) Nakamura, H., Ida, M., Sugimoto, M., et al., "Reduced cost design of liquid lithium target for International fusion material irradiation facility (IFMIF)", JAERI-Tech 2000-78 (2001).
- 16) Nakamura, H., Morimoto, Y., Ochiai, K., et al., "Fusion Neutronics Plan in the Development of Fusion Reactor with the Aim of Realing Electric Power", JAERI-Review 2000-016 (2000) (in Japanese).
- 17) Nishio, S., Ushigusa, K., Ueda, S., et al., "Physics Design of Advanced Steady-State Tokamak Reactor A-SSTR2", JAERI-Research 2000-029 (2000) (in Japanese).
- 18) Nishio, T., Murata, I., Takahashi, A., et al., "Measurement of Secondary Gamma-Ray Spectra from Structural and Blanket Materials Bombarded by D-T Fusion Neutrons," Proceedings of the 2000 Symposium on Nuclear Data, Tokai, Japan, November 2000, JAERI-Conf 2001-006 172 (2001).
- 19) Sato, S., Furuya, K., Hatano, T., et al., "Development of ITER Shielding blanket prototype Mockup by HIP bonding", JAERI-Tech 2000-042 (2000).
- 20) Sato, S., "Proceedings of the First Symposium on Monte Carlo Simulation; 2.12 ITER Nuclear Design by MCNP", JAERI-Conf 2000-018 (2000).
- 21) Sugimoto, M., "Study on the Flow Reduction of Forced Flow Superconducting Magnet and Its Stable Operation Condition", JAERI-Research 2000-096 (2001).
- 22) Takahashi, K., Imai, T., Mori, S., et al., "Conceptual Design of Neutron Shield for ECH Launcher on D-T Fusion Reactors", JAERI-Research 2000-036 (2000).
- 23) Takahashi, K., Komatsuzaki, M., "Stress Analysis of CVD Diamond Window for ECH System", JAERI-Research 2000-054 (2000).
- 24) Uno, Y., Kaneko, J., Nishitani, T., et al., "Technical Feasibility Study for the D-T Neutron Monitor using

Activation of the Flowing Water”, JAERI-Research 2001-007 (2001)

- 25) Urano, H., Kamada, Y., Shirai, H., et al., “Degradation of energy confinement in JT-60U ELMy H-mode plasmas”, JAERI-Research 2000-037 (2000).

### A.1.2 List of papers published in journals

- 1) Ando, T., Hiyama, T., Takahashi, Y., et al., "Completion of the ITER CS Model Coil-Outer Module Fabrication" *IEEE Trans. ASC*, **10**, 568 (2000).
- 2) Ando, T., Hiyama, T., Takahashi, Y., et al., "Development of 13 T – 640 MJ Superconducting Pulse Field Coil for Fusion Machine", *Trans. IEE Japan*, **120-B**, 449 (2000) (in Japanese).
- 3) Asakura, N., Sakurai, S., Shimada, M., et al., "Measurement of natural plasma flow along the field lines in the scrape-off layer on the JT-60U divertor tokamak", *Phys. Rev. Lett.*, **84**, 3093 (2000).
- 4) Cardella, A., Barabash, V., Hatano, T., et al., "Application of Beryllium as first wall armor for ITER primary, Baffle and Limiter modules", *Fusion Technol.*, **38**, 326 (2000).
- 5) Ezato, K., Sato, K., Taniguchi, M., et al., "Critical Heat Flux In Subcooled Water Flow In A Saw-Toothed Finned Tube Under One-Sided Heating Conditions", *Fusion Technol.*, **39**, 885 (2001).
- 6) Fujita, T. and JT-60 team, "Recent progress towards steady state tokamak operation with improved confinement in JT-60U", *J. Plasma Fusion Res., SERIES* **3**, 87 (2000).
- 7) Fujita, T., Ide, S., Kamada, Y., et al., "Quasi-steady High-confinement Reversed Shear Plasma with Large Bootstrap Current Fraction under Full Non-inductive Current Drive Condition in JT-60U", *Phys. Rev. Lett.*, **87**, 085001 (2001).
- 8) Fujiwara, Y., Hanada, M. and Okumura, Y., "Beamlet-beamlet interaction in a multi-aperture negative ion source", *Rev. Sci. Instrum.*, **71**(8), 3059 (2000).
- 9) Fukuda, T., Takizuka, T., Tsuchiya, K., et al., "Reduction of L-H transition threshold power under the W-shaped pumped divertor geometry in JT-60U", *Plasma Phys. Control. Fusion*, **42**, A289 (2000).
- 10) Hamajima, K., Hanai, T., Wachi, Y., et al., "AC loss performance of 100kWh SMES model coil", *IEEE Trans. ASC*, **10**, 812 (2000).
- 11) Hamamatsu, K. and Fukuyama, A., "Controllability of Driven Current Profile in ECCD on ITER", *Fusion Eng. Des.*, **53**, 53 (2001).
- 12) Hamamatsu, K. and Fukuyama, A., "Numerical Analysis of Electron Cyclotron Current Drive with Suppressed Doppler Broadening", *Plasma Phys. Control. Fusion*, **42**, 1309 (2000).
- 13) Hatae, T., Sugihara, M., Hubbard, A., et al., "Understanding of the H-mode Pedestal Characteristics using the Multi-Machine Pedestal Database", *Nucl. Fusion*, **41**, 285 (2001).
- 14) Hatano, T., Gotoh, M., Yamada, T., et al., "Crack Propagation Tests of HIPed DSCu/SS Joints for Plasma Facing Components", *Fusion Eng. Des.*, **49-50**, 207 (2000).
- 15) Hatano, T., Suzuki, S., Yokoyama, K., et al., "High Heat Flux Test of a HIPed Ferritic Steel F-82H First Wall Panel", *J. Nucl. Mater.*, **283-287**, 685 (2000).
- 16) Hayashi, N., Takizuka, T. and Shimizu, K., "Thermoelectric Instability in Externally Induced Asymmetric Divertor Plasmas", *Contrib. Plasma Phys.*, **40**, 387 (2000).
- 17) Hiroki, S., Tanzawa, S., Arai, T., et al., "Fabrication of a Leak Test Unit for Developing a Water Leak Detection Method in Fusion Machines", *J. Vac. Soc. Jpn.*, **44**, 329 (2001) (in Japanese).
- 18) Hoshino, K. and JFT-2M group, "Suppression of the m/n=2/1 Tearing Mode by ECH/ECCD on JFT-2M Tokamak", *Fusion Eng. Des.*, **53/1-4**, 249 (2000).
- 19) Hu, L., Kuriyama, M., Akino, N., et al., "Beam divergence and power loading on the beamline components of the negative-ion based NBI system for JT-60U", *Fusion Eng. Des.*, **54**, 321 (2001).
- 20) Ide, S. and JT-60 team, "Latest Progress in Steady State Plasma Research on Japan Atomic Energy Research Institute Tokamak-60 Upgrade", *Phys. Plasmas*, **7**, 1927 (2000).
- 21) Idomura, Y., Tokuda, S., Kishimoto, Y., et al., "Gyrokinetic theory of drift waves in negative shear tokamaks", *Nucl. Fusion*, **41**, 437 (2001).
- 22) Idomura, Y., Tokuda, S. and Wakatani, M., "Gyrokinetic theory of slab electron temperature gradient mode in negative shear tokamaks", *Phys. Plasmas*, **7**, 2456 (2000).
- 23) Idomura, Y., Tokuda, S. and Wakatani, M., "Stability of ExB zonal flow in electron temperature gradient driven turbulence", *Phys. Plasmas*, **7**, 3551 (2000).
- 24) Iguchi, K., Morimoto, Y., Sugiyama, T., et al., "Chemical Behavior of Energetic Deuterium Implanted into

- SiC, Si and Graphite”, *Fusion Technol.*, **39**, 905 (2001).
- 25) Ikeda, Y. and JT-60 team, “Initial results of electron cyclotron range of frequency (ECRF) operation and experiments in JT-60U”, *Fusion Eng. Des.*, **53**, 351 (2001).
  - 26) Isayama, A. and JT-60 team, “Electron temperature perturbations measured by electron cyclotron emission diagnostic systems in JT-60U”, *Fusion Eng. Des.*, **53**, 129 (2001).
  - 27) Isayama, A., Isei, N., Ishida, S., et al., “Electron Temperature Perturbations Measured by ECE Diagnostic Systems in JT-60U”, *Fusion Eng. Des.*, **53**, 129 (2000).
  - 28) Isayama, A., Kamada, Y., Ide, S., et al., “Complete Stabilization of a Tearing Mode in Steady State High beta-p H-mode Discharges by the First Harmonic Electron Cyclotron Heating/Current Drive on JT-60U”, *Plasma Phys. Control. Fusion*, **42**, L37 (2000).
  - 29) Isayama, A., Kamada, Y., Ozeki, T., et al., “Long Sustainment of Quasi-steady State High beta-p H-mode Discharges in JT-60U”, *Nucl. Fusion*, **41**, 761 (2001).
  - 30) Isayama, A., Kamada, Y., Ozeki, T., et al., “Characteristics of Tearing Modes in Steady State High beta-p H-mode Discharges in JT-60U”, *J. Plasma Fusion Res. SERIES*, **3**, 94 (2000).
  - 31) Isei, N. and JFT-2M group, “Application of Low Activation Ferritic Steel in the JFT-2M Tokamak - Evaluation of Magnetic Effect on the Plasma”, *Fusion Technol.*, **39**, 1101 (2001).
  - 32) Isei, N. and JT-60U team, “ECE Measurements in JT-60U”, *Fusion Eng. Des.*, **53/1-4**, 213 (2000).
  - 33) Ishii, Y., Azumi, M., Kurita, G., et al., “Nonlinear evolution of double tearing modes”, *Phys. Plasmas*, **7**, 4477 (2000).
  - 34) Ivanov, D., Sato, S., Marois, G.Le, “Evaluation of hot isostatic pressing for joining of fusion reactor structural components”, *J. Nucl. Mater.*, **283-287**, 35 (2000).
  - 35) Iwai, Y., Hayashi, T., Kobayashi, K., et al., “Simulation study of tritium release experiments in the caisson assembly for tritium safety at the TPL/JAERI”, *Fusion Eng. Des.*, **54**, 523 (2001).
  - 36) Iwai, Y., Hayashi, T., Yamanishi, T., et al., “A simulation of tritium behavior after intended tritium release in a ventilated room”, *J. Nucl. Sci. Technol.*, **38**, 63 (2001).
  - 37) Iwai, Y., Yamanishi, T., and Nishi, M., “A Design study of advanced hydrogen isotopes separation system for ITER”, *Fusion Technol.*, **39**, 1078 (2001).
  - 38) Johnson, W.R., Trester, P.W., Sengoku, S., et al., “Performance of V-4Cr-4Ti Alloy Exposed to the JFT-2M Tokamak Environment”, *J. Nucl. Mater.*, **283-287**, 622 (2000).
  - 39) Kajiwara, K., Kasugai, A., Takahashi, K., et al., “High and Long pulse ECRF System in JT-60U”, *J. Plasma Fusion Res.*, **3**, 372 (2000).
  - 40) Kakudate, S., Oka, K., Taguchi, K., et al., “Mechanical Characteristics and Position Control of Vehicle/Manipulator for ITER Blanket Remote Maintenance”, *Fusion Eng. Des.*, **51-52**, 993 (2000).
  - 41) Kakuta, T., Konishi, S., Kawamura, Y., et al., “Electrochemical properties of hydrogen concentration cell with ceramic protonic conductor”, *Fusion Technol.*, **39**, 1083 (2001).
  - 42) Kamada, Y., Oikawa, T., Lao, L., et al., “Disappearance of giant ELMs and appearance of minute grassy ELMs in JT-60U high-triangularity discharges”, *Plasma Phys. Control. Fusion*, **42**, A247 (2000).
  - 43) Kamada, Y., “Observations on the formation and control of transport barriers”, *Plasma Phys. Control. Fusion*, **42**, A65 (2000).
  - 44) Kamiya, K., Miura, Y., Ido, T., et al., “Development of Mesh Probe for the Calibration of the HIBP Diagnostic System in the JFT-2M Tokamak”, *Rev. Sci. Instrum.*, **72**, 579 (2001).
  - 45) Kaneko, J., Uno, Y., Nishitani, T., et al., “Technical feasibility study on a fusion power monitor based on activation of water flow”, *Rev. Sci. Instrum.*, **72**, 809 (2001).
  - 46) Kasugai, A., Sakamoto, K., Takahashi, K., et al., “1 MW and long pulse operation of Gaussian beam output gyrotron with CVD diamond window for fusion devices”, *Fusion Eng. Des.*, **53**, 399 (2001).
  - 47) Kasugai, Y., Ikeda, Y., Ikeda, Y., Sakane, H., “Cross-Section Measurement for the  $^{17}\text{O}(n,p)^{17}\text{N}$  Reaction by 14 MeV Neutrons”, *Nucl. Sci. Eng.*, **136**, 238 (2000).
  - 48) Kawai, M., Grisham, L., Itoh, T., et al., “Study of plasma uniformity on JT-60U negative ion source”, *Rev. Sci. Instrum.*, **71(2)**, 755 (2000).

- 49) Kawamura, Y., Iwai, Y., Yamanishi, T., et al., "Analysis of hydrogen isotopes with a micro gas chromatograph", *Fusion Eng. Des.*, **49-50**, 855 (2000).
- 50) Kawamura, Y., Konishi, S. and Nishi, M., "Adsorption isotherms of hydrogen isotopes on molecular sieves 5A at low temperature", *J. Nucl. Sci. Technol.*, **37**, 536 (2000).
- 51) Kawano, Y., Chiba, S. and Inoue, A., "Infrared Laser Polarimetry for Electron Density Measurement in Tokamak Plasmas", *Rev. Sci. Instrum.*, **72**, 1068 (2001).
- 52) Kawano, Y., et al., "Electron Density Measurement for Steady State Plasmas", *J. Plasma Fusion Res., SERIES*, **3**, 397 (2000).
- 53) Kawano, Y., et al., "Infrared Laser Polarimetry for Electron Density Measurement in Tokamak Plasmas", *Rev. Sci. Instrum.*, **72**, 1068 (2001).
- 54) Kawashima, H. and JFT-2M group, "Demonstration of Ripple Reduction by Ferritic Steel Insertion in JFT-2M", *Nucl. Fusion*, **41**, 257 (2001).
- 55) Kawashima, H. and JFT-2M group, "Ripple Reduction Test by Ferritic Steel Board Insertion in the JFT-2M Tokamak", *J. Plasma Fusion Res.*, **76**, 585 (2000) (in Japanese) .
- 56) Kikuchi, M., Seki, Y., Nakagawa, K., "The advanced SSTR", *Fusion Eng. Des.*, **48**, 265 (2000).
- 57) Kikuchi, S., "Numerical analysis model for thermal conductivities of packed beds with high solid-to-gas conductivity ratio", *J. Heat Mass Transfer*, **44**, 1213 (2001).
- 58) Kohagura, J., Cho, T., Hirata, M., et al., "investigation of x-ray-energy response of semiconductor detectors under deuterium-tritium fusion produced neutron irradiation", *Rev. Sci. Instrum.*, **72**, 805 (2001).
- 59) Koide, Y., Sakasai, A., Sakamoto, Y., et al., "Multichordal Charge Exchange Recombination Spectroscopy on the JT-60U Tokamak", *Rev. Sci. Instrum.*, **72**, 119 (2001).
- 60) Kondoh, T. and Lee, S., "Collective Thomson scattering using a pulsed CO2 laser in JT-60U", *Rev. Sci. Instrum.*, **72**, 1143 (2001).
- 61) Konishi, S., Asaoka, Y., Hiwatari, R., et al., "Start up of DT fusion plant without initial loading of tritium", *J. Plasma Fusion Res.*, **76**, 1309 (2000).
- 62) Konno, C., Maekawa, F., Kasugai, Y., et al., "Neutronics experiments for ITER at JAERI/FNS", *Nucl. Fusion*, **41**, 333(2001).
- 63) Konno, C., Maekawa, F., Uno, Y., et al., "Overview of Straight Duct Streaming Experiments for ITER", *Fusion Eng. Des.*, **51-52**, 797 (2000).
- 64) Kubo, H., Sakurai, S., Asakura, N., et al., "High-Radiation and High-Density Experiments in JT-60U", *Nucl. Fusion*, **41**, 227 (2001).
- 1) Kumagai, A., Kubo, H., Takenaga, H., et al., "Spatial variation of D line spectral profile and emission process in the divertor region of JT-60U", *Plasma Phys. Control. Fusion*, **42**, 529 (2000).
- 66) Kurihara, R., Nishio, S., Ueda, S., et al., "Control of Fusion Power in a Steady-State Tokamak Reactor", *J. Plasma Fusion Res. Series*, **3**, 553 (2000).
- 67) Kuriyama, M., Akino, N., Ebisawa, N., et al., "Power flow in the negative-ion based neutral beam injection for JT-60", *Rev. Sci. Instrum.*, **71(2)**, 751 (2000).
- 68) Lao, L.L., Kamada, Y., Oikawa, T., et al., "Dependence of Edge Stability on Plasma Shape and Local Pressure Gradients in the DIII-D and JT-60U Tokamaks", *Nucl. Fusion*, **41**, 295 (2001).
- 69) Lee, S., Kondoh, T., Yonemoto, Y., et al., "A Filter Bank System for Scattered Spectrum Analysis in Collective Thomson Scattering Diagnostic on JT-60U", *Rev. Sci. Instrum.*, **71**, 4445 (2000).
- 70) Lee, S., Kondoh, T., Yoshino, R., et al., "Collective Thomson Scattering Diagnostic for Fast Ion and Deuterium to Tritium Ratio Measurement in Open Magnetic Systems", *Trans. Fusion Technol.*, **39**, Number 1T, 151 (2001).
- 71) Lee, S. and Kondoh, T., "Advanced Impurity Measurement for Deuterium-Tritium Burning Plasmas using Pulsed CO2 Laser Collective Thomson Scattering", *Rev. Sci. Instrum.*, **71**, 3718 (2000).
- 72) Maebara, S., Goniche, M., Kazarian, F., et al., "Outgassing of plasma Facing antenna front for lower hybrid wave launcher" *Fusion Eng.Des.*, **49-50**, 269 (2000).
- 73) Matsuda, S., "Status of Fusion Technology Development in JAERI Stressing Steady-State Operation for

- Future Reactor”, *Fusion Eng. Des.*, **49-50**, 27 (2000).
- 74) Matsuda, T., Tsugita, T., Oshima, T., et al., “Status of JT-60 Data Processing System”, *Fusion Eng. Des.*, **48**, 99 (2000).
  - 75) Matsukawa, M., Ishida, S., Sakasai, A., et al., “A Design Study of the Power Supply System for Superconducting JT-60”, *Fusion Tech.*, **39** (2-Part2), 1106 (2000).
  - 76) Mori, S., Ito, A., Sato, S., et al., “Dose Rate Analyses around the Equatorial and Divertor Ports during ITER In-Vessel Components Maintenance”, *J. Nucl. Sci. Technol.*, **Supplement 1**, 248 (2000).
  - 77) Mori, Y., Mori, S., Nishio, S., et al., “Neutron Streaming Evaluation for the DREAM Fusion Power Reactor”, *J. Nucl. Sci. Technol.*, **Suppl.1**, 268 (2000).
  - 78) Murata, I., Nishio, T., Kokoo, et al., “Benchmark Experiment on  $\text{LiAlO}_2$ ,  $\text{Li}_2\text{TiO}_3$  and  $\text{Li}_2\text{ZrO}_3$  Assemblies with D-T Neutrons -Leakage Neutron Spectrum Measurement-,” *Fusion Eng. Des.*, **51-52**, 821 (2000).
  - 79) Nakamura, H., Hayashi, T., Iwai, Y., et al., “The Effect of Annealing on the Transient Deuterium Permeation Characteristics of Tungsten”, *Fusion Technol.*, **39**, 894 (2001).
  - 80) Nakano, H., Tanabe, T., Kimura, T., et al., “Analysis of the Current Distortion Factor of a Three-Phase, Three-Wire System”, *Electrical Eng. in Japan*, **131**, 279 (2000).
  - 81) Neudatchin, S.V., Takizuka, T., Shirai, H., et al., “Analysis of internal transport barrier heat diffusivity from heat pulse propagation induced by an ITB event in JT-60U reverse shear plasmas”, *Plasma Phys. Control. Fusion*, **43**, 661 (2001).
  - 82) Ninomiya, N. and JT-60 Team, “JT-60U Experimental Results aimed at Steady-State Operation of a Tokamak Reactor”, *Fusion Eng. Des.*, **51-52**, 1023 (2000).
  - 83) Nishio, S., Ueda, S., Kurihara, R., et al., “Prototype Tokamak Fusion Power Reactor Based on SiC/SiC Composite Material, Focusing on Easy Maintenance”, *Fusion Eng. Des.*, **48**, 271 (2000).
  - 84) Nishitani, T., Shibata, Y. and Kusama, Y., “Fusion Gamma-Ray Measurement for D-3He Experiments in JT-60U”, *Rev. Sci. Instrum.*, **72**, 877 (2001).
  - 85) Nishitani, T., Shikama, T., Fukao, M., et al., “Irradiation Effects on Magnetic Probes made of Mineral Insulated”, *Fusion Eng. Des.*, **51-52**, 153 (2000).
  - 86) Ogawa, T. and JFT-2M group, “Coupling and Heating Experiments using Fast Wave Antenna with Back Faraday Shield on JFT-2M”, *Trans. Fusion Technol.*, **39**, 305 (2001).
  - 87) Ogawa, T., Ogawa, H., Miura, Y., et al., “Compact Troid Injection as Fueling in the JFT-2M Tokamak” *J. Nucl. Mater.*, **290-293**, 454 (2001).
  - 88) Oikawa, T. and JT-60 team, “High Performance and Prospects for Steady-State Operation on JT-60U”, *Nucl. Fusion*, **40**, 1125 (2000).
  - 89) Oikawa, T., et al., “Disappearance of Giant ELMs and Appearance of Minute Grassy ELMs in JT-60U High-triangularity Discharges”, *Plasma Phys. Control. Fusion*, **42**, A283 (2000).
  - 90) Oikawa, T., et al., “Heating and Non-inductive Current Drive by Negative Ion Based NBI in JT-60U”, *Nucl. Fusion*, **40**, 435 (2000).
  - 91) Oya, Y., Kobayashi, K., Shu, W., et al., “Decontamination of candidate materials for ITER remote handling equipment exposed to tritiated moisture”, *Fusion Technol.*, **39**, 1023 (2001).
  - 92) Oya, Y., Shu, W., O'hira, S., et al., “A study of tritium decontamination of deposits by UV irradiation”, *J. Nucl. Mater.*, **290-293**, 469 (2001).
  - 93) Ozeki, T., Hamamatsu, K., Isayama, A., et al., “Effects of Profiles on the Neo-classical Tearing Mode”, *Fusion Eng. Des.*, **53**, 65 (2001).
  - 94) Saigusa, M., Kikuchi, Y., Takei, N., et al., “The evaluation of mode purity for ECCD using single deep grooved polarizer”, *Fusion Eng. Des.*, **53**, 505 (2000)..
  - 95) Saigusa, M., Takei, N., Kikuchi, Y., et al., “New application of a deep grooved polarizer for ECCD”, *J. Plasma Fusion Res.*, **3**, 383 (2000).
  - 96) Sakamoto, Y., Kamada, Y., Ide, S., et al., “Characteristics of Internal Transport Barrier in JT-60U Reversed Shear Plasmas”, *Nucl. Fusion*, **41**, 865 (2001).
  - 97) Sakasai, A., Takenaga, H., Kubo, H., et al., “Helium Exhaust in Divertor-Closure Configuration with W-shaped Divertor of JT-60U”, *J. Nucl. Mater.*, **290-293**, 957 (2001)

- 98) Sakata, S., Koiwa, M., Aoyagi, T., et al., "Real Time Processor in JT-60 Data Processing System", *Fusion Eng. Des.*, **48**, 225 (2000).
- 99) Sato, K., Ishitsuka, E., Uda, M., et al., "Erosion Characteristics Of Neutron Irradiated Carbon Based Materials Under The Simulated Disruption Heat Loads", *J. Nucl. Mater.*, **283-287**, 1157 (2000).
- 100) Sato, M., Isei, N., Isayama, A., et al., "Effects of Polarization Change on the Measurement of Electron Temperature Profile from ECE in Tokamak Plasma", *Fusion Eng. Des.*, **53**, 161 (2001).
- 101) Sato, M., Kawashima, H., Miura, Y., et al., "Design and First Experimental Results of Toroidal Field Ripple Reduction Using Ferritic Insertion in JFT-2M", *Fusion Eng. Des.*, **51-52**, 1071 (2000).
- 102) Sato, S., Iida, H., "Monte Carlo Analyses for ITER NBI Duct by 1/4 Tokamak Model", *J. Nucl. Sci. Technol.*, **Supplement 1**, 258 (2000).
- 103) Sato, S., Plenteda, R., Valenza, D., et al., "Evaluation of Biological Dose Rates around the ITER NBI Ports by 2-D SN/Activation and 3-D Monte Carlo Analyses", *Fusion Eng. Des.*, **47**, 425 (2000).
- 104) Sato, S., "Estimation of Helium Production due to Neutron Streaming and Establishment of Shielding Design Conditions in Fusion Shielding Blanket by 3-D Monte Carlo Calculation", *J. Nucl. Sci. Technol.*, **Supplement 1**, 253 (2000).
- 105) Seki, M., Ohara Y., Tada E., et al., "Development and testing of large-scale nuclear components and remote handling system in JAERI", *Fusion Eng. Des.*, **51-52**, 941 (2000).
- 106) Seki, Y., "Overview of the Japanese Fusion reactor Studies Programme", *Fusion Eng. Des.*, **48**, 247 (2000).
- 107) Seki, Y., Tabara, T., Aoki, I., et al., "Composition Adjustment of Low Activation Material for Shallow Land Disposal", *Fusion Eng. Des.*, **48**, 435 (2000).
- 108) Shibata, Y., Iguchi, T., Hoek, M., et al., "Time-of flight neutron spectrometer for JT-60U", *Rev. Sci. Instrum.*, **72**, 828 (2001).
- 109) Shikama, T., Yamamoto, S., Snider, R., et al., "Fission-reactor-irradiation tests of MI-cables and magnetic coils for fusion burning plasma", *Fusion Eng. Des.*, **51-52**, 171(2000).
- 110) Shimomura, Y., "New ITER", *J. Plasma Fusion Res.*, **9**, 135 (2000).
- 111) Shimomura, Y., "Towards the construction of ITER", *J. of Atomic Energy Society of Japan*, **43**, 217 (2001).
- 112) Shirai, H., Kikuchi, M., Takizuka, T., et al., "Role of Radial Electric Field and Plasma Rotation in the Time Evolution of Internal Transport Barrier in JT-60U", *Plasma Phys. Control. Fusion*, **42**, A109 (2000).
- 113) Shirai, H., Takizuka, T., Koide, Y., et al., "Nondimensional Transport Study on ELMy H-mode Plasmas in JT-60U", *Plasma Phys. Control. Fusion*, **42**, 1193 (2000).
- 114) Shoyama, H., Sakamoto, K., Kasugai, A., et al., "Development of long pulse Gyrotron for fusion application", *J. Plasma Fusion Res.*, **3**, 368 (2000).
- 115) Shu, W. and Oya, Y., "Tritium decontamination from plasma facing materials", *J. Plasma Fusion Res.*, **76**, 1021 (2000) (in Japanese) .
- 116) Shu, W.M., O'hira, S., Gentile, C. A., et al., "Tritium decontamination of TFTR carbon tiles employing ultra violet light", *J. Nucl. Mater.*, **290-293**, 482 (2001).
- 117) Skinner, C. H., Gentile, C. A., Ascione, G., et al., "Studies of Tritiated Co-deposited Layers in TFTR", *J. Nucl. Mater.*, **290-293**, 486 (2001).
- 118) Sugai, H., "Radiation effects on intermetallic compound -LiAl", *Radiation Chemistry*, **69**, 55 (2000).
- 119) Sugihara, M., Suttrop, W., Igitkhanov, Y., et al., "A model of H-mode pedestal width scaling using International Pedestal Base", *Nucl. Fusion*, **40**, 1743 (2000).
- 120) Sugimoto, M., Isono, T., Nunoya, Y., et al., "Completion of CS insert fabrication", *IEEE Trans. ASC*, **10**, 564 (2000).
- 121) Suzuki, S., Ezato, K., Sato, K., et al., "Thermal Fatigue Damage Of The Divertor Plate", *Fusion Eng. Des.*, **49-50**, 343 (2001).
- 122) Suzuki, Y., Hayashi, T. and Kishimoto, Y., "Deceleration mechanism of spheromak-like compact toroid penetrating into magnetized plasmas", *Phys. Plasmas*, **7**, 5033 (2001).
- 123) Takahashi, K., Kajiwara, K., Kasugai, A., et al., "High power transmission and polarization measurement in

- 110 GHz transmission line”, *Fusion Eng. Des.*, **53**, 511 (2001).
- 124) Takahashi, K., Sakamoto, K., Kasugai, A., et al., “Chemical vapor deposition diamond window as vacuum and tritium confinement barrier for fusion application”, *Rev. Sci. Instrum.*, **71**, 4139 (2000).
  - 125) Takahashi, Y., Ando, T., Hiyama, T., et al., “Test Results of ITER Model Coil – 13 T – 640 MJ Nb<sub>3</sub>Sn Pulsed Coil–”, *Japanese Cryo. Engn.*, **35**, 357 (2000) (in Japanese) .
  - 126) Takahashi, Y., Nunoya, Y., Nishijima, G., et al., “Development of 46-kA Nb<sub>3</sub>Sn Conductor Joint for ITER Model Coils”, *IEEE Trans. ASC*, **10**, 580 (2000).
  - 127) Takeji, S., Tokuda, S., Fujita, T., et al., “Stability of Reversed Shear Discharges in JT-60U”, *J. Plasma Fusion Res.*, **76**, 575 (2000).
  - 128) Takizuka, T., Hosokawa, M. and Shimizu, K., “Advanced Particle Simulation of Open-field Plasmas in Magnetic Confinement Systems”, *Trans. Fusion Tech.*, **39**, 111 (2001).
  - 129) Takizuka, T., Hosokawa, M. and Shimizu, K., “Particle Simulation of Detached Plasma in the Presence of Diffusive Particle Loss and Radiative Energy Loss”, *J. Nucl. Mater.*, **290-293**, 753 (2001).
  - 130) Takizuka, T. and Hosokawa, M., “Particle Simulation Study of the Effect of Radial Electric Field on Scrape-off Layer Plasma and Sheath Formation”, *Contrib. Plasma Phys.*, **40**, 471 (2000).
  - 131) Takizuka, T., JT-60 team and JFT-2M team, “Tokamak Experiments in JT-60U and JFT-2M”, *Chinese Physics Letters*, **362**, 9 (1999).
  - 132) Tanaka, T., Kaneko, J., Takeuchi, H., et al., “Diamond radiation detector made of ultrahigh-purity type IIa diamond crystal grown by high-pressure and high-temperature synthesis”, *Rev. Sci. Instrum.*, **72**, 1406 (2001).
  - 133) Taniguchi, M., Sato, K., Ezato, K., et al., “Disruption Erosion Tests on La<sub>2</sub>O<sub>3</sub> Containing Tungsten Material”, *Fusion Technol.*, **39**, 890 (2001).
  - 134) Tsuzuki, K., Sato, M., Kawashima, H., et al., “Ripple Reduction and Surface Coating Tests with Ferritic Steel on JFT-2M”, *J. Nucl. Mater.*, **283-287**, 681 (2000).
  - 135) Ueda, S., Nishio, S., Yamada, R., et al., “Maintenance and Material Aspects of DREAM Reactor”, *Fusion Eng. Des.*, **48**, 521(2000).
  - 136) Umeda, N., Kuriyama, M., Itoh, T., et al., “Development of negative ion based NBI system for JT-60U”, *Fusion Technology*, **39** (2-Part2), 1135 (2001).
  - 137) Ushigusa, K. and JT-60 team, “Progress in the Steady-state High Performance Plasma and Related Technologies in the JT-60 Tokamak”, *Fusion Technol.*, **39**, 315 (2000).
  - 138) Ushigusa, K., Isayama, A., Kurita, G., et al., “Vibration analysis in JT-60SU design”, *Fusion Eng. Des.*, **51-52**, 371 (2000).
  - 139) Watanabe, K., Akiba, M., Hatano, T., et al., “Development of key technologies for steady state tokamak reactor in JAERI”, *J. Plasma Fusion Res.*, **SERIES 3**, 525 (2000).

### A.1.3 List of papers published in conference proceedings

- 1) Akiyama, I., Umehara, T., Tayama, T., et al., "Radiation Protection in the Large Tokamak Device (JT-60) Facility", Proc. 10th International Congress of the International Radiation Protection Association(IRPA-10), P-6a-314, Hiroshima, Japan, May 2000.
- 2) Aoki, I., Ushigusa, K., Kurihara, R., et al., "Development of Dynamic Simulation Code for Fuel Cycle of Fusion Reactor", Proc. of 21st Symp. on Fusion Technology, p.90 (2000).
- 3) Araki, M., Sato, S., Senda, I., et al., "Conceptual tokamak design at higher neutron fluence for the next generation fusion experimental devices", Proc. of 21st Symposium on Fusion Technology, p.250 (2000).
- 4) Asaoka, Y., Konishi, S., Hiwatari, R., et al., "Commissioning of a DT Fusion reactor without External Supply of Tritium", Fusion Energy 2000 (CD-ROM, IAEA, Vienna), POP/8 (2001).
- 5) Bosia, G., Ioki, K., Kobayashi, N., et al., "Design of ITER-FEAT RF heating and current drive systems", Fusion Energy 2000 (CD-ROM, IAEA, Vienna), ITERP/14 (2001).
- 6) Bykov, V., Nishikawa, A., Carbonare G., et al., "The thermal shields for the ITER magnet system: thermal, structural and assembly aspects", Proc. of 21st Symposium on Fusion Technology, p.224 (2000).
- 7) Cardella, A., Elio, F., Ioki, K., et al., "Improvements in the design and manufacture of the ITER-FEAT first wall towards cost minimization", Proc. of 21st Symposium on Fusion Technology, p.16 (2000).
- 8) Costley, A., Di Pietro, E., (Inoue, T.), et al., "Conceptual design and integration of A diagnostic neutral beam in ITER", Proc. of 21st Symposium on Fusion Technology, p.202 (2000).
- 9) Donne, A.J.H., Costley, A., Ebisawa, K., et al., "Measurement requirements and diagnostic system design for ITER-FEAT", Fusion Energy 2000 (CD-ROM, IAEA, Vienna), IERP/09 (2001).
- 10) Dänner, W., Ioki, K., Cardella, A., et al., "Progress of and future plans for the L-4 blanket project Fusion Energy 2000 (CD-ROM, IAEA, Vienna), ITERP/18 (2001).
- 11) Ebisawa, K., Kasai, T., Yamamoto, S., et al., "Plasma Diagnostic for ITER-FEAT", Proc. of 13th Topical Conference on High Temperature Plasma Diagnostics, June 18-22, 2000, Tucson, Arizona, USA.
- 12) Elio, F., Ioki, K., Yamada, M., "Design of blanket cooling manifolds system for ITER-FEAT", Proc. of 21st Symposium on Fusion Technology, p.104 (2000).
- 13) Ezato, K., Taniguchi, M., Sato, K., et al., "Ultrasonic Non-Destructive Testing On Cfc Monoblock Divertor Mock-Up", Proc. of 9th International Workshop on Carbon Materials, 110 (2001).
- 14) Fujisawa, N., Inoue, T., Di Pietro, E., et al., "Neutral beam heating and current drive system and its role in ITER-FEAT operation scenarios", Fusion Energy 2000 (CD-ROM, IAEA, Vienna), ITERP/01 (2001).
- 15) Gordon, C., Bartels, H-W., Honda, T., et al., "ITER-FEAT Safety Approach", Fusion Energy 2000 (CD-ROM, IAEA, Vienna), ITERP/16 (2001).
- 16) Gribov, Y., Cavinato, M., Fujieda, H., et al., "ITER-FEAT scenarios and plasma position/shape control", Fusion Energy 2000 (CD-ROM, IAEA, Vienna), ITERP/02 (2001).
- 17) Grisham L., Kuriyama, M., Kawai, M., et al., "Progress in Development of Negative Ion Sources on JT-60U", Fusion Energy 2000 (CD-ROM, IAEA, Vienna), FTP1/17 (2001).
- 18) Hatae, T., Sugihara, M., Hubbard, A., et al., "Understanding of the H-mode pedestal characteristics using the multi-machine pedestal database", Fusion Energy 2000 (CD-ROM, IAEA, Vienna), ITERP/03 (2001).
- 19) Hemmings, R., Baulo, V., Gotoh, Y., et al., "The ITER-FEAT building layout-design considerations for the reduction in scale", Proc. of 21st Symposium on Fusion Technology, p.254 (2000).
- 20) Hino, T., Hirohata, Y., (Sengoku, S.), et al., "Low Activated Materials as Plasma Facing Components", Fusion Energy 2000 (CD-ROM, IAEA, Vienna), FTP1/08 (2001).
- 21) Honda, T., Bartels, H.-W., Neyatani, Y., et al., "Safety-related plasma events for ITER-FEAT", Proc. of 21st Symposium on Fusion Technology, p.268 (2000).
- 22) Hosogane, H., and JT-60 team, "Progress of JT-60 facilities and experimental research towards steady high performance plasmas", Proc. of 21st Symposium on Fusion Technology, p.287 (2000).
- 23) Idomura, Y., Tokuda, S., Kishimoto, Y., et al., "Gyrokinetic theory of drift waves in negative shear tokamaks", Fusion Energy 2000 (CD-ROM, IAEA, Vienna), TH2/6 (2001).
- 24) Iguchi, T., Iizuka, S., Uritani, A., et al., "Conceptual design of compact neutron camera with directional

- neutron detector for nuclear fusion experiment”, Proc. of 14<sup>th</sup> Top. Meet. on Technol. Fus. Energy (September, 2000).
- 25) Iida, T., Sato, F., Sato, H., et al., “Electrical Properties of Ceramic Insulators under Irradiation”, Proc. of the 1st International Symposium on Supercritical Water-Cooled Reactors, Design and Technology, Tokyo, pp.251-256 (2000).
  - 26) Ikeda, Y., and JT-60 team, “ECRF experiments for local heating and current drive in JT-60U”, Fusion Energy 2000 (CD-ROM, IAEA, Vienna), EXP4/03 (2001).
  - 27) Inoue, T., Di Pietro, El, Hanada, M., et al., “Design of neutral beam system for ITER-FEAT”, Proc. of 21st Symposium on Fusion Technology, p.36 (2000) .
  - 28) Ioki, K., Barabash, V., Cardella, A., et al., “Design and fabrication methods of FW/Blanket and vessels for ITER-FEAT”, Proc. of 21st Symposium on Fusion Technology, p.102 (2000).
  - 29) Ioki, K., Dänner, W., Koizumi, K., et al., “ITER-FEAT vacuum vessel and blanket design features and implications for the R&D programme”, Fusion Energy 2000 (CD-ROM, IAEA, Vienna), ITER/5 (2001).
  - 30) Ishitsuka, E., Uchida, M., Sato, K., et al., “High heat load tests of neutron irradiated divertor mockups”, 21th Symp. on Fusion Technology, p.303 (2000).
  - 31) Kakudate, S., Oka, K., Yoshimi, T., Hiyama, M., et al., “Status of the Extended Performance Tests for Blanket Remote Maintenance in ITER L6 Project”, Fusion Energy 2000 (CD-ROM, IAEA, Vienna), ITERP/23 (2001).
  - 32) Kardaun, O.J.W.F., (Takizuka, T., Fukuda, T.), et al., “Next Step Tokamak Physics: Confinement-Oriented Global Database Analysis”, Fusion Energy 2000 (CD-ROM, IAEA, Vienna), ITERP/04 (2001).
  - 33) Kato, T., Tsuji, H., Okuno, K., et al., “First test results for the ITER central solenoid model coil”, Proc. of 21st Symposium on Fusion Technology, p.143 (2000).
  - 34) Kizu, K., et al., “A Repetitive Pellet Injection System for JT-60U”, Proc. of 21st Symposium on Fusion Technology, p.86 (2000).
  - 35) Koizumi, N., Azuma, K., Tsuchiya, Y., et al., “Evaluation of critical current performance of 13t-46kA steel-jacketed Nb3Al conductor”, Proc. of 21st Symposium on Fusion Technology, p.144 (2000).
  - 36) Konishi, S., “Use of Fusion Energy as a Heat for Various Applications”, Proc. of 21st Symp. on Fusion Technology, p.135 (2000).
  - 37) Konno, C., Maekawa, F., Kasugai Y., et al., “Neutronics Experiments for ITER at JAERI/FNS”, Fusion Energy 2000 (CD-ROM, IAEA, Vienna), ITERP/22 (2001).
  - 38) Kuriyama, M., Akino, N., Ebisawa, N., et al., “Study of increasing the beam power on the negative ion based neutral beam injector for JT-60U”, Proc. of 21st Symp. on Fusion Technology, p.37 (2000).
  - 39) Kuriyama, M., Grisham, L., Itoh, T., et al., “Performance of the negative ion source for JT-60U”, Proc. of 13th Inter. Conf. on High-Power Particle Beams (CD-ROM, Beam2000), PB-093, 780 (2000).
  - 40) Lad, P., Antipenkov, A., (Konishi, S.), et al., “ITER-FEAT Fuel Cycle”, Fusion Energy 2000 (CD-ROM, IAEA, Vienna), ITERP/12 (2001).
  - 41) Lister, J.B., Khayrutdinov, R., (Nakamura, Y.), et al., “Plasma Equilibrium Response Modeling Experiments on the JT-60U and TCV Tokamaks”, Proc. of 27th European Conference on Controlled Fusion and Plasma Physics (EPS, Budapest, 2000), **24B**, 181-184 (2000).
  - 42) Loarte, I., Saibene, G., (Sugihara, M.), et al., “Predicted ELM energy loss and power loading in ITER-FEAT”, Fusion Energy 2000 (CD-ROM, IAEA, Vienna), ITERP/11(R) (2001).
  - 43) Maebara, S., Morimoto, I., Zheng, X., et al., “Beam transport experiment In JLA Induction linac for mm-meter wave FEL”, Proc. of 13th Inter. Conf. on High-Power Particle Beams (CD-ROM, Beam2000) PC-086, 1059 (2000).
  - 44) Maisonnier, D., Cerdan, G., (Tada, E.), et al., “ITER-FEAT Divertor Remote Maintenance”, Fusion Energy 2000 (CD-ROM, IAEA, Vienna), ITERP/24 (2001).
  - 45) Malaquias, A., Costley, A., Ebisawa, K., et al., “Integration of Direct coupling Diagnostics in ITER Equatorial and Upper Ports”, Proc. of 21st Symposium on Fusion Technology, p.195 (2000).
  - 46) Martin, E., Tivey, R., (Honda, T.), et al., “ITER-FEAT divertor maintenance and integration”, Proc. of 21st Symposium on Fusion Technology, p.373 (2000).
  - 47) Massmann, P., de Esch, H.P.L., (Inoue, T.), et al., “Cadarache 1MV ceramic SINGAP bushing”, Proc. of

21st Symposium on Fusion Technology, p.40 (2000).

- 48) Matsukawa, M., Miura, Y., Terakado, T., et al., "Development of a vacuum switch carrying a continuous current of 36 kA DC", Proc of 19th International Symposium on Discharges and Electrical Insulation in Vacuum, Xi'an, China., p.415 (2000).
- 49) Matsukawa, M., Miura, Y., Terakado, T., et al., "A Modification Plan of the Power Supply System for the JT-60 using Superconducting Coils", Proc. of the 2000 Japan Industry Application Society Conference, **1**, 287 (2000) (in Japanese).
- 50) Matsumoto, T., Naitou, H., Tokuda, S., et al., "Gyro-kinetic Simulations of Internal Collapse in Reversed Magnetic Shear Tokamak", Fusion Energy 2000 (CD-ROM, IAEA, Vienna), TH3/3 (2001).
- 51) Mazul, I., Akiba, M., Arkhipov, I., et al., "Status of R&D of the Plasma Facing Components for the ITER Divertor", Fusion Energy 2000 (CD-ROM, IAEA, Vienna), ITER/6 (2001).
- 52) Miki, N., Ioki, K., Elio, F., et al., "VDE/disruption EM analysis for the ITER-FEAT VV and in-vessel components", Proc. of 21st Symposium on Fusion Technology, p.98 (2000).
- 53) Mikkelsen, D.R., Shirai, H., Asakura, N., et al., "Correlation Between Core and Pedestal Temperatures in JT-60U: Experiment and Modeling", Fusion Energy 2000 (CD-ROM, IAEA, Vienna), EXP5/20 (2001).
- 54) Miura, Y. and JFT-2M group, "Relation among Potential, Fluctuation Change and L/H Transition in the JFT-2M Tokamak", Fusion Energy 2000 (CD-ROM, IAEA, Vienna), EX2/7 (2001).
- 55) Miura, Y.M., Matsukawa M. and Nakano, H., "A Dead Beat Control Method For A PWM Converter Applied To A Superconducting Magnet", Proc. of 21st Symposium on Fusion Technology, p.70 (2000).
- 56) Morimoto, Y., Ochiai, K., Takeuchi, H., et al., "Benchmark experiment on Silicon Carbide with D-T neutrons and validation of nuclear data libraries", Proc. of 21st Symposium on Fusion Technology, p.107 (2000).
- 57) Murakami, Y., Senda, I., Matsumoto, H., et al., "Performance assessment of ITER-FEAT", Fusion Energy 2000 (CD-ROM, IAEA, Vienna), ITERP/06 (2001).
- 58) Murata, I., Nishio, T., Kondo, T., et al., "Neutron-Nuclear Data Benchmark for Copper and Tungsten by Slab Assembly Transmission Experiments with DT Neutrons", Proc. of 21st Symposium on Fusion Technology, p.112 (2000).
- 59) Murayama, S., Sekine, C., Nakano, T., et al., "Magnetic properties of heavy-fermion  $Ce(Ru_{1-x}Pd_x)_2Si_2$ ", Physica B, **281&282**, 343 (2000).
- 60) Nagata, M. and JFT-2M group, "Behavior of Compact Toroid Injected into the External Magnetic Field", Fusion Energy 2000 (CD-ROM, IAEA, Vienna), EXP4/10 (2001).
- 61) Naka, R., Kawarabayashi, J., Uritani, A., et al., "Radiation distribution sensing with normal optical fiber", 2000 IEEE Nucl. Sci. Symp. (October, 2000).
- 62) Nakahira, M., Takahashi, H., Koizumi, K., et al., "Progress and achievements on the R&D activities for ITER vacuum vessel", Fusion Energy 2000 (CD-ROM, IAEA, Vienna), ITERP/17 (2001).
- 63) Nakahira, M., Takahashi, H., Koizumi, K., et al., "Evaluation of Welding Deformation on ITER Vacuum Vessel", Proc. of 18th Symp. on Fusion Engineering, 245-248 (2000).
- 64) Nakamura, H., Ida, M., Sugimoto, M., et al., "Status of Lithium Target System for International Fusion Materials Irradiation Facility (IFMIF)", Proc. of 21st Symposium on Fusion Technology, p.255 (2000).
- 65) Neudatchin, S.V., Takizuka, T., Dnestrovskij, Yu.N., et al., "Dynamic Behavior of Transport in Normal and Reversed Shear Plasmas with Internal Barriers in JT-60U", Fusion Energy 2000 (CD-ROM, IAEA, Vienna), EXP5/01 (2001).
- 66) Neyatani, Y., Tsuru, D., Nakahira, M., et al., "Study of Decay Heat Removal and Structural Assurance by LBB concept of Tokamak Components", Fusion Energy 2000 (CD-ROM, IAEA, Vienna), SEP/01 (2001).
- 67) Niimi, H., Ogawa, T., Ogawa, H., et al., "Analysis of Magnetic Fluctuation Induced by CT Injection on JFT-2M", Proc. International Conference of Plasma Physics (ICPP2000), **3**, 1987 (2000).
- 68) Nishio, S., Ushigusa, K., Ueda, S., et al., "Conceptual Design of Advanced Steady-State Tokamak Reactor (A-SSTR2) -Compact and Safety Oriented Commercial Power Plant-", Fusion Energy 2000 (CD-ROM, IAEA, Vienna), FTP2/4 (2001).
- 69) Nishitani, T., Shikama, T., Fukao, M., et al., "Neutron irradiation tests on diagnostic components at JAERI," Proc. of 21st Symposium on Fusion Technology, p.198 (2000).

- 70) Obara, K., Tada, E., Yagi, T., et al., "Development of Colored Alumilite Dosimeter for High Radiation use", Proc. RADECS 2000, pp. 214-218, Louvain-la-Neuve, Belgium (2000).
- 71) Ogawa, T. and JFT-2M group, "Radio Frequency Experiments in JFT-2M: Demonstration of Innovative Applications of a Travelling Wave Antenna", Fusion Energy 2000 (CD-ROM, IAEA, Vienna), EXP4/06 (2001).
- 72) Okumura, Y., Amemiya, T., Fujiwara, Y., et al., "Advanced Negative Ion Beam Technology to Improve the System Efficiency of Neutral Beam Injectors", Fusion Energy 2000 (CD-ROM, IAEA, Vienna), FTP1/18 (2001).
- 73) Okuno, K., Bessette, D., Ferrari, M., et al., "Key features of the ITER FEAT magnet system", Proc. of 21st Symposium on Fusion Technology, p. 220 (2000).
- 74) Onozuka, M., Ioki, K., Yoshimura, Y., et al., "Design and Thermal/Hydraulic Characteristics of the ITER-FEAT Vacuum Vessel", Proc. of 21st Symposium on Fusion Technology, p.244 (2000).
- 75) Oohara, H., Akino, N., Ebisawa, N., et al., "Operation of the positive-ion based NBI system for JT-60U", American Nuclear Society 14<sup>th</sup> Topical Meeting on the Technology of Fusion Energy, Fusion Technology, **39** (2-Part2), p.1140-1144 (2001).
- 76) Oshima, T., Matsuda, T., Tsugita, T., et al., "Mass Data Acquisition Systems in JT-60 Data Processing System", Proc. 13th Topical Conference on High-Temperature Plasma Diagnostics, p.517 (2000).
- 77) Prater, R., Austin, M.E., (Isayama, A.), et al., "Highly Localized Electron Cyclotron Heating and Current Drive and Improved Core Transport in DIII-D", Fusion Energy 2000 (CD-ROM, IAEA, Vienna), EX8/1 (2001).
- 78) Pustovitov, V.D., Mikhailovskii, A.B., (Kobayashi, N.), et al., "Theory of neoclassical tearing modes and its application to ITER", Fusion Energy 2000 (CD-ROM, IAEA, Vienna), ITERP/07 (2001).
- 79) Roshal, A., Bareyt, B., (Shoji, T.), et al., "The ITER-FEAT power supply system and interface with the site HV power grid", Proc. of 21st Symposium on Fusion Technology, p.76 (2000).
- 80) Saigusa, M., Kanazawa, S., Ogawa, T., et al., "Direct Measurement of Electromagnetic Field Pattern of Fast Wave in FWCD Experiments using Ponderomotive Potential Produced by Beat Wave in JFT-2M", Proc. of International Conference of Plasma Physics (ICPP2000), **3**, 844 (2000).
- 81) Sakamoto, K., Kasugai, A., Shouyama, H., et al., "Development of 110GHz band gyrotrons and its application for JT-60U and ITER", Proc. of 25th Int. Conf. on Infrared and Millimeter Waves, p.11 (2000).
- 82) Sakamoto, K., Kasugai, A., Shouyama, H., et al., "Development of 100GHz band high power gyrotrons for fusion experimental reactor", Fusion Energy 2000 (CD-ROM, IAEA, Vienna), FTP1/20 (2001).
- 83) Sakasai, A., Takenaga, H., Higashijima, S., et al., "Helium Exhaust and Forced Flow Effects with Both-leg Pumping in W-shaped Divertor of JT-60U", Fusion Energy 2000 (CD-ROM, IAEA, Vienna), EX5/5 (2001).
- 84) Sannazzaro, G., Elio, F., Ioki, K., et al., "Critical issues of the structural integrity of the ITER-FEAT vacuum vessel", Proc. of 21st Symposium on Fusion Technology, p.245 (2000).
- 85) Sato, K., Ezato, K., Taniguchi, M., et al., "Thermal Fatigue Experiment of the CuCrZr Diverter Mock-Ups", Proc. of 7th Conference on Creep and Fatigue at Elevated Temperatures, p.55 (2001).
- 86) Sato, K., Ishitsuka, E., Uchida, M., et al., "Thermal Cycle Experiments of the Neutron-Irradiated CFC/Cu Mock-Ups", Proc. of 9<sup>th</sup> International Workshop on Carbon Materials, p.111 (2000).
- 87) Seki, M., Maebara, S., Fujii, T., "R&D of the heat-resistant LH antenna", Proc. of 21th Symp. on Fusion Technology, p.172 (2000).
- 88) Senda, I., Takase, H., Shoji, T., et al., "Study on the steady state tokamak reactor with combined heating and current drive", Fusion Energy 2000 (CD-ROM, IAEA, Vienna), FTP2/13 (2001).
- 89) Shimada, M., Campbell D.J., Wakatani, M., et al., "Physics Bases of ITER-FEAT", Fusion Energy 2000 (CD-ROM, IAEA, Vienna), ITERP/05 (2001).
- 90) Shimizu, K. and Takizuka, T., "Impurity Behavior in MARFE Plasma", Proc. of 27th European Conference on Controlled Fusion and Plasma Physics, (Budapest, Hungary), p.4.094 (2000).
- 91) Shimomura, Y., Aymar, R., Chuyanov, V., et al., "ITER-FEAT operation", Fusion Energy 2000 (CD-ROM, IAEA, Vienna), ITER/1 (2001).
- 92) Shimomura, Y., Sugio, K., Ohkubo, H., et al., "Point Defects Observed in D-T neutron irradiated Copper, Silver and Gold at 15°C with a Rotating Target in FNS\_JAERI", 2000 Material Research Society Fall, (2000).

- 93) Shinohara, K., Kusama, Y., Kramer, G.J., et al., "Alfven eigenmodes driven by energetic ions in JT-60U", Fusion Energy 2000 (CD-ROM, IAEA, Vienna), EXP2/05 (2001).
- 94) Sugimoto, M., Kanamasa, T., Takeuchi, H., et al., "Concept of staged approach for international fusion material irradiation facility," 20th International Linear Accelerator Conference, Montley (August, 2000).
- 95) Takahashi, H., Nakahira, M., Koizumi, K., et al., "Lead Behavior of High Compression Lead Rubber Bearing Second Report Section Photograph of Rubber Bearing by X-Ray CT and Assessment of Analysis", Summaries of Technical Papers of Annual Meeting B-2 (in Japanese), Architectural Institute of Japan, Tohoku, Japan, pp. 695-696 (2000).
- 96) Takahashi, K., Imai, T., Sakamoto, K., et al., "Development and design of ECRF launching system for ITER", Proc. of 21st Symposium on Fusion Technology, p.174 (2000).
- 97) Takeda, N., Nakahira, M., Takahashi, H., et al., "Vibration Test Using Sub-Scaled Tokamak Model to Validate Numerical Analysis on Seismic Response of Fusion Reactor", Fusion Energy 2000 (CD-ROM, IAEA, Vienna), FTP1/16 (2001)..
- 98) Takeji, S. and JT-60 team, "Improvement of Plasma Performance Toward Steady-state High-beta Tokamak Operation in JT-60U", Proc. of 27th EPS Conference on Controlled Fusion and Plasma Physics (Budapest, Hungary), **24B**, 77 (2000).
- 99) Takeuchi, H., Sugimoto, M., Nakamura, H., et al., "Staged Deployment of the International Fusion Materials Irradiation Facility (IFMIF)", Fusion Energy 2000 (CD-ROM, IAEA, Vienna), FTP2/03 (2001).
- 100) Takizuka, T., Shimizu, K., Hayashi, N., et al., "Simulation Study of the Detached Plasmas by Using Advanced Particle Model and Fluid Model", Fusion Energy 2000 (CD-ROM, IAEA, Vienna), THP1/22 (2001).
- 101) Tamai, H., Yoshino, R., Tokuda, S., et al., "Runaway Current Termination in JT-60U", Fusion Energy 2000 (CD-ROM, IAEA, Vienna), EX9/3 (2001).
- 102) Tesini, A., Honda, T., Maisonnier, D., et al., "ITER in-vessel components transfer using remotely controlled casks", Proc. of 21st Symposium on Fusion Technology, p.375 (2000).
- 103) Tokuda, S., "An innovative method for ideal and resistive MHD stability analysis of tokamaks", Fusion Energy 2000 (CD-ROM, IAEA, Vienna), THp2/10 (2001).
- 104) Tsuji, H., Okuno, K., Ando, T., et al., "Progress of the ITER central solenoid medel coil program", Fusion Energy 2000 (CD-ROM, IAEA, Vienna), ITER/4 (2001).
- 105) Tsuneoka, M., Kasugai, A., Ikeda, Y., et al., "Development of a d.c. power supply for a multi-MW CW CPD gyrotron", Proc. Inter. Power Electronics Conf., Tokyo, **3** 1529 (2000).
- 106) Uno, Y., Kaneko, J., Nishitani, T., et al., "Absolute Measurement of D-T Neutron Flux with a Monitor Using Activation of Flowing Water", Proc. of 21st Symposium on Fusion Technology, p.196 (2000).
- 107) Urano, H., Kamada, Y., Shirai, H., et al., "Density Dependence of Thermal Energy Confinement properties of ELMy H-mode in JT-60U", Proc. of 27th EPS Conference on Controlled Fusion and Plasma Physics (Budapest, Hungary), **24B**, 956 (2000).
- 108) Utin, Y., Ioki, K., Komarov, V., et al., "Vacuum vessel port structures for ITER-FEAT", Proc. of 21st Symposium on Fusion Technology, p.116 (2000).
- 109) Walker, C.I., Costley, (Ebisawa, K.), et al., "Integration of In-Vessel Diagnostics in ITER", Proc. of 21st Symposium on Fusion Technology, p.194 (2000).
- 110) Watanabe, K., Akiba, M., Hatano, T., et al., "Development of key technologies for steady state tokamak reactor in JAERI", Proc. of 10<sup>th</sup> International Toki Conference on Plasma Physics and Controlled Nuclear Fusion (ITC-10), 525-529 (2000).
- 111) Weber, H.W., Humer, K., (Okuno, K.), et al., "Irradiation and mechanical testing of ITER relevant magnet insulation", Proc. of 21st Symposium on Fusion Technology, p. 217 (2000).
- 112) Zheng, X., Morimoto, I., Maebara, S., et al., "200MW relativistic backward-wave oscillator", Proc. of 13th Inter. Conf. on High-Power Particle Beams (CD-ROM, Beam2000) PC-075, 1024 (2000).

#### A.1.4 List of other papers

- 1) Fukuda, T., "Plasma Control in Tokamaks", J. Plasma Fusion Research, **76**, 21 (2000) (in Japanese).
- 2) Hatae, Y., Yoshida, H., Yamauchi, T., Naito, O., "Non-collective Thomson Scattering in JT-60U and JFT-2M", J. Plasma Fusion Research, **76**, 868(2000) (in Japanese).
- 3) Hayashi, T., Kobayashi, K. and Nishi, M., "Tritium Confinement and Detritiation Demonstration Program for Fusion Reactor Rooms using Caisson Assembly for Tritium Safety Study (CATS) at TPL/JAERI", J. Health Phys., **35**, 112 (2000) (in Japanese).
- 4) Kamada, Y., Fukuda, T., Takizuka, T., et al., "Activities of ITER Physics R&D Expert Group", J. Plasma Fusion Res., **76**, 1091 (2000) (in Japanese).
- 5) Kawano, Y., "Polarimetry measurement in JT-60U", J. Plasma Fusion Research, **76**, 855 (2000) (in Japanese).
- 6) Kobayashi, K., "Study of Tritium Confinement in the Facility of a Fusion Reactor", J. Plasma Fusion Res., **76**, 1051 (2000) (in Japanese) .
- 7) Kondoh, T., Li, S. and Miura, Y., "Measurements of ion temperature and energetic ions in JT-60U by using collective Thomson scattering of CO<sub>2</sub> lazer", J. Plasma Fusion Research, **76**, 883 (2000) (in Japanese).
- 8) Zushi, H., Sugie, T., Kusama, Y., et al., "Progress in ITER Physics R&D - 7. Plasma Diagnostics", J. Plasma Fusion Research, **76**, 145 (2000) (in Japanese).

**A.2 Scientific Staff in the Naka Fusion Research Establishment  
(April 2000 - March 2001)**

Naka Fusion Research Establishment

MATSUDA Shinzaburo	(Director General)
HINO Syuji	(Vice Director General)
MIYAMOTO Kenro	(Invited Researcher)
NISHIKAWA Kyoji	(Invited Researcher)
HORIOKA Kazuhiko	(Invited Researcher)
SHIMAMOTO Susumu	(Invited Researcher)
KOYAMA Akira	(Invited Researcher)
KONDO Tatsuo	(Invited Researcher)
SEKIMURA Naoto	(Invited Researcher)
AZUMI Masafumi	(Director)
YAMAMOTO Takumi	(Staff for Director General)
OGAWA Toshihide	(Staff for Director General)
IIZUKA Takayuki	(Staff for Director General)

Department of Administrative Services

HINO Syuji	(Director)
KAWAKAMI Hideki	(Deputy Director)

Department of Fusion Plasma Research

KITSUNEZAKI Akio	(Director)
NINOMIYA Hiromasa	(Deputy Director)
KANEKO Sadao	(Administrative Manager)

Tokamak Program Division

KIKUCHI Mitsuru	(General Manager)	
ISHIDA Shinichi	KAWANO Yasunori	KURITA Gen-ichi
KUSAMA Yoshinori	MORI Katsuharu (*14)	ODAMAKI Masayoshi (*14)
OGURI Shigeru (*14)	OIKAWA Akira	SAKASAI Akira
SAKURAI Shinji (#)	TAMAI Hiroshi (#)	YAMAZAKI Takeshi (*14)

Plasma Analysis Division

OZEKI Takahisa	(General Manager)	
HAMAMATSU Kiyotaka	HAYASHI Nobuhiko	IWASAKI Keita (*31)
KOIWA Motonao (*31)	MATSUDA Toshiaki	NAITO Osamu
NAKAMURA Yukiharu	NEUDATCHIN Sergei V. (*9)	OHSHIMA Takayuki
SAKATA Shinya	SATO Minoru	SHIMIZU Katsuhiro
SHIRAI Hiroshi	SUZUKI Masaei (*31)	SUZUKI Mitsuhiro (*26)
TAKIZUKA Tomonori	TSUGITA Tomonori	WANG Shaojie (*7)

Large Tokamak Experiment Division I

USHIGUSA Kenkichi	(General Manager)	
CHIBA Shinichi	CUI Zhengying (*32)	FUJITA Takaaki
FUKUDA Takashi	GAO Xiang (*7)	HAMANO Takashi (*25)

INOUE Akira (*25)	ISAYAMA Akihiko	KAMADA Yutaka
KASHIWABARA Tsuneo (*22)		KITAMURA Shigeru KOIDE Yoshihiko
KOKUSEN Shigeharu (*22)	KRAMER Gerrit Jakob (*9)	MORIOKA Atsuhiko
NAGAYA Susumu	NISHITANI Takeo	OIKAWA Toshihiro
SAKAMOTO Nobuteru	SAKUMA Takeshi (*25)	SHIBATA Yasunari (*21)
SHITOMI Morimasa	SUNAOSHI Hidenori	SUZUKI Takahiro
TAKECHI Manabu (*29)	TAKEJI Satoru	TAKI Yoshiaki (*22)
TSUCHIYA Katsuhiko	TSUKAHARA Yoshimitsu	UEHARA Kazuya
URAMOTO Yasuyuki	URANO Hajime (*6)	

#### Large Tokamak Experiment Division II

MIURA Yukitoshi	(General Manager)	
ASAKURA Nobuyuki	BAK Paul Eric (*9)	BAKHTIARI Mohammad (*38)
CHANKIN Alex V. (*9)	HATAE Takaki	HIGASHIJIMA Satoru
IDE Shunsuke	ISHIKAWA Masao (*37)	ITAMI Kiyoshi
KONDOH Takashi	KONOSHIMA Shigeru	KUBO Hirotaka
LEE Seishu (*29)	NAKANO Tomohide	OYAMA Naoyuki (*29)
SUGIE Tatsuo	TAKENAGA Hidenobu	

#### Plasma Theory Laboratory

KISHIMOTO Yasuaki	(Head)	
IDOMURA Yasuhiro	ISHII Yasutomo	LI Jiquan (*33)
MATSUMOTO Taro	MIYOSHI Takahiro (*29)	SUGAHARA Akihiro (*31)
SUZUKI Yoshio (*29)	TOKUDA Shinji	TUDA Takashi

#### Experimental Plasma Physics Laboratory

KIMURA Haruyuki	(Head)	
HOSHINO Katsumichi	ISEI Nobuaki	KAWASHIMA Hisato
OASA Kazumi	OGAWA Hiroaki	OGAWA Toshihide
SATO Masayasu	SENGOKU Seio	SHIINA Tomio
SHINOHARA Koji	TSUZUKI Kazuhiro	

#### Reactor System Laboratory

KONISHI Satoshi	(Head)	
AOKI Isao	HE Kaihui (*32)	HU Gang (*32)
KURIHARA Ryoichi	NISHIO Satoshi	OKADA Hidetoshi (*5)
TOBITA Kenji		

#### Department of Fusion Facilities

SHIMIZU Masatsugu	(Director)
KIMURA Toyoaki	(Deputy Director)

#### JT-60 Administration Division

OOTAKE Masaki	(General Manager)
---------------	-------------------

JT-60 Facilities Division I

HOSOGANE Nobuyuki	(General Manager)	
AKASAKA Hiromi	FURUKAWA Hiroshi (*25)	HOSHI Yoshiyuki (*18)
KAWAMATA Youichi	MATSUKAWA Makoto	MIURA M Yushi
NODA Masaaki (*14)	OHMORI Shunzo	OHMORI Yoshikazu
OKANO Jun	SEIMIYA Munetaka	SHIMADA Katsuhiko
SUEOKA Michiharu	TAKANNO Shoji (*1)	TERAKADO Tsunehisa
TOTSUKA Toshiyuki	UEHARA Toshiaki (*25)	YAMASHITA Yoshiki (*14)
YONEKAWA Izuru		

JT-60 Facilities Division II

MIYA Naoyuki	(General Manager)	
ITOH Takao	(Deputy General Manager)	
ARAI Masaru (*14)	ARAI Takashi	HIRATSUKA Hajime
HONDA Masao	ICHIGE Hisashi	IWAHASHI Takaaki (*22)
KAMINAGA Atsushi	KIKUCHI Hiroshi (*5)	KIZU Kaname
KODAMA Kozo	MASAKI Kei	MASUI Hiroshi (*10)
MIYATA Katsuyuki (*5)	MIYO Yasuhiko	MORIMOTO Masaaki (*20)
OKABE Tomokazu	SASAJIMA Tadayuki	SASAKI Noboru (*5)
URATA Kazuhiro (*20)	YAGYU Jun-ichi	

RF Facilities Division

FUJII Tsuneyuki	(General Manager)	
HIRANAI Shinichi	IGARASHI Koichi (*22)	IKEDA Yoshitaka
ISAKA Masayoshi	ISHII Kazuhiro (*25)	KAJIYAMA Eiichi (*22)
MORIYAMA Shinichi	SEKI Masami	SHIMONO Mitsugu
SHINOZAKI Shin-ichi	TAKAHASHI Masami (*34)	TERAKADO Masayuki
YOKOKURA Kenji		

NBI Facilities Division

KURIYAMA Masaaki	(General Manager)	
OHGA Tokumichi	(Deputy General Manager)	
AKINO Noboru	EBISAWA Noboru	GRISHAM Larry (*30)
HIKITA Shigenori	HONDA Atsushi	KAWAI Mikito
KAZAWA Minoru	KUSANAGI Naoto (*25)	LEE Pengyuan (*7)
LEI Guangjiu (*7)	MOGAKI Kazuhiko	OOHARA Hiroshi
SEKI Hiroshi (*25)	TANAI Yutaka (*25)	TOYOKAWA Ryoji (*22)
UMEDA Naotaka	USUI Katsutomi	YAMAZAKI Haruyuki (*5)

JFT-2M Facilities Division

MIYACHI Kengo	(General Manager)	
YAMAMOTO Masahiro	(Deputy General Manager)	
AKIYAMA Takashi (*14)	KASHIWA Yoshitoshi	KIKUCHI Kazuo
KIYONO Kimihiro	KOMATA Masao	OKANO Fuminori
SAWAHATA Masayuki	SHIBATA Takatoshi	SUZUKI Sadaaki
TANI Takashi	UMINO Kazumi (*25)	

## Department of Fusion Engineering Research

SEKI Masahiro (Director)  
SEKI Shogo (Deputy Director)  
NEMOTO Shinichiro (Administrative Manager)  
SHIHO Makoto

## Blanket Engineering Laboratory

OHARA Yoshihiro (Head)  
ABE Tetsuya ENOEDA Mikio HATANO Toshihisa  
HIROKI Seiji KASAI Satoshi KIKUCHI Shigeto (\*36)  
KOSAKU Yasuo KURODA Toshimasa (\*17) SATO Satoshi  
TANZAWA Sadamitsu YANAGI Yoshihiko (\*5)

## Superconducting Magnet Laboratory

TSUJI Hiroshi (Head)  
ANDO Toshinari HAMADA Kazuya HARA Eiji (\*8)  
HIYAMA Tadao ISONO Takaaki KATO Takashi  
KAWANO Katsumi KOIZUMI Norikiyo KUBO Hiroatsu (\*3)  
MATSUI Kunihiro NAKAJIMA Hideo NISHIJIMA Gen (\*29)  
NUNOYA Yoshihiko OSHIKIRI Masayuki (\*25) SHIMBA Toru (\*8)  
SUGIMOTO Makoto TAKAHASHI Yoshikazu TSUCHIYA Yoshinori (\*29)  
WAKABAYASHI Hiroshi (\*25)

## NBI Heating Laboratory

OKUMURA Yoshikazu (Head)  
AKIBA Masato AMEMIYA Toru (\*24) DAIRAKU Masayuki  
EZATO Koichiro HANADA Masaya IGA Takashi (\*5)  
KASHIWAGI Mieko (\*29) SATO Kazuyoshi SAWAHATA Osamu (\*25)  
TANIGUCHI Masaki WATANABE Kazuhiro YOKOHAMA Kenji

## RF Heating Laboratory

IMAI Tsuyoshi (Head)  
HAYASHI Kenichi (\*36) IKEDA Yukiharu INOUE Yoji (\*23)  
KASUGAI Atsushi MAEBARA Sunao OHUCHI Hitoshi (\*23)  
SAKAMOTO Keishi SHIHO Makoto SHOYAMA Hiroaki (\*29)  
TAKAHASHI Koji TSUNEOKA Masaki WATANABE Akihiko (\*23)  
YAMAMOTO Masanori (\*5)

## Tritium Engineering Laboratory

NISHI Masataka (Head)  
HAYASHI Takumi IMAIZUMI Hideki (\*20) ISOBE Kanetsugu  
IWAI Yasunori KAKUTA Toshiya (\*17) KAWAMURA Yoshinori  
KOBAYASHI Kazuhiro MISAKI Yohnosuke (\*34) NAKAMURA Hirofumi  
OYA Yasuhisa (\*29) SHU Wataru SUZUKI Takumi  
TADOKORO Takahiro (\*5) TERADA Osamu (\*16) YAMADA Masayuki

Reactor Structure Laboratory

KOIZUMI Koichi	(Head)	
AKOU Kentaroo (*17)	HIGASHIJIMA Takeshi (*12)	HIYAMA Masayuki (*29)
KAKUDATE Satoshi	KOSUGE Shin-ichi (*8)	NAKAHIRA Masataka
OBARA Kenjiro	OKA Kiyoshi	SHIBANUMA Kiyoshi
TAGUCHI Kou (*25)	TAKAHASHI Hiroyuki (*5)	TAKEDA Nobukazu
YOSHIMI Takashi (*36)		

Fusion Neutron Laboratory

TAKEUCHI Hiroshi	(Head)	
ABE Yuichi	IDA Mizuho (*8)	KUTSUKAKE Chuzo
NAKAMURA Hiroo	NISHIO Takashi (*27)	NISHITANI Takeo
OCHIAI Kentaro (*29)	OGINUMA Yoshikazu (*25)	MORIMOTO Yuichi (*5)
SEKI Masakazu	SUGIMOTO Masayoshi	TANAKA Shigeru

Office of Fusion Materials Research Promotion

TAKEUCHI Hiroshi	(Head)	
NAKAMURA Kazuyuki	FURUYA Kazuyuki	ANDO Masami (*27)

Department of ITER Project

TSUNEMATSU Toshihide	(Director)
NAGAMI Masayuki	(Deputy Director)
SHIMOMURA Yasuo	(Prime Scientist)
FUJISAWA Noboru	
INABE Teruo	
ODAJIMA Kazuo	

Administration Group

KIMURA Toshiyuki	(Leader)
------------------	----------

Project Management Group

MORI Masahiro	(Leader)
KURIHARA Kenichi	
TSURU Daigo	

Joint Central Team Group

ANDO Toshiro	(Leader)	
EBISAWA Katsuyuki (*36)	HONDA Takuro (*5)	HONDA Tsutomu (*36)
IIDA Hiromasa	INOUE Takashi	IOKI Kimihiro (*20)
KATAOKA Yoshiyuki (*5)	KITAMURA Kazunori (*36)	KOBAYASHI Noriyuki (*36)
KURIBAYASHI Takashi (*8)	MARUYAMA So	MATSUMOTO Hiroshi
MATSUMOTO Yasuhiro (*36)	MATSUNOBU Takashi (*5)	MIKI Nobuharu (*36)
MIZOGUCHI Tadanori (*5)	MOCHIZUKI Eiji (*35)	NISHIKAWA Akira (*8)
OHSAKI Toshio (*17)	OKUNO Kiyoshi	ONOZUKA Masanori (*20)
SATO Kouichi (*1)	SHIMADA Michiya	SUGIHARA Masayoshi
TAKIGAMI Hiroyuki (*36)	YAMADA Masao (*20)	YAMAMOTO Shin
YOSHIDA Hiroshi	YOSHIDA Kiyoshi	YOSHIMURA Hideto (*19)

#### Home Team Design Group

SHOJI Teruaki	(Leader)	
ARAKI Masanori	GOTO Yoshinori (*19)	HORI Akio (*4)
KASHIMURA Shinji (*16)	KATAOKA Takahiro (*19)	KUCHIISHI Keiichi (*5)
MATSUMOTO Kiyoshi	MURAKAMI Yoshiki (*36)	OHKAWA Yoshinao
OHMORI Junji (*36)	OHNO Isamu (*8)	SAITO Keiji (*5)
SATO Shinichi (*17)	SENDA Ikuo (*36)	SHIMA Hiroaki (*15)

#### Safety Evaluation Group

TADA Eisuke	(Leader)	
ARAKI Takao (*36)	HADA Kazuhiko	HASHIMOTO Masayoshi (*8)
ISHIDA Toshikatsu (*17)	MARUO Takeshi	NEYATANI Yuzuru
NOMOTO Kazuhiro (*19)	OHIRA Shigeru	

- \*1 Atomic Data Service Corp.
- \*2 Cooperative Graduate School System
- \*3 Fuji Electric Co., Ltd.
- \*4 Hazama Corp.
- \*5 Hitachi Co., Ltd.
- \*6 Hokkaido University
- \*7 Institute of Plasma Physics, Academy of Science (China)
- \*8 Ishikawajima-Harima Heavy Industries, Co., Ltd.
- \*9 JAERI Fellowship
- \*10 Japan Expert Clone Corp.
- \*11 Japan Steel Works Co., Ltd.
- \*12 JGC Corp.
- \*13 JST Fellowship
- \*14 Kaihatsu Denki Co.
- \*15 Kajima Corporation
- \*16 Kandenko Corp.
- \*17 Kawasaki Heavy Industries, Co., Ltd.
- \*18 Mito Software Engineering Co.
- \*19 Mitsubishi Electric Co., Ltd.
- \*20 Mitsubishi Heavy Industries, Co., Ltd.
- \*21 Nagoya University
- \*22 Nippon Advanced Technology Co., Ltd.
- \*23 Nissei Sangyo Co., Ltd.
- \*24 Nissin Electric Co., Ltd.
- \*25 Nuclear Engineering Co., Ltd.
- \*26 Nuclear Information Service Co.
- \*27 Osaka University
- \*28 Osaka Vacuum Co., Ltd.
- \*29 Post-Doctoral Fellow
- \*30 Princeton Plasma Physics Laboratory (USA)
- \*31 Research Organization for Information Science Technology

- \*32 Southwestern Institute of Physics (China)
- \*33 STA Fellowship
- \*34 Sumitomo Heavy Industries, Co., Ltd.
- \*35 Takenaka Corp.
- \*36 Toshiba Corp.
- \*37 Tsukuba University
- \*38 Utsunomiya University